INTEGRATED RESERVOIR CHARACTERIZATION:

A CASE STUDY OF AN ONSHORE RESERVOIR IN NIGER DELTA BASIN

A

THESIS

Presented to the Graduate Faculty
of the African University of Science and Technology

in Partial Fulfilment of the Requirements
for the Degree of

MASTER OF SCIENCE IN PETROLEUM ENGINEERING

By

Oladipo, Musliu Kehinde.

Abuja-Nigeria

October 2011.

RECOMMENDED:.....

.....

.....
Committee Chair

APPROVED: .....
Chair, The Chief Academic Officer

.....
Date

ABSTRACT

Reservoir characterization has long been identified as the ultimate process employed in detailed description of a reservoir in order to properly book the reserve and also to optimally place the wells and drain the reservoir.

This report details the workflow of reservoir 'X' study, right from 3D seismic interpretation to delivery of a 3D static model of the reservoir by fully integrating all the available data in the field: 3D seismic data, well logs, deviation data, core data, checkshot data, PVT data, and production data

The field of study is located in the Northern Depobelt of the Niger Delta basin in the Gulf of Guinea. 21 wells have been drilled to date, penetrating 7 hydrocarbon-bearing sands (6 oils and 1 gas) between 5900 and 8500 ftss. The field was discovered by well-1 in 1965. 4 of the 21 wells were completed on this reservoir.

Reservoir 'X' is one of the 7 hydrocarbon-bearing sands in the field and has never been fully studied, that is, it does not have a static model and thus necessitated this research.

The objectives of this research were to properly characterize this reservoir by integrating all the available data in the field; produce a high resolution

static model of the reservoir; and re-evaluate the reserve using the 3D model.

Fault and Horizon interpretations were done using Petrel (A Schlumberger software) which culminated in delivery of a 3D structural map of the reservoir.

Sequence stratigraphic analyses were done using both seismic and well data to delineate the system tracts the reservoir belongs. Facies modelling and well correlation were done in Petrel to properly delineate the reservoir.

Petrophysical parameters were evaluated using Techlog® (a Schlumberger software).

Structural, stratigraphic and Petrophysical models were then integrated to produce a high resolution geological model (3D static model).

The generated 3D static model was used to rebook the reserve of Reservoir X. Both deterministic and stochastic volumes were estimated for the reservoir.

Volume (Bulk volume, net volume, Hydrocarbon Pore volume, STOIIP, Recoverable reserves etc) calculations were also done in Petrel.

Structural and stratigraphic analyses revealed that the reservoir is a rollover anticline with dip closure and fault boundary. It belongs to a prograding clastic sequence of transitional marine origin. The reservoir

rock properties are generally fair to good; the fluid properties and the performance plot typed the reservoir as an undersaturated reservoir with an active water drive. Uncertainty analyses showed the Stochastic most likely STOIIP, UR and reserve as 34.76MMSTB, 24.33MMSTB, and 4.33MMSTB respectively having produced 20MMSTB circa from the reservoir.

Conclusively, integration of subsurface data led to building of a consistent 3-D static model of the reservoir which can be used as input into a reservoir simulation model and provides a basis for a very effective reservoir management strategy. Well prognosis was better done using the 3D model (which considers both structure and property) as against prognosis in 2D map that only considers structure. This clearly underscores the superiority of a 3D model to a 2D map and showcases the significance of reservoir characterization.

DEDICATION

This Thesis work is dedicated to Almighty God; The Omniscient, The Omnipotent, The Creator of all creatures, The first and The last.

To my Late parents: Alhaji Jimoh Babalola Oladipo and Alhaja Wasilat Jadesola Oladipo, they were around when I started this program but are no more today. May they continue to rest in the bosom of Almighty God. Amen.

ACKNOWLEDGEMENTS

This work would not have been successful if not for immeasurable contribution of my colleagues in NPDC, IDSL and AUST. You are all appreciated. My tribute also goes to my lovely wife (my Queen) for her understanding, support and encouragement throughout the duration of the program. I also appreciate my supervisor, Prof Mosto Onuoha and co-sponsors, Prof Godwin Chukwu and Prof Debasmita Misra for their great contribution in this work. I will not forget to mention the psychological boost given to me by my children: Azimat and Mahfuz Oladipo.

Lastly, big thanks go to all my friends and everyone that contributed one way or the other to the successful completion of this work.

TABLE OF CONTENTS

LIST OF FIGURES

LIST OF TABLES

CHAPTER 1

1.0 INTRODUCTION

According to John W Kramers[1], Reservoir characterisation is the development of a detailed understanding of the reservoir, how it is put together and how it reacts to the production strategy.

The ultimate goal of an E&P company in the oil industry is to explore and produce hydrocarbon in an economic, safe and environment-friendly manner. In other words, the purpose of being in the oil and gas business is to maximize the NPV of the asset[2].

Modern Reservoir Characterization has become extremely important to oil companies since its advent around 1980[3]. Reservoir Characterization involves a holistic description of a reservoir by integrating all the available data, tools, disciplines, and knowledge. The aim of reservoir characterization is to understand and identify the flow units of the reservoir and predict the inter-well distributions of relevant reservoir properties[3] (φ, k, Sw, NTG). By applying reservoir characterization techniques in a field, asset holders will be able to maximally recover hydrocarbon while minimizing costs. Optimal placements of new wells and infill wells are also possible.

The field under study is located in the Northern Depobelt of Niger Delta Basin. 21 wells had been drilled in the field from 1965 till date. The general structure of the field (see enclosure 1.1 and figure 1.1)[4] is a large

rollover structure with dip closure located to the south, east and west and growth fault to the north. All the wells penetrated the reservoir under study (Reservoir X) but only 4 of the wells were completed on the reservoir. Several studies had been done on the largest reservoir in the field[4] but no study had ever been undertaken on Reservoir X, hence no existing model of the reservoir.

One of the objectives of this study is to build a reservoir static model of reservoir X. Another one is to validate the hydrocarbon volumes obtained from 3D seismic data interpretation and compare with the volumes estimated using 2D interpretation.

1.1 Reservoir Description/ Study objectives

1.1.1 Reservoir Description

The field under study is located onshore, in the seasonally flooded area of Niger Delta (See Figure 1.1.1)[4]. The field was discovered in 1965 by Well-1. To date 21 wells have been drilled, penetrating seven hydrocarbon-bearing sands (6 oils and 1 gas) between 5900 and 8500 ftss. 4 of the wells were completed on the studied reservoir. It is covered by good to fair 3D seismic[4].

Reservoir X is one of the oil sands in this field with expectation STOIIP of 44.9 MMstb and UR of 23.8 MMstb based on 2D interpretation[5]. The reservoir is a rollover anticline, bounded to the north by a major regional boundary fault and dip closure to the east, west and south. (Figure 2.3.2)

The reservoir is an undersaturated one and came on stream in August 1974. The major production problem encountered in some of the wells was early water breakthrough[4].

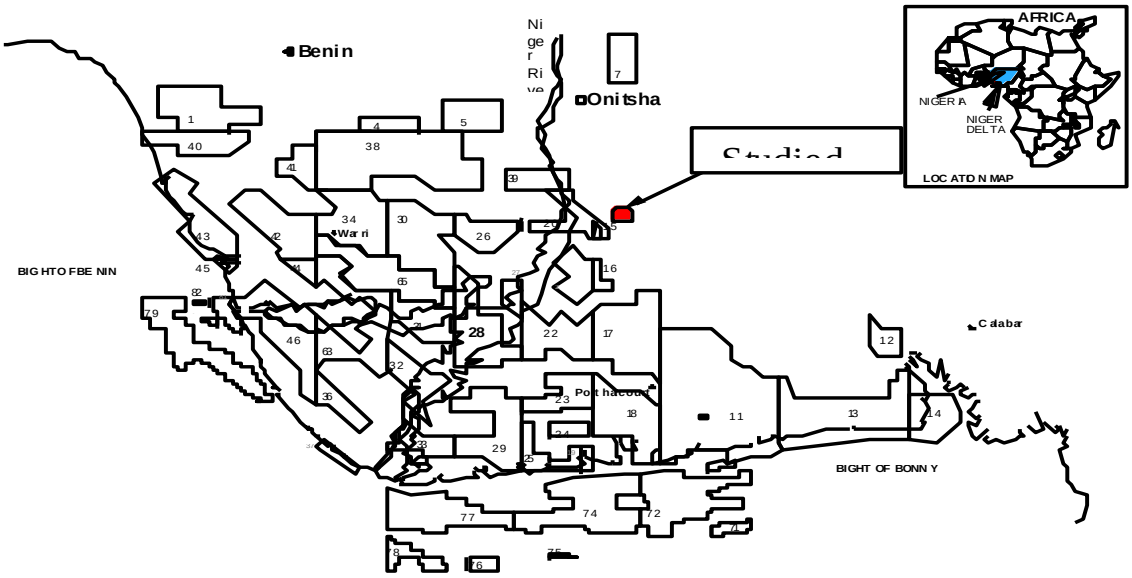

Figure 1.1.1: Location Map of the field.

1.1.2 Study Objectives

The objectives of this study are:

- Consistently describe and characterize Reservoir X
- Build a High Resolution Geo model (Static model) of the reservoir
- Re-evaluate the volumes (HCPV, STOIIP and UR) in the reservoir
- Showcase the significance of reservoir characterization by comparing the 3D volumes with the existing 2D volumes

1.2 Thesis Justification

The undertaking of this work was borne out of the fact that Oil and Gas companies often run into problems of poor reservoir performance due to inadequate reservoir description. The author decided to embark on this project to resoundingly underscore the importance of Reservoir Characterization in maximizing hydrocarbon recovery from a reservoir by ensuring a consistent reservoir description which helps in optimal well placement.

1.3 Scope of Work

The following scope of work was earmarked towards realizing the study objectives:

- Gather and QC all available data and subsequently identify the major subsurface uncertainties in respect of the reservoir.

- Quantify the impacts of these uncertainties by evaluating the range of Stock Tank Oil Initially in place (STOIIP) in the reservoir

- Carry out 3-D seismic interpretation, detailed correlation, generate top structure map

- Build a High Resolution Geological Model (Static model) in Petrel

1.4 Reservoir Volumes

As at 01/01/2011, the expectation STOIIP and oil UR of Reservoir X were estimated to be 44.9MMSTB and 23.8MMSTB respectively of which some 20MMSTB has been produced leaving reserves of 3.8MMSTB[4]. The resource volumes are tabulated below:

Table 1.4: Reservoir X resource volumes[4] before this study

Resource category (expt.)	Oil (MMSTB)
STOIIP	44.9
Ultimate Recovery	23.8
Cum. Production	20
Reserves	3.8

1.5 Key Benefits

This project will afford the author the opportunity to build capacity in **Practical** Reservoir characterization techniques and also learn the usage of oil industry-recognized softwares. The expected reserve to be added to the existing reserve is about 1MMSTB. The 3D Static model will also enable an optimal well placement to drain the remaining reserve in the reservoir. The project also provides a platform upon which future authors could build on in undertaking **Practical** Reservoir Characterization.

1.6 Project Schedule

See the attached for the Project Schedule.

1.7 Project Risks and Uncertainties

Projects (Theses) by nature are highly risky due to their unique outcome. Any uncertain event that can impact any of the Project objective(s) is a Risk. Not managing the risk(s) properly can lead to issues / Project failure. Listed in the simple Risk Matrix below:

Table 1.7a: Simple Risk Matrix

S/No.	Risk Title	Probability of Occurrence	Impact	Risk
1.	Inadequate number of Petrel Licences	High	High	High
2.	Outage of Internet connection	Very Low	Medium	Low
3.	Delay in Thesis Start-up due to extra coursework	Low	Low	Low
4.	Unrealistic Project/ Thesis scope	Medium	High	Medium
5.	Unavailability of Petrophysical evaluation software	High	High	High

Table 1.7b: Risk Response Planning/ Mitigation Plan

Risk Name	Mitigation Plan
Inadequate number of Petrel Licences	Develop a time table of usage among various researchers
Outage of Internet Connection	Outsource for Internet modem
Delay in Thesis Start-up due to extra coursework	Start early by prioritizing the optional courses
Unrealistic/ Wide Project Scope	Start early to finish within stipulated time
Unavailability of Petrophysical evaluation software	Outsource for software (Techlog)

CHAPTER 2

2.0 LITERATURE REVIEW

Reservoir characterization has evolved from the time that geologists and engineers were encouraged to work side by side in an asset team[1]. Initially, this cooperation had the objective to understand the non-homogeneous nature of the reservoir[6, 7]. This has grown to include geophysics, petrophysics, statistics and numerical modelling as new tools and techniques were developed to obtain a better understanding of the reservoir and reservoir heterogeneities. The literature on reservoir characterization has grown by leaps and bounds since the landmark papers by Haldorsen and Lake[8] and Begg and King[9] on characterizing and modelling of random shales in a sandstone reservoir. Professional societies such as the AAPG and SPE regularly have symposia and special publications on various aspects of reservoir characterization and heterogeneities[11]. Specialist conferences, such as those held by the National Institute for Petroleum and Energy Research in the USA have greatly added to our knowledge of reservoirs and recovery technique[10, 11, 12].

Several workers have published papers about Reservoir Characterization and its applications using case studies of fields in their regional basins. None of these papers ever applied this technique to Niger Delta basin.

G.R. King et al[13] published a SPE paper written in 1998 about Reservoir characterization of N'Sano field, Upper Pinda Reservoir, which is located offshore of Angolan province of Cabinda in approximately 250ft of water. They delineated the reservoir structure and Stratigraphy from the available data. A fine-scale geological model of the reservoir was produced using a facies-based geological modelling approach. The geological model was scaled-up using the dynamic scale-up approach of Durlofsky et al.'[14] The scaled-up model was converted into a reservoir simulation model which was successfully history matched (on a flow unit basis) against metered production data. The history- matched model was then used to make prediction forecasts for the N'Sano U. Pinda reservoir. OOIP estimates from Volumetrics and Material balance of 177MMSTB and 170MMSTB respectively are fairly in agreement. However, they fail to run uncertainty/ risk analyses on the OOIP estimates.

P.K. Neog and N.M. Borah[15] in their own work (in Oct. 2000) used Well Test Analysis technique in addition to other reservoir characterization techniques to dynamically describe Dikom field, an onshore field in the Upper Assam basin located in the Assam-Arakan geological province in the north-eastern part of India. They concluded that modern well test analysis is an effective tool for reservoir description for a field like Dikom with thin and deep seated sand units. It provides dynamic reservoir description by providing insight into fluid process taking place in the

reservoir. However, they relied too much on Well Test data while relegating the hardest data (Core data) to the background.

M.A. Naguib et al[16] presented a paper (in Oct., 2000) on how to improve reservoir management for a mature field using reservoir characterization. It's a case study of Ras Budran field (R/B) located at the eastern coast of the

Gulf of Suez area, Egypt. Several detailed reservoir characterization studies were carried out as parts of reservoir management strategy in order to optimize field performance and maximize field recovery. In conclusion, detailed understanding of the reservoir drive mechanism and reservoir characterization helps to optimize the reservoir management strategy leading to formulate short and long-term work programs.

CHAPTER 3

3.0 METHODOLOGY

As mentioned earlier, the current study involved a detailed description of an onshore Niger Delta reservoir by integrating all the available data in the field.

3.1 Data Availability and Quality

The dataset available for this study includes:

- ✓ 3D Seismic data (Soft)
- ✓ Well deviation survey data (Soft)
- ✓ Checkshot survey data (in one well)
- ✓ Core data (from analogue reservoir)
- ✓ Digital wireline log data (Soft)
- ✓ Formation tops files
- ✓ Production data
- ✓ Pressure data

3.1.1 3D Seismic Data

The field is fully covered by fair to good 3D Seismic data, though the resolution of the data is bad at the deeper levels (beyond 2 seconds).

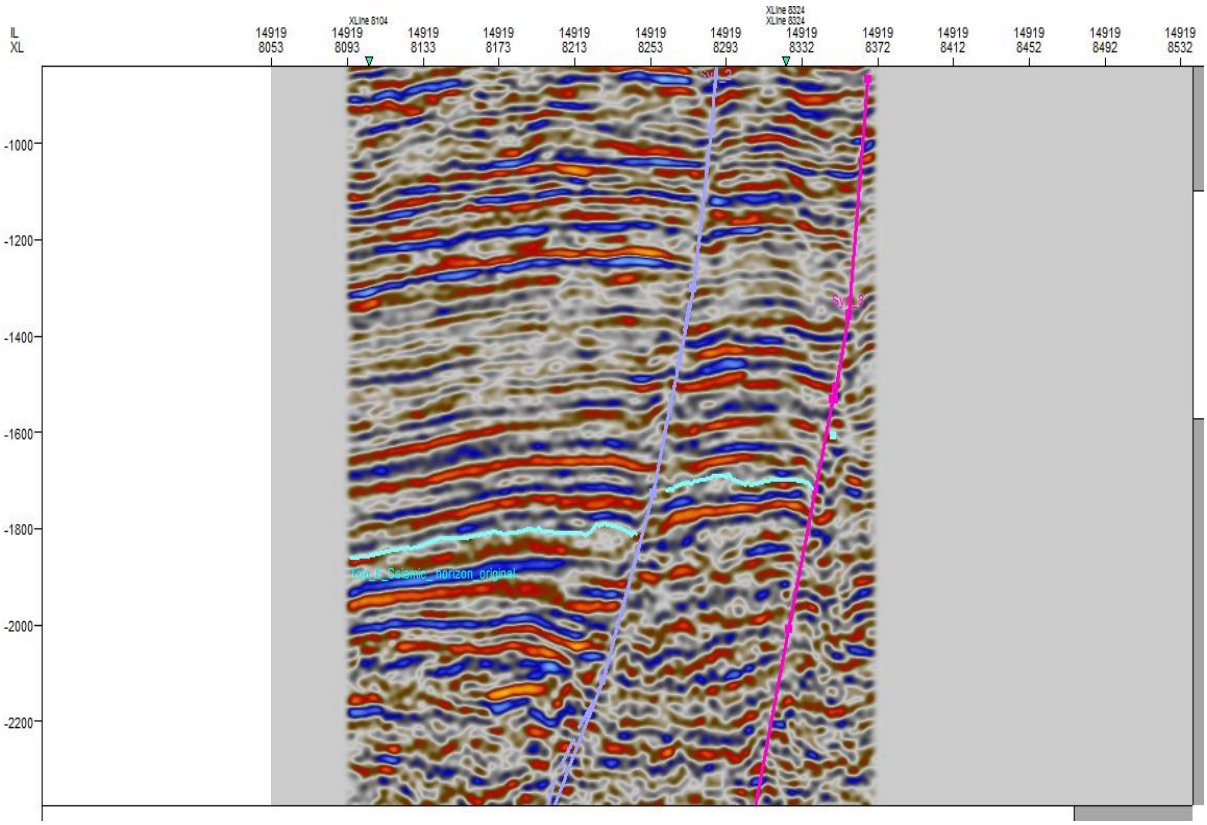

Figure 3.1.1: 3D Seismic inline showing the major synthetic growth faults.

3.1.2 Well Deviation Data

The deviation survey data from the 21 wells (all penetrated Reservoir X) were all available for the study. This usually indicates if a well is vertical or deviated.

3.1.3 Checkshot Data

Checkshot velocity data was shot in only 1 of the 21 wells. This was used in establishing Seismic to well tie during horizon interpretation.

3.1.4 Core Data

No core data exists for this interval (Reservoir X). However, core data was taken in one of the reservoirs in the field within well 21 with 96% recovery rate. Thus an analogue routine core analysis was available for this study.

3.1.5 Formation Tops Files

Tops and bases of the reservoir exist in most of the wells files. Tops and bases were not available in some of the wells though. These data was used as a guide when picking the tops and bases of Reservoir X.

3.1.6 Well log Data

Log data are available for all the 21 wells in the field. The data is generally of good quality. Table 3.1.6 below shows the log data availability in the field.

The 21 wells were drilled with water-based mud. The log types used for quantitative analysis in this study are the gamma ray, resistivity, density and neutron logs. The SP and caliper logs were mainly used for lithology identification and hole washout detection respectively. Eight of the wells (Wells-1, -2, -3, -5, -10,-13, 15 and –16) do not have density log acquired across the sand (Reservoir X).

The resistivity logs for the early wells (Wells-001, -002, and -003) were old vintage electrical logs (LN/SN) supplemented by lateral logs (LAT) in wells Wells-001 and -003. Wells-001 and -005 had the I6FR resistivity logs. All the other wells had deep and shallow lateral logs. Wells -019, -020 and -021 additionally had micro-spherically focused logs.

Table 3.1.6: Summary of the field well logs

Well	GR	SP	CAL	LL3R	LATL	LN	SN	16FR	LL9D	LL9S	MSFL	BCSL	FDC	CNL	DATE LOGGED
Well-1	X	X	X	X	X	X	X	X				X			06/08/65
Well- 2	X	X	X	X		X	X								15/04/66
Well-3	X	X	X	X	X	X	X								05/04/67
Well-4	X		X	X									X		03/05/73
Well-5	X		X					X					X		30/07/73
Well-6	X	X	X						X				X		27/01/74
Well-7	X	X	X						X				X		02/09/74
Well-8	X	X							X	X					21/02/74
Well-9	X	X							X	X					07/07/74
Well-10	X		X						X	X			X		07/03/74
Well-11	X	X	X						X	X			X		06/05/75
Well-12	X	X	X						X	X			X	X	27/06/75
Well-13	X	X	X						X	X			X		08/03/75
Well-14	X	X	X						X	X			X	X	19/02/76
Well-15	X	X	X				X						X		07/08/76
Well-16	X	X	X				X						X	X	13/05/76
Well-17	X	X	X				X						X	X	06/03/77
Well-18	X	X	X				X						X	X	27/06/77
Well-19	X	X	X						X	X	X				06/02/78
Well-20	X	X	X						X	X	X		X	X	07/06/78
Well-21	X	X	X						X	X	X	X	X		31/07/91

X Indicates Data availability

3.1.7 Production Data

Performance/ Production data (from 1974 till 2010) was available for integration into the study. The reservoir daily oil rate, cumulative production, solution gas produced and utilized were all available and of good quality.

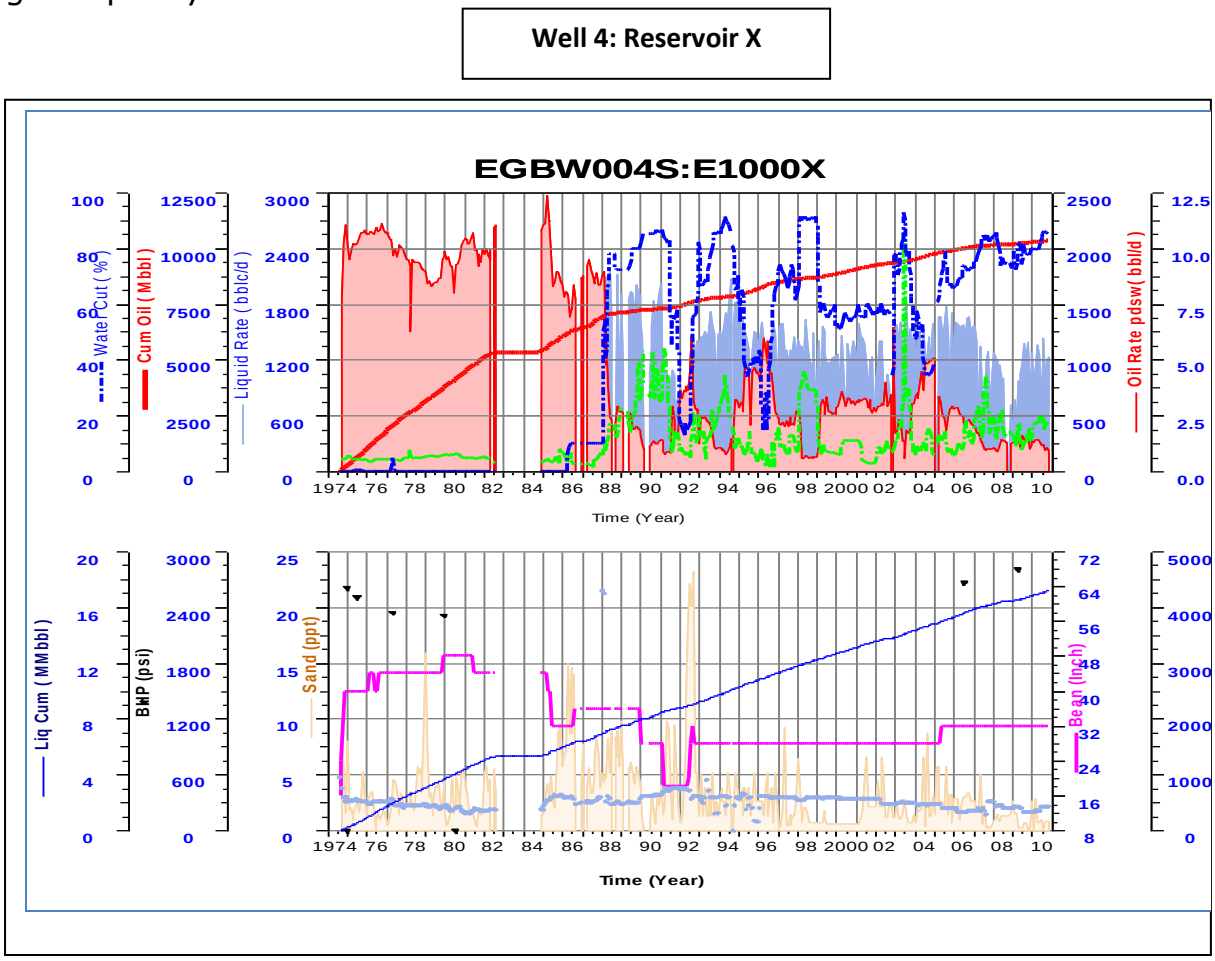

Figure 3.1.7: Performance plot of well 4 in Reservoir X

3.1.8 Pressure Data

The BHP survey data in the reservoir is shown in figure 2.1.7 above. It shows the reservoir has an active aquifer support, hence fairly uniform pressure.

3.1.9 PVT Data

PVT data got through Surface Samples Recombination method was available for the study.

Table 3.1: Data Availability and Quality Summary

Discipline		Comment
Geosciences	1. Seismic surveys	Field is covered by fair to good 3D seismic data, acquired in 1994.
	2. Well-ties	Synthetics from Well-21 showed good match with seismic data.
	3. Interpretations	Confidence level is high due to high amplitude mapable event, and good attributes supporting structural pattern.
	4. Reservoir Models	No static model for Reservoir X
	5. Reports	No dedicated previous studies on Reservoir X
Petrophysics	1. Wells and Log data	Reference log availability table. Well data available in 21 wells. Data quality considered fair.
	2. Core data	Available for one of the reservoirs in well 21. No core data for Reservoir X.
Petroleum Engineering	1. Production data	36 years production data exists for the producing well in the reservoir.
	2. Well Data	Available in well files
	3. Pressure data	BHP data exists for reservoir X in the field. There is no RFT data.
	4. PVT data/reports	Available for Reservoir X

3.1.10 Data Gaps and Limitations

The absence of core data from the reservoir (even though there is analogue) is a major uncertainty in the study since core data is the

hardest reservoir sample for all the important Petrophysical parameters. Lack of biostratigraphic data for better inter-well correlation and to ascertain environment of deposition was another challenge. An incomplete log suite (especially Neutron-Density and deep resistivity data) to accurately delineate the fluid type and contacts was another constraint. Lack of capillary pressure data to validate the Oil-water contact

3.2 Tools/ Applications employed

Petrel® (A Schlumberger software) was employed in Geological and Geophysical Interpretation.

Techlog was employed in Petrophysical Interpretation.

3.3 Subsurface Assessment

This section details the methods employed in characterizing the studied reservoir including Seismic data interpretation, structural interpretation and mapping, reservoir geology, Petrophysical evaluation and Static modelling. Oil in place and Reserves were then estimated from the interpretations. A bit of Static uncertainty analyses/ risk assessment were also carried out.

3.3.1 Seismic Interpretation

The 3D Seismic volume and well data were systematically loaded into Workstation in readiness for interpretation. Structural Smooth and Trace AGC volume attribute processes were then applied on the 3D volume

before being realized. These were done to increase the continuity of the seismic reflectors; boost weak events for improved interpretability; and to eliminate boosted noise**.**

Fault Interpretation

Geological fault interpretation was done on every 10th inline and 10th cross line. Arbitrary lines were taken where the fault pattern did not show clearly on the inline or trace (cross line). Major and minor discontinuities on the seismic lines were identified and picked. These are the major and minor faults respectively. The faults were identified on the Inlines, traces and time slices at the representative levels. These identified faults were assigned names, colour-coded and correlated. The major faults in the field were mostly synthetic faults which are generally downthrown to the basin because of progradation. Antithetic faults were few and minor ones.

Seismic to well tie

A synthetic seismogram was generated for the only well that has checkshot data and this was used to tie seismic to well data. Being that the field is a mature field with many wells, an arbitrary line was taken across the field inside the seismic to calibrate the seismic to well data. Both methods produced the same results (Figures 3.3.1 a and b).

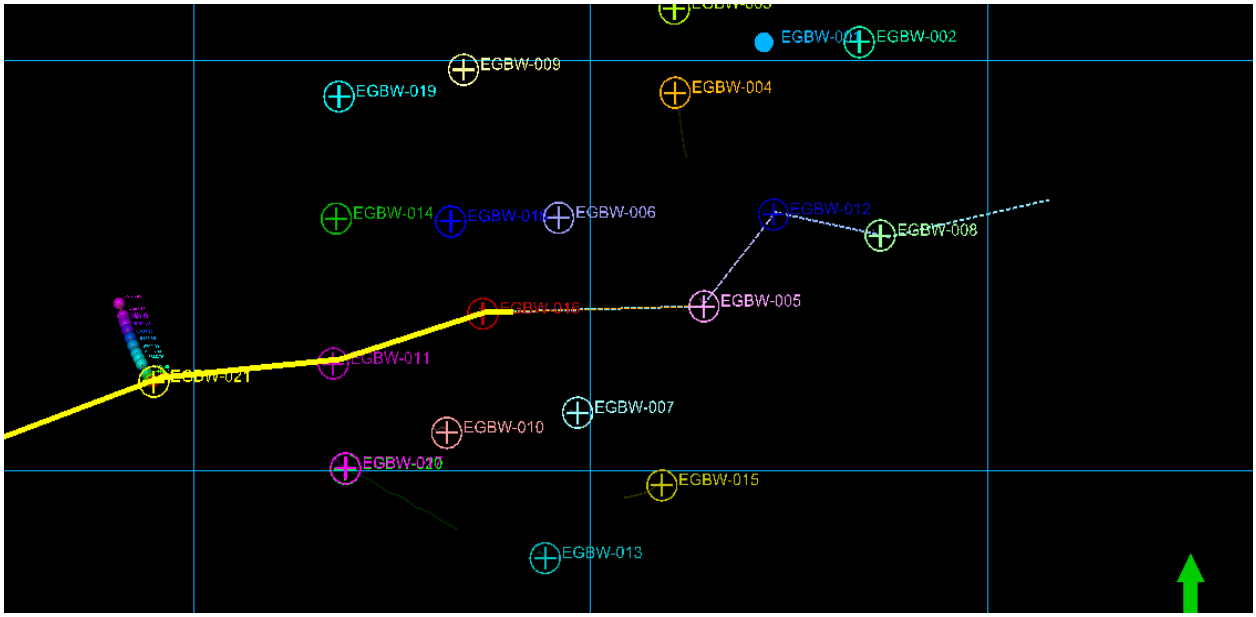

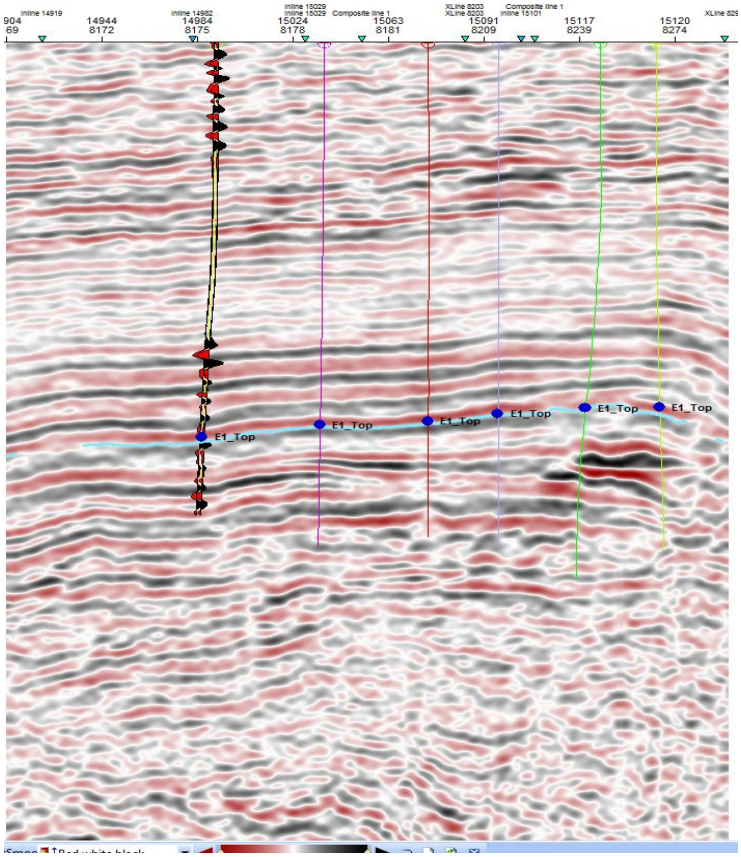

Figures 3.3.1 a and b: Seismic to well tie using Synthetic Seismogram and using checkshot data.

Horizon Interpretation:

Having tied seismic to well data, reservoir X time horizon was identified, picked and interpreted. Horizon tracking was carried out on every 10th in-lines and cross-lines before being refined to a denser grid on every 5th inlines and crosslines. This mapping/ digitization was done across the entire seismic volume

3.3.2 Structural Interpretation and Mapping

The field structure is a rollover anticline, it is bounded to the north and to the Southwest by major synthetic growth faults that defines the field.

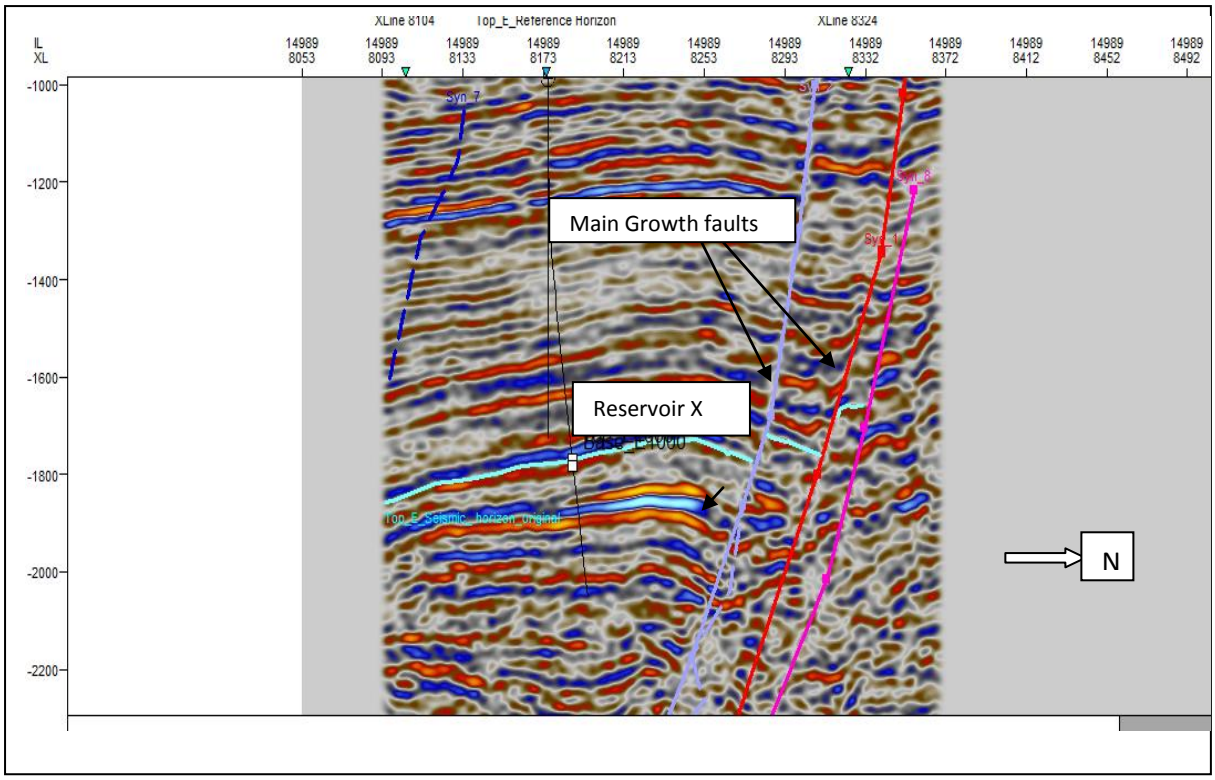

Figure 3.3.2: Reservoir X Rollover anticline and Growth Fault

As it can be seen from the above figure, Reservoir X is a Rollover anticline structure bounded to the North by the major (E-W trending) regional synthetic growth fault and to the Northwest by the Egbema-west boundary fault with dip closures to the East and South. There is no occurrence of intra-reservoir faults. The oil accumulation is preserved by both fault and structural dip closure.

Having finished with fault and horizon interpretation, fault polygons were generated from the interpreted main faults. The polygons were renamed (Reservoir X fault polygon) and converted from time to depth using both Look-up function and velocity model. Afterwards, time grid and time map of Reservoir X were generated. The time grid was then depth converted

using both look-up function and the generated velocity model while respecting the well data (that is, well adjustment). The time horizon interpretation seed grid, TWT map and depth map are shown in figures 3.3.2_1, 3.3.2_2 and 3.3.2_3 respectively.

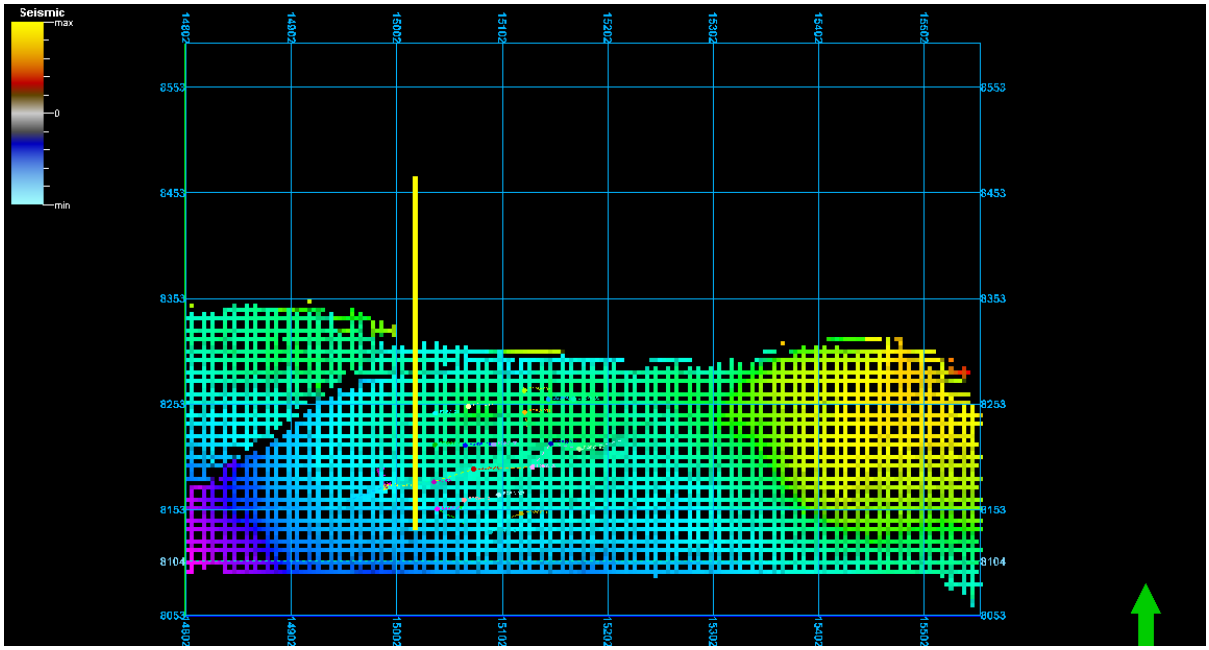

Figure 3.3.2_1: Reservoir X Time horizon interpretation Seed grid

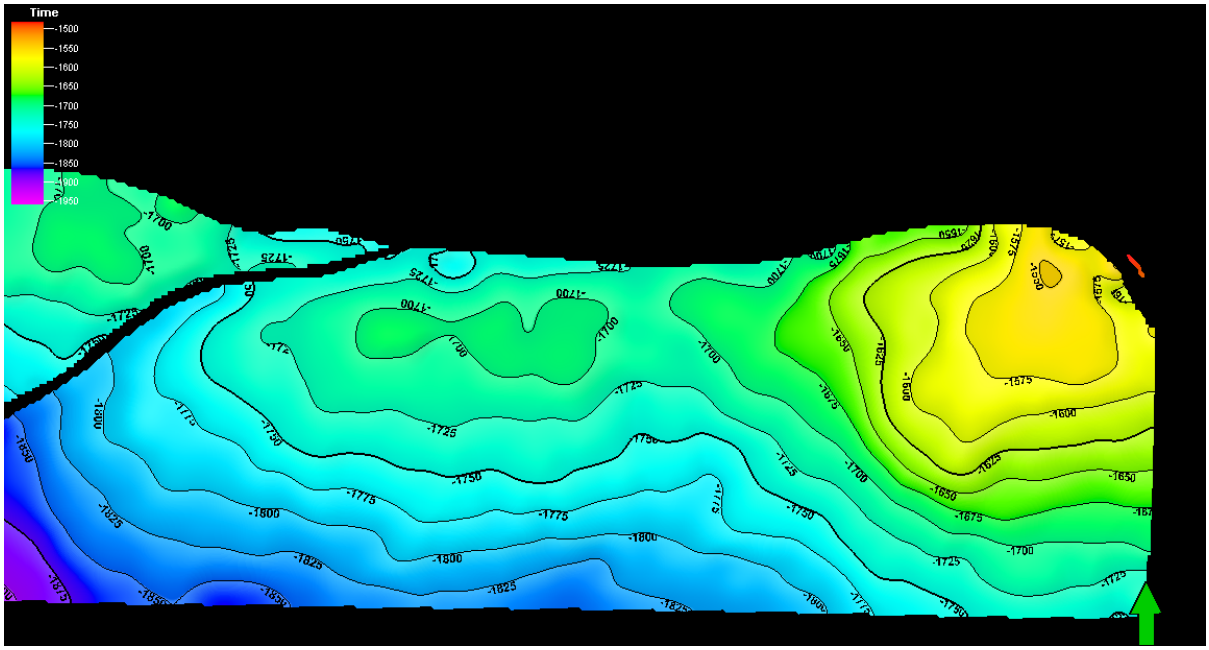

Figure 3.3.2_2 : Reservoir X Smoothened TWT Map

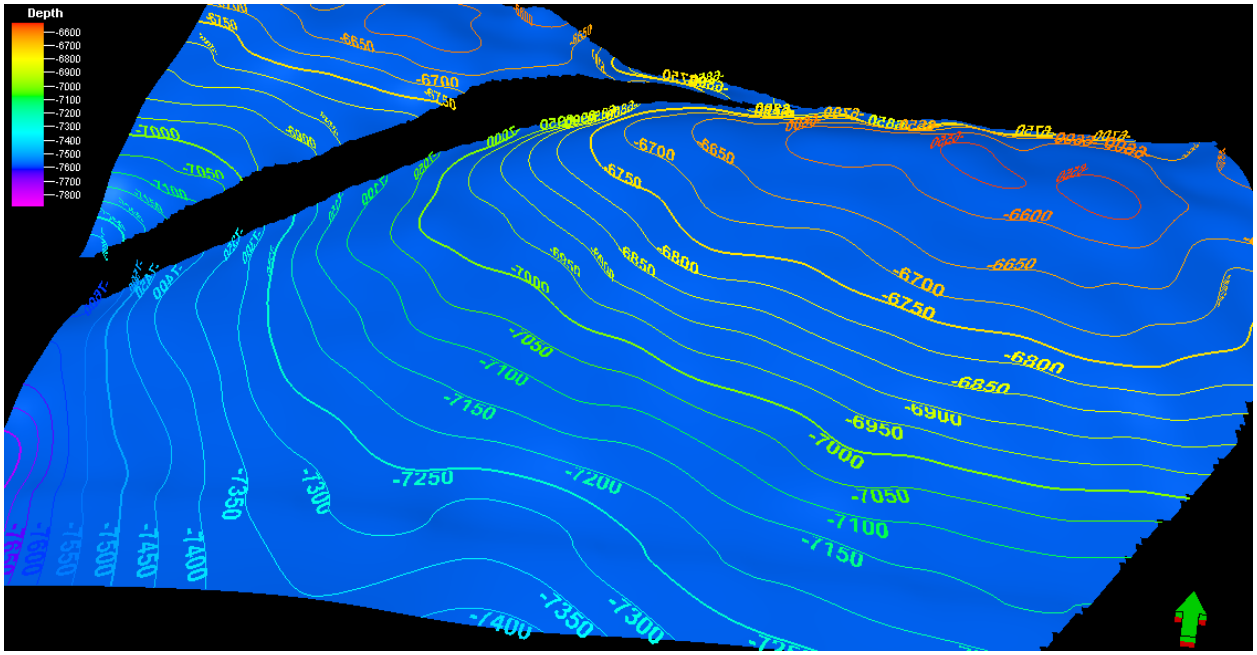

Figure 3.3.2_3: Reservoir X Top structure smoothened Depth Map

3.3.3 Reservoir Geology

3.3.3.1 Stratigraphy and Depositional Environment:

The depositional environment of Reservoir X was inferred from wireline logs. The environment of deposition was interpreted to be Shoreface / Barrier island environment (transitional marine setting). The logs generally coarsen upward indicating paralic facies[17]. The Reservoir exists within Lowstand Systems Tract (LST) and generally overlain by Transgressive Systems Tract TST) which means the two tracts are separated by Transgressive surface of erosion (TSE)[18]. LST generally gets deposited as part of prograding shoreline during relative fall in sea level.

This LST may have been deposited during Pliocene sea level fall. The top shale regionally forms the top seal for the reservoir. Though the reservoir has shale baffles in some wells, the stacking patterns are generally progradational. The reservoir sands vary in thickness and properties from north to south. Figure 3.3.3.1 illustrates this.

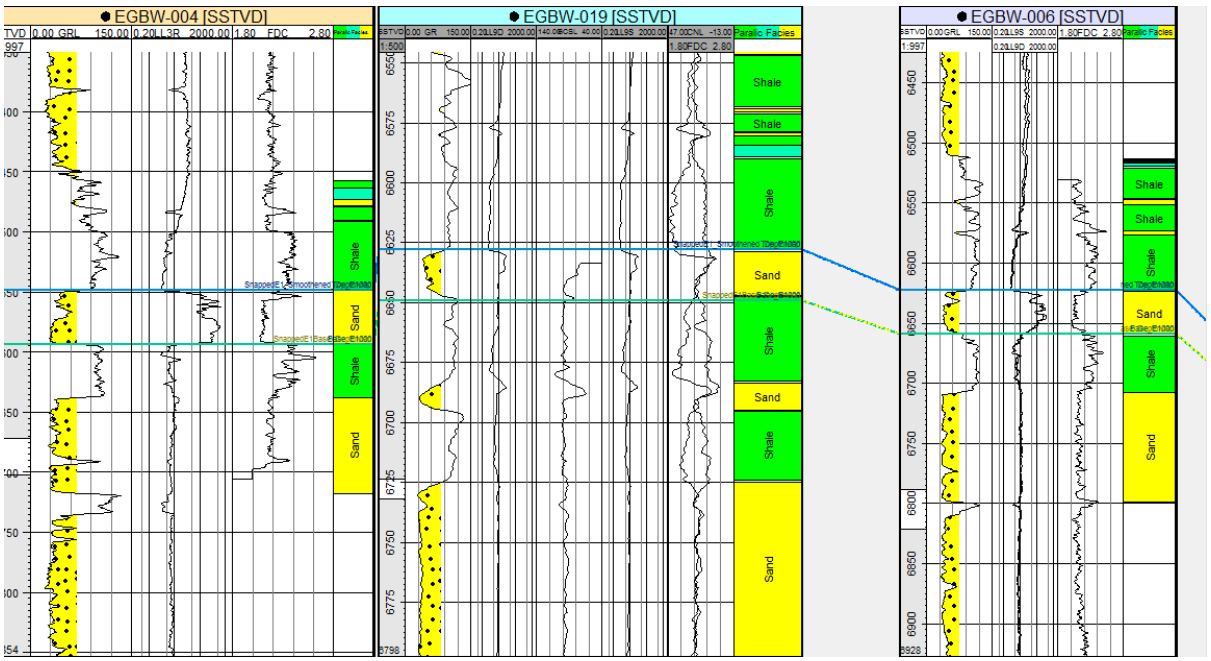

Figure 3.3.3.1: Wireline logs showing the stacking patterns and top-seal.

3.3.3.2 Well Correlation and Flow unit Description:

The correlation shows that the reservoir is of good continuity and generally elongated since it's a barrier bar deposit. Reservoir X generally thins from north to south (i.e. it thins towards the basin) signifying a prograding sequence (Figure 3.3.3.2). The thickness of the flow unit ranges between 3 and 49ft. The implication is that we should move northward or landward to get more sand. Likewise, sand development

was shown to be better at the western flank and get worse as we move eastward. That is, the reservoir pinches out towards the east due to a clay filled channel at the eastern flank. Appendices 3.3.3.2_1 and 3.3.3.2_2 show the well correlation panels indicating sand pinch out towards the south and east. Two different flow units were observed in some wells (wells 9, 16, 18 and 21) separated by shale baffles which can cause vertical permeability barrier in that part of the reservoir.

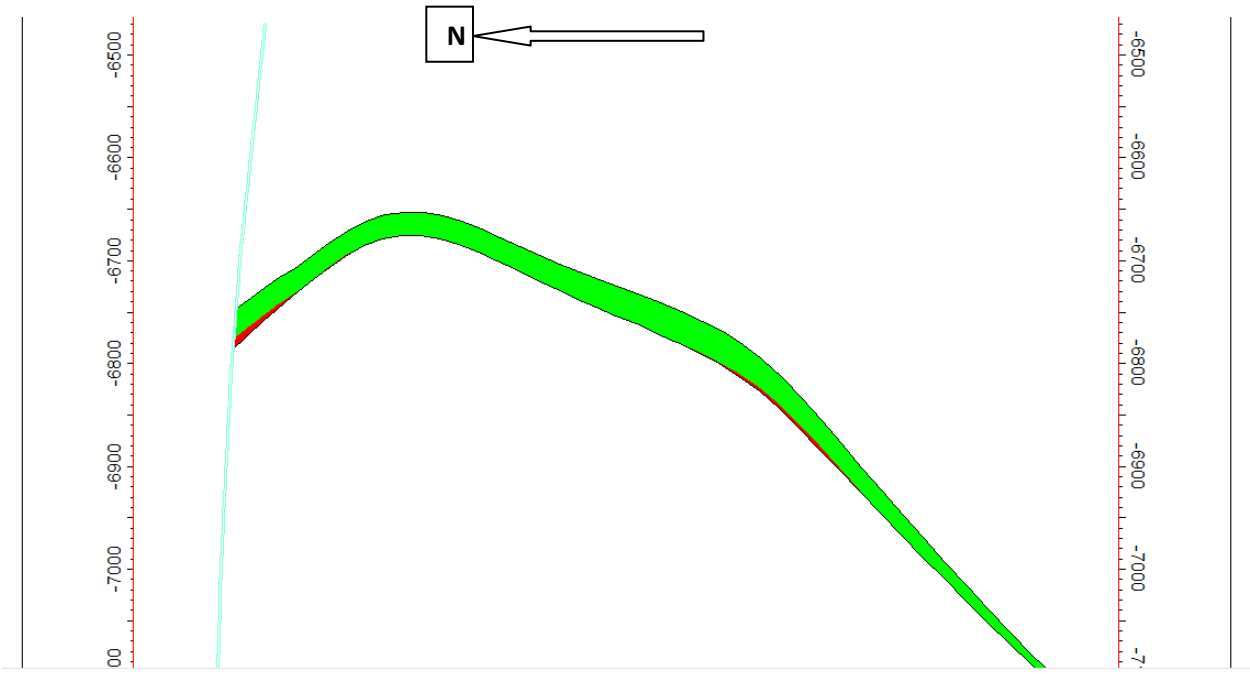

Figure 3.3.3.2: North- South (Inline) Cross-sectional view of Reservoir X

3.3.4 Petrophysical Interpretation

The log data (in LAS format) of all the 21 wells were loaded into Techlog Workstation and used to generate curves. Gamma Ray, Caliper and SP curves were placed in Track 1; Resistivity (Micro resistivity, Shallow,

Medium and deep) curves were placed in Track 2 while Density, Neutron and Sonic curves were placed in Track 3.

3.3.4.1 Log Editing and Normalization

The electronic logs in Techlog were validated with the hard copy logs. This was to ensure the imported log data were not corrupted during data transfer. Logs were checked and depth-matched where necessary. Harmonization of dataset names and assigning to their respective families and units were all done using appropriate Techlog process. The first Gamma Ray log run in each well was used as the primary depth reference. The GR logs were normalized in Techlog using quantile normalization by linear transformation, at 5% and 95% percentiles. The minimum and maximum percentile values (after normalization) were subsequently calibrated to typical sand and shale peak gamma ray readings of 20 API and 140 API, respectively. Well-5 was used as the calibration logs because it has the most consistent signature. Having normalized the GR logs of all the wells, a cut off of 80 was used across the field. Figure 2.3.4.1 depicts the histogram/ statistics of the calibration well log (Well-5). Sonic logs were checked for spikes (which occur as a result of cycle skipping during logging) and were de-spiked where necessary. The corrected and processed logs were used in geological and petrophysical analyses, and in construction of Reservoir X static model.

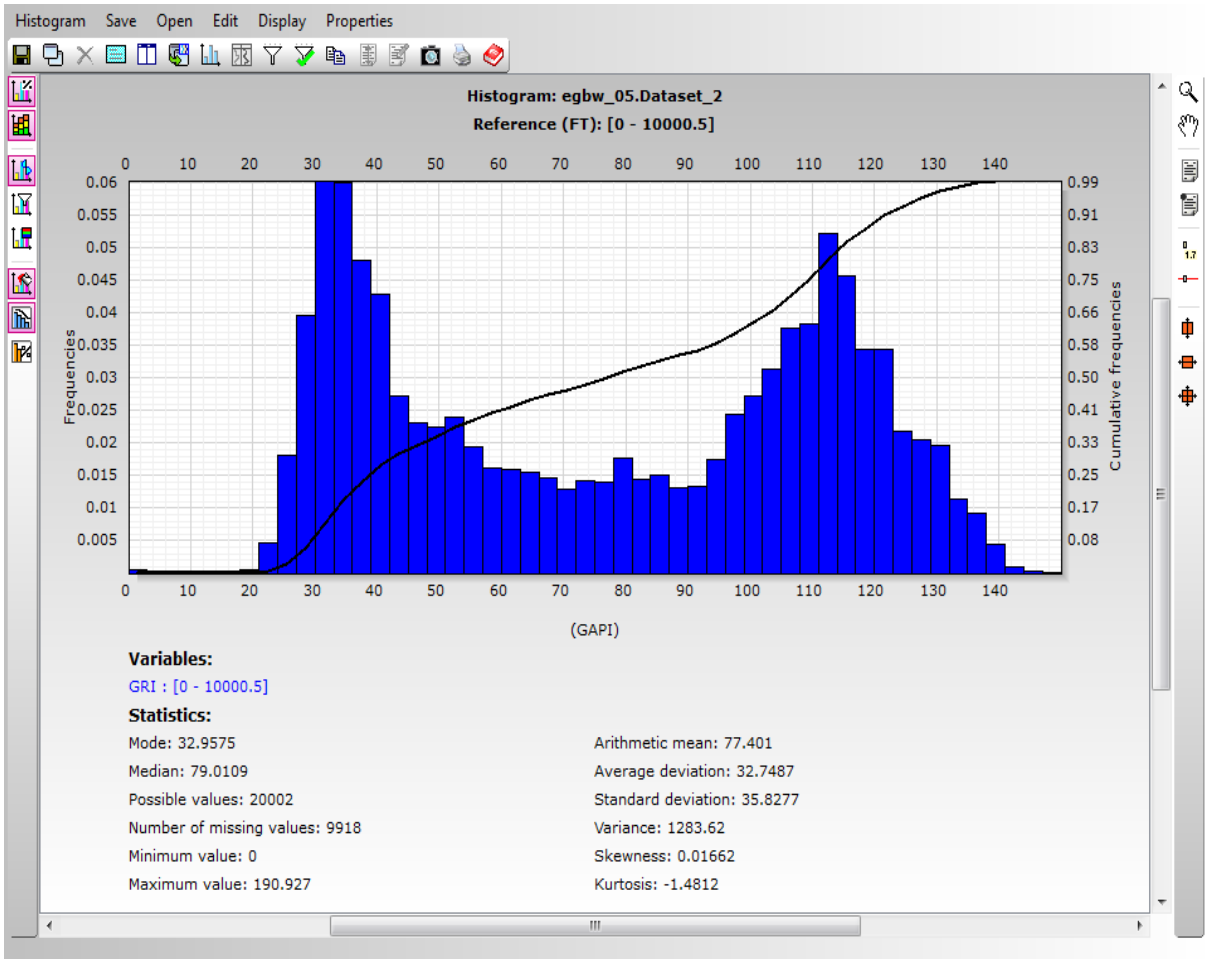

Figure 3.3.4.1: Histogram of well-5 GR log (Calibration log)

3.3.4.2 Qualitative Interpretation of logs

Permeable zones (sands) were differentiated from non-permeable zones using GR, SP and Neutron/Density logs. Based on this, tops and bases of Reservoir X were delineated in all the 21 wells. Table 3.3.4.2 shows the tops and bases of Reservoir X in all the 21 wells.

Hydrocarbon-bearing intervals were discriminated from water-bearing intervals using the resistivity logs (especially deep resistivity). Fluid Contacts (GOC/OUT and OWC/ODT) were therefore inferred from resistivity logs. However, some wells don't have deep resistivity to be

used for contact delineation. Figure 3.3.4.2 shows the fluid distribution across the reservoir.

Fluid typing (oil, gas or water) was done using Neutron/ Density logs. Reservoir X was interpreted as an oil reservoir because there is little separation between neutron and density curves in the reservoir. Gas usually shows high neutron-density separation, mostly referred to as GAS EFFECT.

Table 3.3.4.2: Tops, bases and contacts of Reservoir X

Well	Tops of sand		Bases of sand		Gross thickness(ft)		Contact(TVDSS,ft)	
	MD(ft)	TVDSS(ft)	MD(ft)	TVDSS(ft)	MD	TVDSS	WDT/OUT	OWC/ODT
1	6633.84	6574	6697.84	6638	64.00	64.00	6574(OUT)	6634(ODT)
2	6640.73	6588	6654.73	6602	14.00	14.00	Wet	Wet
3	6703.75	6635	6719.80	6651	16.05	16.00	6638(WDT)	6648(OWC)
4	6761.19	6549	6810.04	6594	48.81	45.00	6549(OUT)	6594(ODT)
5	6692.56	6629	6699.56	6636	7.00	7.00	6634(WDT)	6636(OWC)
6	6689.27	6623	6728.10	6662	39.04	39.00	6624(WDT)	6662(ODT)
7	6813.83	6743	6830.89	6760	17.06	17.00	6747(WDT)	6750(OWC)
8	6630.15	6563	6637.16	6570	7.01	7.00	6567(WDT)	6569(OWC)
9	6649.02	6585	6683.70	6619.11	34.68	34.11	6586(OUT)	6621(ODT)
10	6892.86	6823	6931.93	6862	39.07	39.00	6827(WDT)	6831(OWC)
11	6837.68	6768	6869.71	6800	32.03	32.00	6771(WDT)	6776(OWC)
12	6634.63	6577	6640.65	6583	6.02	6.00	6578(WDT)	6583(ODT)
13	6986.59	6915	6992.59	6920	6.00	5.00	6918(WDT)	6920(OWC)
14	6733.74	6669	6758.77	6694	25.03	25.00	6671(WDT)	6676(OWC)
15	6921.59	6806	6931.17	6815	9.58	9.00	Wet	Wet
16	6783.94	6717	6810.95	6744	27.01	27.00	No data	No data
17	6970.73	6895	6990.77	6915	20.04	20.00	6899(WDT)	6905(OWC)
18	6698.06	6635	6734.07	6671	36.01	36.00	6636(WDT)	6641(OWC)
19	6694.62	6628	6715.63	6649	21.01	21.00	6630(WDT)	6639(OWC)
20	7391.40	6930	7397.95	6936	6.55	6.00	6932(WDT)	6936(ODT)
21	7265.10	6911	7330.79	6969	65.69	58.00	6914(WDT)	6962(OWC)

Fluid distribution and delineation

An integrated approach was used to establish fluid contacts. Since there is no RFT data from the reservoir, the fluid contacts seen by wells were taken as the actual contacts in the reservoirs. The contacts in the wells were identified using the logs (resistivity and density – neutron), and delineated by log correlation and contour mapping. The figure below (3.3.4.2) depicts the fluid distribution in the reservoir.

Table 3.3.4.2: Summary of fluid contacts based on logs

Sand	Well	OUT/ WDT	OWC/ ODT
Reservoir X	1	6574(OUT)	6634(ODT)
	2	Wet	Wet
	3	6638(WDT)	6648(OWC)
	4	6549(OUT)	6594(ODT)
	5	6634(WDT)	6636(OWC)
	6	6624(WDT)	6662(ODT)
	7	6747(WDT)	6750(OWC)
	8	6567(WDT)	6569(OWC)
	9	6586(OUT)	6621(ODT)
	10	6827(WDT)	6831(OWC)
	11	6771(WDT)	6776(OWC)
	12	6578(WDT)	6583(ODT)
	13	6918(WDT)	6920(OWC)
	14	6671(WDT)	6676(OWC)
	15	Wet	Wet
	16	No data	No data
	17	6899(WDT)	6905(OWC)
	18	6636(WDT)	6641(OWC)
	19	6630(WDT)	6639(OWC)
	20	6932(WDT)	6936(ODT)
	21	6914(WDT)	6962(OWC)

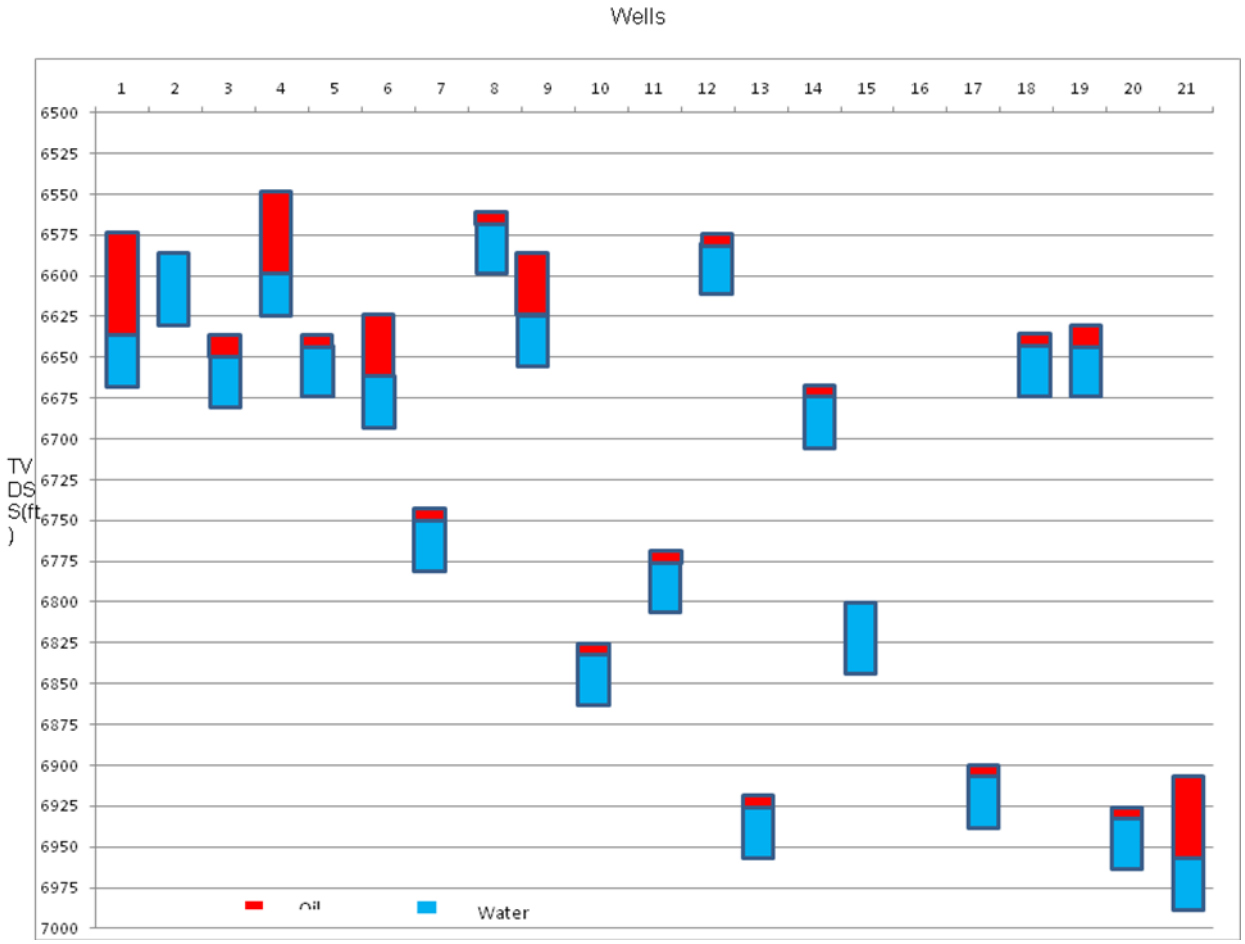

Figure 3.3.4.2: Fluid distribution plot in Reservoir X

3.3.4.3 Quantitative Evaluation from Logs

Edited well logs were used in evaluating rock properties in Techlog software.

Shale Volume (V_{sh}) Determination

Shale volumes were evaluated using both GR and Neutron/ Density curves. Since both results were close or similar, all the other shale volumes were calculated using GR curves by applying 'Larionov Tertiary Rock' method. GR curves were used in the evaluation because all the 21 wells have GR curves; very few of them have Neutron/ Density pair. Figure 3.3.4.3 (a) compares V_{sh} from GR to that from Neutron/ Density. Larionov method was chosen because it goes well with Tertiary Niger Delta rocks and is widely used in the industry. The applied equations[19] are shown below:

$$GR_{index} = \frac{GR - GR_{matrix}}{GR_{shale} - GR_{matrix}}$$

- Larionov Tertiary rocks method:

$$VSH = 0.083 * (2^{(3.7 * GR_{index})} - 1)$$

Where GR is the GR log reading in the zone of interest;

GR_{matrix} is the GR log reading in 100% matrix rock;

GR_{shale} is the GR log reading in 100% shale

GR_{index} is the Gamma Ray index

VSH is the Volume of Shale

Reservoir delineation (reservoir vs. non-reservoir) was done by applying cut-offs of 75% on evaluated volume of shale, Vsh.

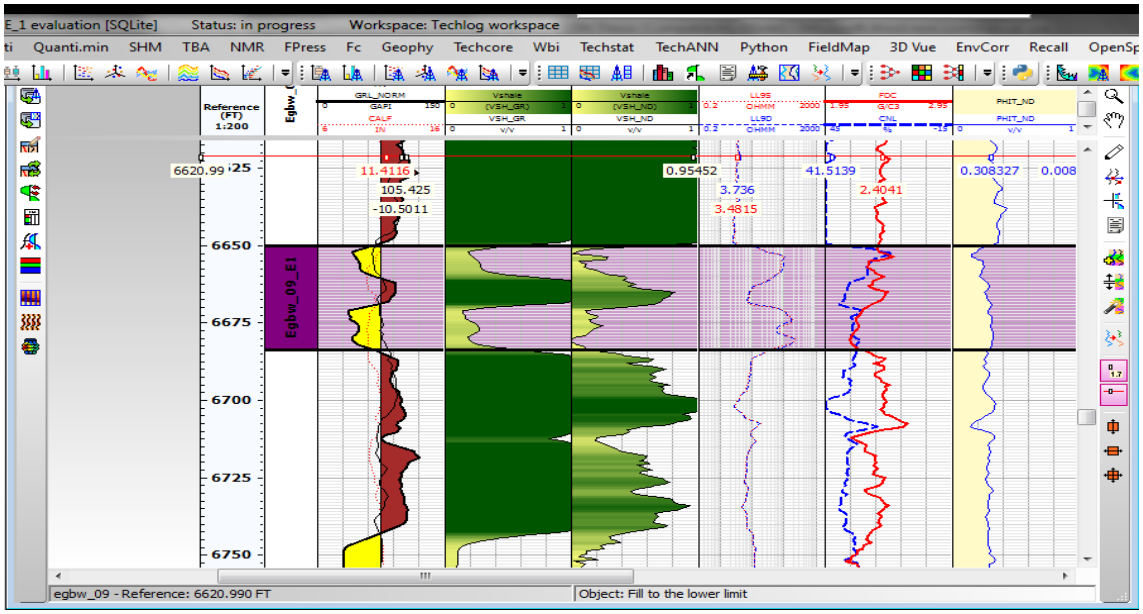

Figure 3.3.4.3 compares V_{sh} from GR to that from Neutron/ Density curves

Porosity Determination

Total porosity was estimated majorly from density logs using a *rho-matrix* value of 2.65 gm/cc and *rho-fluid* value of 0.808 gm/cc from PVT data. The effective porosity was then deduced by introducing shale volume into the equation. The deduced effective porosities were validated using the core data from well 21 in a deeper reservoir. The effective porosities from Techlog compare well with core porosity. Equations[19] below were used in the computation. Porosity ranges between average of 9% and 36.6% in the wells across the reservoir.

$$\phi_T = \frac{\rho_{ma} - \rho_B}{\rho_{ma} - \rho_f} \qquad \phi_{T_{sh}} = \frac{\rho_{ma} - \rho_{sh}}{\rho_{ma} - \rho_f}$$

$$\phi_E = \phi_T - (\phi_{T_{sh}} * VSH)$$

Where P_{ma} is the Matrix Bulk density,

P_{sh} is the Shale Bulk density,

P_f is the fluid density (density log reading in 100% water),

P_B is the Bulk density (density log reading in the zone of interest),

VSH is the Volume of shale,

Φ_T is the Total porosity in the zone of interest,

$\Phi_{T\,sh}$ is the Total porosity in shale,

Φ_E is the Effective porosity in the zone of interest.

Water Saturation Determination

Water saturation was estimated from Archie's and Modified Simandoux equations. In order to estimate Water saturation from any of the methods, Formation water resistivity (R_w) needs to be estimated. R_w is usually estimated in a clean water-bearing interval (water leg) using deep resistivity reading, Sw=1 and the computed porosity (Φ). However, deep resistivity (R_t) and Φ (porosity) may vary widely within the water-bearing zone making it difficult to get single values of R_t and Φ. For this reason, a double logarithmic plot of R_t against Φ is generally used to estimate R_w. R_w is the intersection on the R_t axis of a best fit line produced from the plot. The plot is

commonly referred to as 'Picket plot'. In this study, a Picket plot was used in estimating R_w from water-bearing interval. Therefore, S_w (Archie's equation) was then estimated using the computed R_w and Φ; local correction factor or tortuosity factor (a) of 1 was assumed; saturation exponent (n) of 2 was also assumed; and cementation exponent (m) of 1.80-1.82. These values commonly apply to reservoirs in this field. R_w ranges from 0.57 to 1.5 ohm.m across the reservoir. Figure 3.3.4.3 (b) shows the Picket plot in well 4. Other wells' Picket plots are showcased in the appendix.

Effective porosity saturation was estimated using Simandoux equation by taking cognizance of Volume of shale (V_{sh}). The equations[19] used are highlighted below:

$$SW = \left(\frac{a * R_w}{R_t * \phi_t^m} \right)^{\frac{1}{n}}$$ - Archie's equation

$$\frac{phi_e^m}{a * R_w * (1 - V_{sh})} * S_w^2 + \frac{V_{sh}}{R_{sh}} * S_w - \frac{1}{R_t} = 0$$

$$BVWE = SW_e * \varphi_e$$ - Modified Simandoux equations

Note that $S_h = 1 - S_w$

Where S_w is the Water saturation

a is the tortuosity factor

R_w is the formation water resistivity

R_t is the formation resistivity

n is the saturation exponent

m is the cementation exponent

Φ_t is the calculated porosity

Phi_e or Φ_e is the calculated effective porosity

V_{sh} is the calculated Volume of shale in the zone of interest

R_{sh} is the resistivity log reading in 100% shale

BVWE is the effective bulk volume of water

S_h is the hydrocarbon saturation

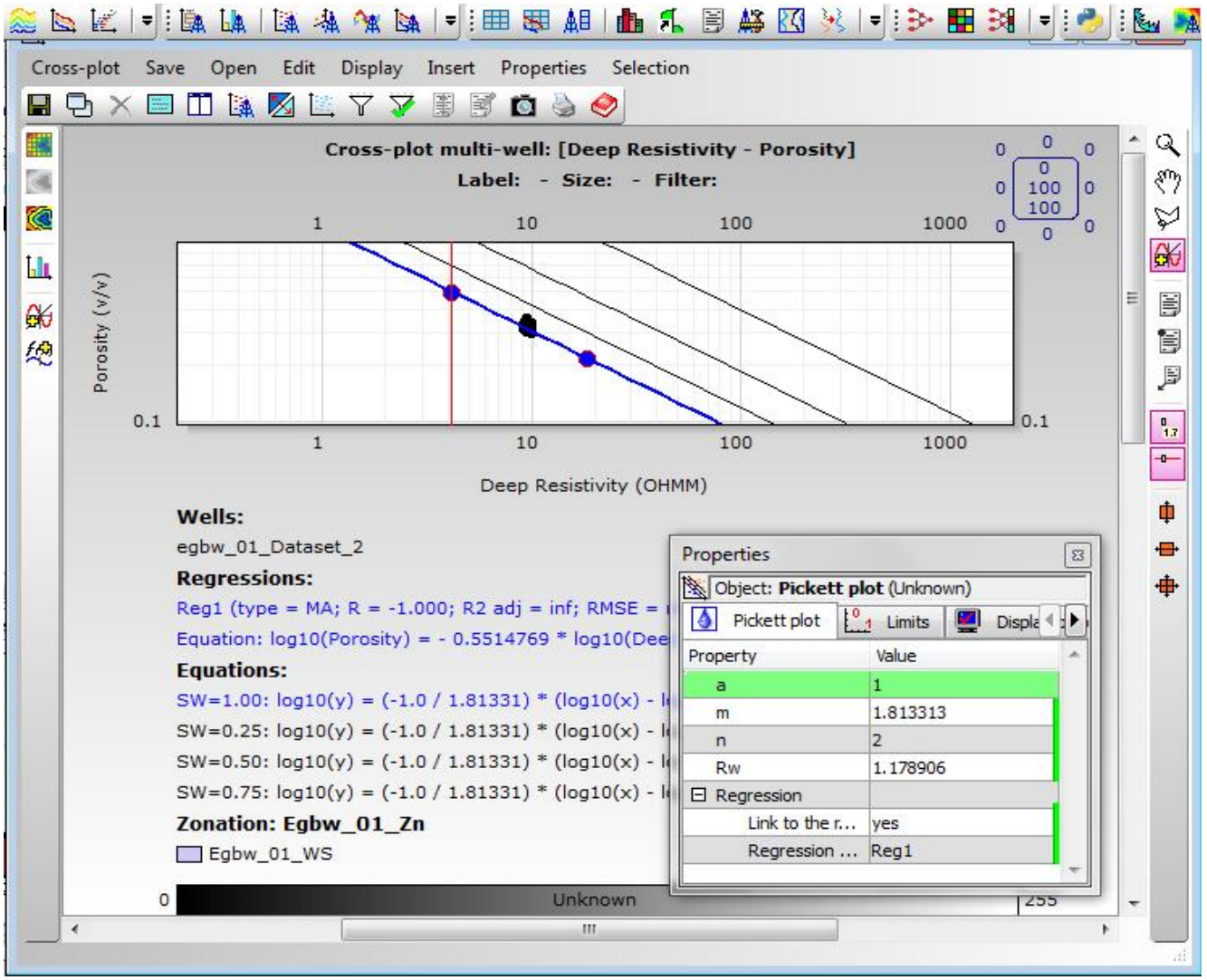

Figure 3.3.4.3_1: Picket plot for well-1 indicating petrophysical properties

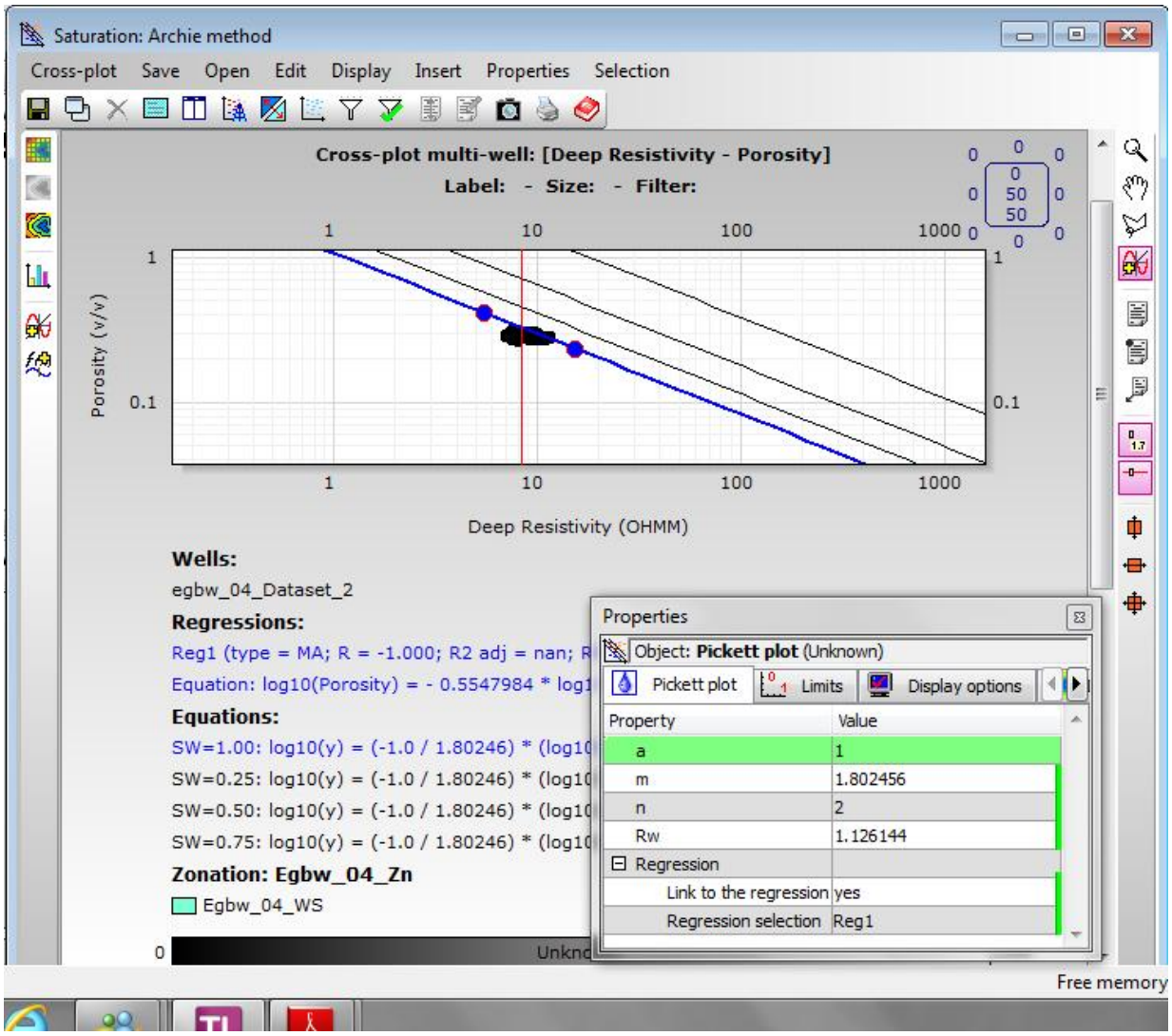

Figure 3.3.4.3(b): Well-4 Picket plot indicating petrophysical parameters

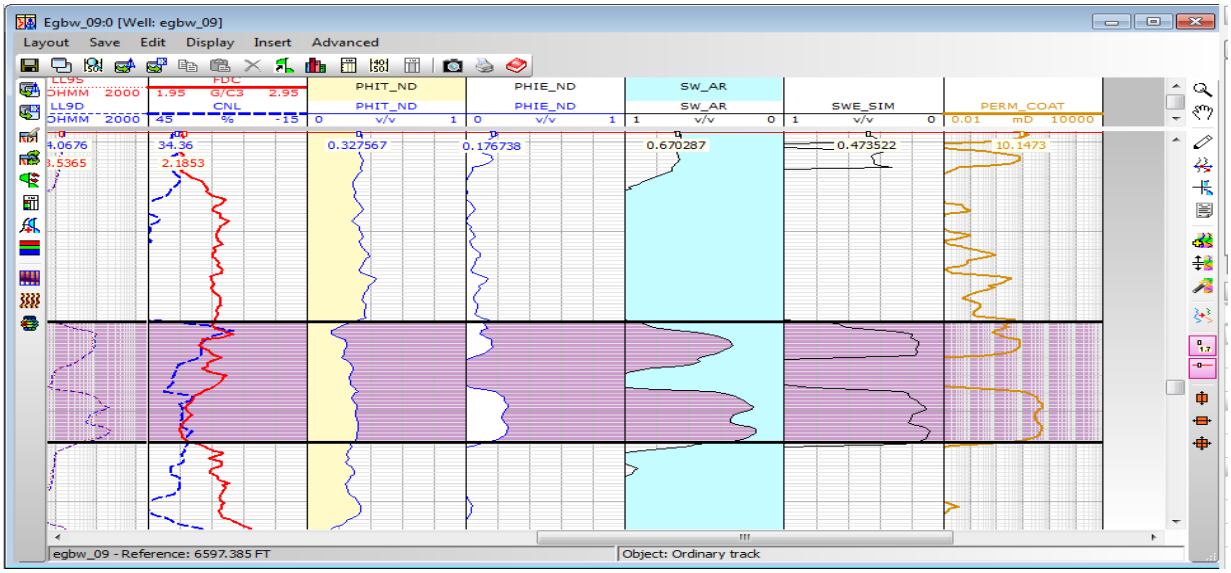

Figure 3.3.4.3 (c): Porosity and Saturation logs in well 9

Permeability estimation

Since core data was not available for Reservoir X, empirical correlation was used to predict permeability in the reservoir. Coates method (1981) was employed in this study for that purpose. The equations are stated below[19]:

- Clean zones

$$PERM = kc * PHIe^4 * \left(\frac{1 - Sw}{Sw}\right)^2$$ (Coates 1981)

- else

$$PERM = kc * PHIe^4 * \left(\frac{PHIt - PHIe * Sw}{PHIe * Sw}\right)^2$$

Where PERM or K is the Permeability in millidarcies

k_c is Coates' constant

PHIe is the effective porosity

PHI_t is the total porosity

S_w is the irreducible water saturation

Analogue Core data from a deeper reservoir in this same field was however used to validate the estimated permeability and a wide variance was discovered. Permeability from core of the deeper reservoir ranges between 50md to 5000md as against estimated permeability that ranges between 1md and 150md. The worst-case permeability values for Reservoir X should be 50md to 5000md going by core data analyses. Therefore, the estimated permeability was discarded and analogue core permeability was applied in permeability modelling during static modelling process.

Reservoir Pressure, Temperature and PVT Data

Analysis of the pressure in the reservoir showed that the initial average reservoir pressure (static) was 2915psig while the flowing bottom-hole pressure was 2765psig. The current average BHP (pressure) is about 2700psig. Well head pressure of well-4 was 795psig.

The initial reservoir temperature (average) was 181^{o}F.

The bubble point pressure at reservoir temperature was 1750psig; the solution GOR was 690 cf/bbl; formation volume factor was 1.45

RB/STB; viscosity and specific gravity at reservoir condition were 0.4cp and 0.622 respectively while API gravity was around 43.6^0API.

Reservoir Sums and Averages

Cut-off values were established for the following answer curves based on experience in the Niger Delta and the general data trend: volume of shale (V_{sh}), effective porosity (Phi_e) and water saturation (S_w). The cut-off values adopted are 0.5, 0.10 and 0.7 respectively. Pay zones were delineated on the basis of these cut-off values.

Sums and averages were determined using the previously defined net reservoir counts. Based on log interpretation, curves were constructed. These curves were used as discriminators to calculate sums and averages for the reservoir

The results of the computed sums and averages for the reservoir is presented in Table 3.3.4.3

Gross Rock Volume Computation

This was computed using Reservoir X 2D map in Petrel. It was computed as the volume within top surface and base surface while respecting the Oil water contact (using the 'volume above surface' calculation in Petrel). The GRV was computed to be 8.90689E+8 Barrels while the area was 3644.66 acre.

Table 3.3.4.3: Petrophysical Sums and Averages for Reservoir X

Well	Sand	Top (MD,ft)	Base (MD,ft)	Gross (MD,ft)	Net (MD,ft)	NTG	Av_Eff Φ	Av_Eff. Sw	Av_Vsh	Av_Total Φ	Av_Sw (Darcie)	Av_K, md)	Av-Core K(md)
1	X	6635	6698	63	61	0.968	0.366	0.177	0.158	0.375	0.267	205.7	4346
4	X	6761	6810	49	48.5	0.99	0.287	0.148	0.125	0.306	0.231	85.286	2113
6	X	6689	6726	37	35.5	0.959	0.318	0.225	0.178	0.345	0.357	116.93	3213
7	X	6813.83	6821.17	7.34	3	0.409	0.09	0.92	0.31	0.137	1	0.863	60
8	X	6630.15	6637.16	7.01	0	0	0	0	0	0	0	0	5
9	X	6650	6683	33	22.5	0.682	0.197	0.19	0.25	0.272	0.322	23.295	584
11	X	6837.68	6873.43	35.75	27.5	0.769	0.231	0.188	0.154	0.254	0.802	40.394	1010
12	X	6634	6641	7	3	0.429	0.093	0.589	0.364	0.202	0.922	1.603	93
14	X	6734	6759	25	23.5	0.94	0.192	0.857	0.195	0.251	0.906	19.007	486
17	X	6972	6992	20	13.5	0.675	0.187	0.772	0.28	0.271	0.957	16.056	404
18	X	6699	6736	37	29	0.784	0.225	0.871	0.189	0.281	0.973	32.816	822
19	X	6695	6715	20	17.5	0.875	0.161	0.848	0.201	0.192	0.994	12.689	321
20	X	7392	7396	4	2	0.5	0.034	0.668	0.381	0.092	1	0.057	9
21	X	7265	7330.79	65.79	28	0.426	0.188	0.816	0.212	0.218	0.895	29.12	743

Average effective Porosity= 0.1976
Average effective water saturation= 0.559
Average Volume of shale= 0.231
Average Net to Gross= 0.724
Average Permeability= 1092.6 md

3.3.5 3D Static Reservoir Modelling

Geological modelling or Static modelling generally involves bringing together the stratigraphic, structural and property models into one single model. In other words, it involves populating the reservoir architecture (Structure and Stratigraphy) with rock properties. A cell size of 114 x 72 x 2 was selected in building the 3D Grid, being small enough to capture all the reservoir details. Total number of 3D grid cells came up to 16416.

3.3.5.1 Stratigraphic Modelling

This has already been carried out earlier on, using log correlation to delineate the reservoir architecture and continuity. A field and reservoir wide (for the modelled levels) correlation exercise was carried out as a means of validating the reservoir tops and bases, to ensure consistency of the reservoir picks, and to correlate the reservoir. This was done within the established sequence stratigraphic framework.

3.3.5.2 Structural Modelling

This (in Petrel) involves Fault Modelling, Pillar Gridding and Horizon Making.

Fault Modelling involved definition of the various faults in the model which formed the basis for generating the 3D Grid. This field is bounded to the north by an east-west trending synthetic growth fault

and to the west by another synthetic fault which links the major fault at the northern part of the field (Figure 3.3.5.2_1). These two faults were modelled, defining their lateral shape and geometries. The modelled faults and the horizon structure formed the basis of the 3D structural framework in Petrel. The faults used in this study were named Major and Minor faults respectively. The faults were built using key pillars and joints of these key pillars formed the fault plane. These faults defined breaks in the 3D grid.

Having modelled the faults, the next thing was to generate the 3D grid from the fault model. This is called Pillar Gridding in Petrel.

Horizon making involved building of vertical layering in the grid (model) generated during Pillar Gridding. Make zone process in Petrel was then employed in zoning the reservoir model into flow units. After zoning, Gas-Oil Contact and Oil-Water Contact were then specified in the model (Appendix 3.3.5.2_2).

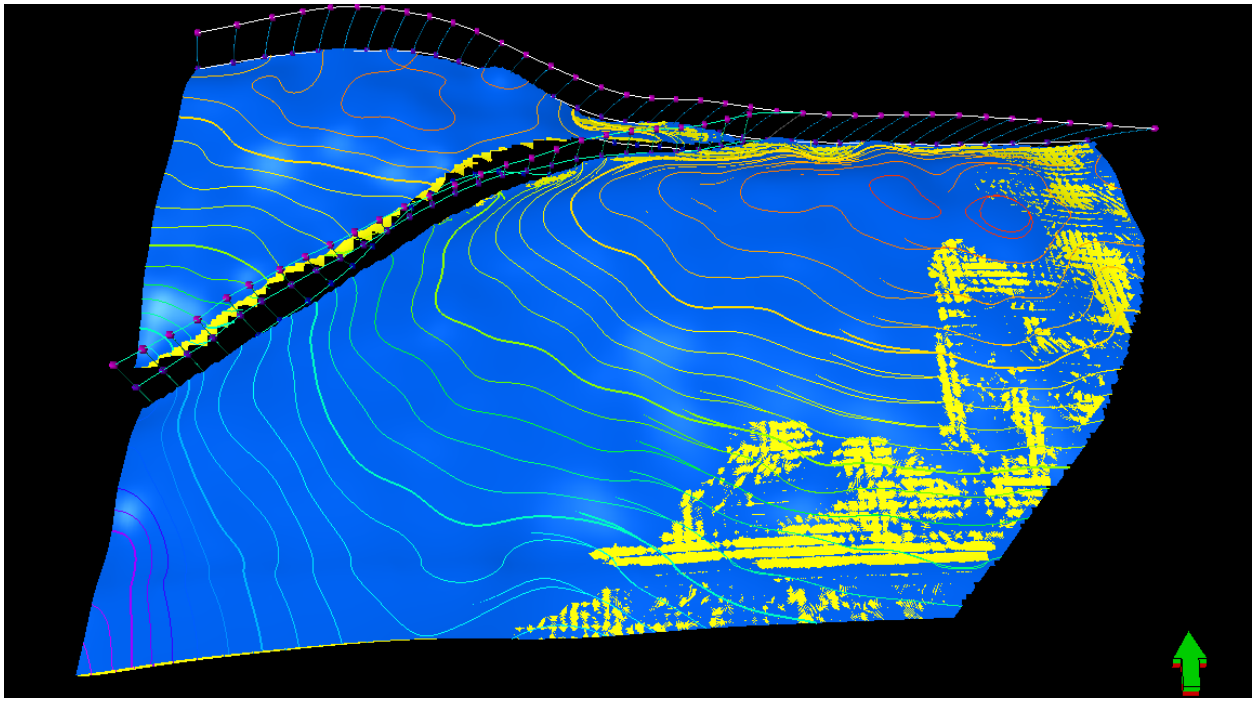

Figure 3.3.5.2_1: Reservoir X surface showing the modelled faults

3.3.5.3 Property Modelling

This is the process of filling the cells of the grid with discrete (facies) or continuous (Petrophysical) properties including facies, Porosity, saturation, Net to gross and Permeability. The first thing was to import into Petrel all the property logs prepared in Techlog (validated with analogue core data). These logs were then scaled up. Scale up of well logs involves sampling property values from well logs into the 3D grid in such a way that each grid cell will have a single value for each property. Having assigned property values (both facies and petrophysical) to each grid cell at well locations, the next thing was to distribute properties in the inter-well grid cells in order to realistically preserve the heterogeneity of the studied reservoir. This was achieved in Petrel by first performing Data analysis and then

modelling the properties. Data analysis was done in order to identify trends in the data; remove the identified trends; apply transformations on the residual property data, and eventually define Variogram model that describe the data and serve as input into property modelling process. Variogram map for each property was generated to identify anisotropy and infer the direction of maximum data continuity before generating each property's sample variogram and variogram model. It is these Variogram models that were used in populating properties in 3D grid using various algorithms during modelling of properties. A variogram is simply a description of the spatial variations in a reservoir property. The two major Geostatistical methods (Deterministic and Stochastic) were applied in modelling the properties. Both Kriging algorithm (deterministic) and Sequential Gausian Simulation algorithm or Sequential Indicator Simulation (stochastic) were applied in geostatistically assigning properties and compared.

Figures 3.3.5.3 (a), (b) and (c) show the variogram map, Variogram model for porosity and Porosity model (using Sequential Gausian Simulation algorithm) respectively.

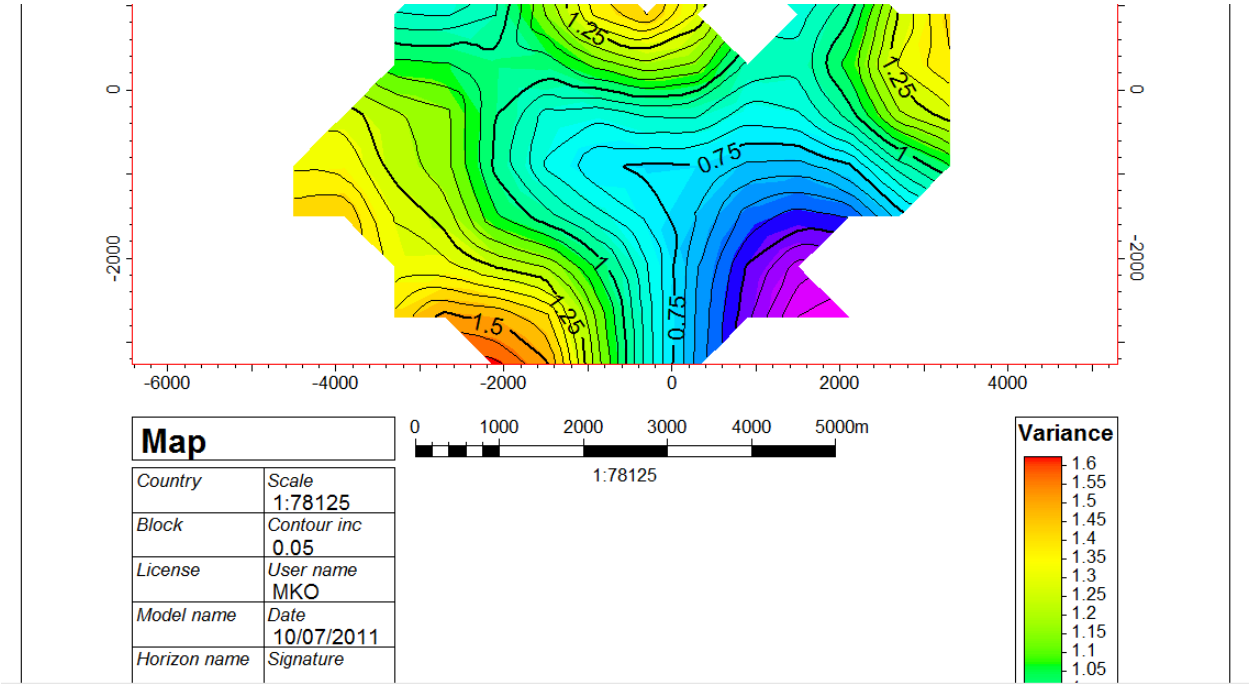

Figure 3.3.5.3 (a): Variogram map for Porosity

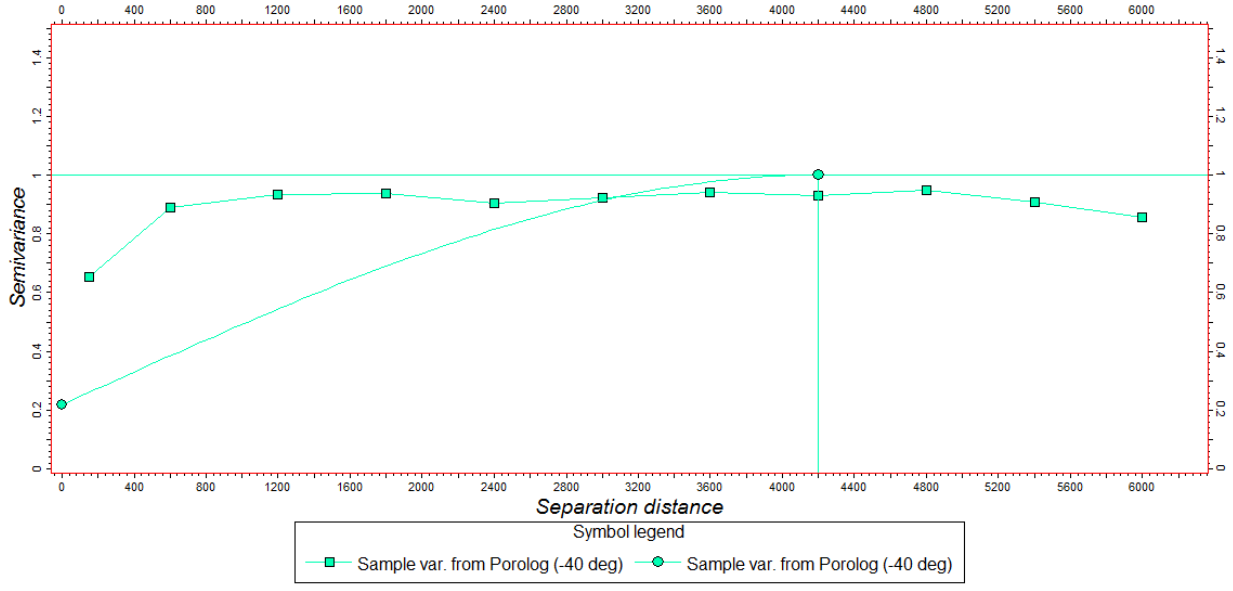

Figure 3.3.5.3 (b): Sample Variogram and Variogram model from Porolog

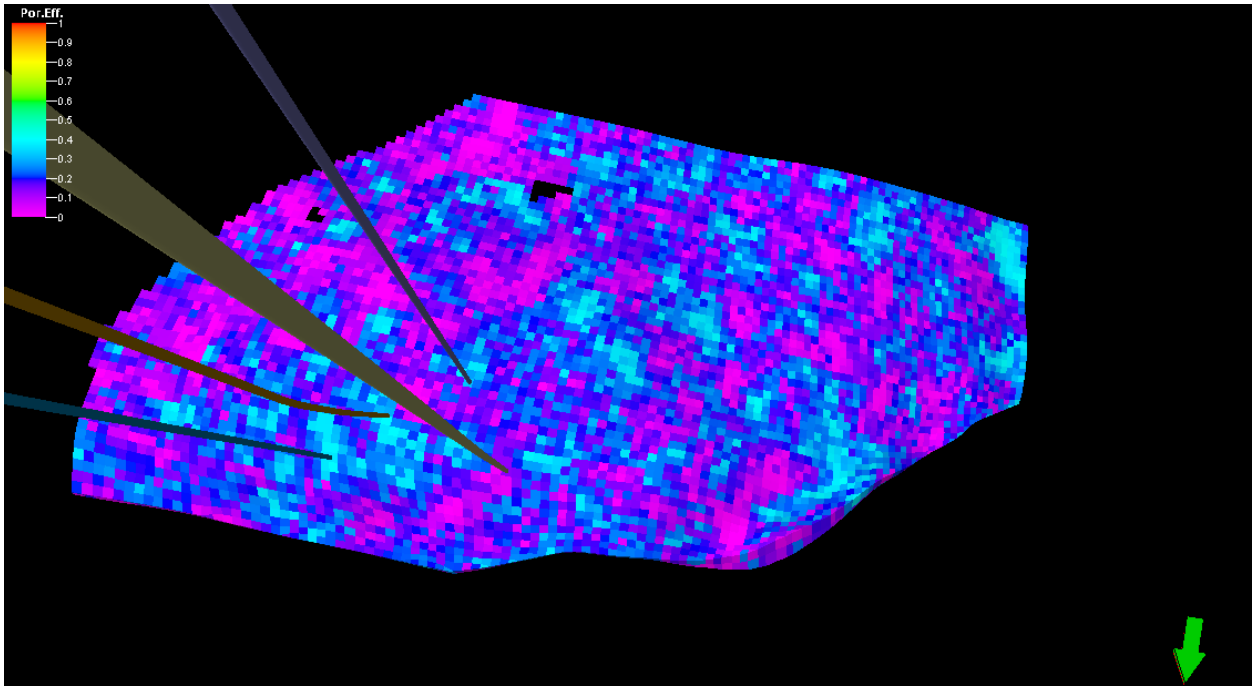

Figure 3.3.5.3 (b): Porosity model (from SGS) for Reservoir X

The products of the property distribution within the 3D grid are the property models: Facies, Porosity, Water Saturation, NTG and Permeability models. Porosity model for reservoir X using Sequential Gausian Simulation algorithm is shown in the figure above. The other property variogram maps and models are highlighted in appendices 3.3.5.3_1-5.

3.3.6 Oil volume Estimates

3.3.6.1 Gross Rock Volume Computation

This was computed using Reservoir X 2D map in Petrel. It was computed as the volume within top surface and base surface of the reservoir while respecting the Oil water contact (using the 'volume above surface' calculation in Petrel). The GRV was computed to be 4.29893E+8 Barrels (55,413 acre-ft) while the area was 2450.8 acre.

The computed GRV was combined with the other petrophysical parameters to estimate the STOIIP and UR as represented by the equation below[19]:

$$N = \frac{7758 \times GRV \times NTG \times \phi \times (1 - S_w)}{B_O}$$

where,

N = stock-tank oil initially in place expressed in stock-tank barrels, stb

7758 = conversion factor: acre-ft to barrels

GRV = gross rock volume, expressed in acre-ft

NTG = net to gross ratio, expressed as fraction

φ = average reservoir rock porosity, expressed as a fraction

S_w = average reservoir rock water saturation, expressed as a fraction

B_o = initial oil formation volume factor, expressed in reservoir barrels per stock-tank barrel.

3.3.6.2 Static Model Volume Estimates

Estimates of Oil initially in place (OIIP) within Reservoir X 3D grid were done using two different scenarios:

OIIP was estimated in PETREL from the rock and property models earlier on generated. These were combined with the B_{oi} (Formation volume factor) and the actual recovery factor (RF) to estimate the

STOIIP (Stock Tank Oil Initially in Place) and UR (Ultimate Recovery).See Table 3.3.6.2

The second scenario involved estimate of OIIP within the 3D grid using the petrophysical averages. Reservoir average porosity of 0.2, average S_w of 0.56, and average NTG of 0.72 were combined with B_{oi} and RF to estimate the STOIIP and UR of the reservoir. Table 3.3.6.2 presents the comparisons among the various volumes.

UR= N * RF

Where,

UR = Ultimate Recovery, STB

N = STOIIP, STB

RF = Recovery factor or Recovery Efficiency, %

RF was initially estimated from Guthrie and Greenberger Correlation for water-drive sandstone reservoir[20] and compared with the Actual Recovery Factor:

$E_R = 0.114 + 0.272\log k + 0.256S_w - 0.136\log \mu_0 - 1.538\,\phi - 0.0003h$

where,

E_R= Recovery Efficiency, %

k= Permeability, md

S_w= Water Saturation, %

μ_0= Oil viscosity, cp

$\phi =$ Porosity, %

Actual RF till date= Cumulative Production till date
STOIIP

Table 3.3.6.2: Comparisons among volumes from various sources

Reservoir	Method	GRV(acre-ft)	Bulk Volume(acre-ft)	STOIIP(MMSTB)	UR(MMSTB)
X	2008 ARHR(2D)[5]	46,944		44.9	23.8
X	2D Mapped volume(this study)	55,412			
X	3D Static model(using property averages)		55,298	52	36.4
X	3D Static model (using property models @OWC=6656 & RF=50%)		55,298	15	7.5
X	3D Static model (using property models @OWC=6936 & RF=70%)		153,390	35	24

3.3.7 Uncertainty and Sensitivity Analyses

Reserves estimation is never complete until it is accompanied by a quantitative statement of its uncertainties. The essence of the uncertainty analysis is to measure the effect of variations on the STOIIP (base case). The variations can be due to: Structural uncertainty, velocity model uncertainty, fluid contact uncertainty,

petrophysical and facies models uncertainties etc. Petrel uses Monte Carlo Simulation which was used to stochastically determine the probabilistic spread of Reservoir X STOIIP. The input data were the base case models of the reservoir 3D grid and property combined with their respective distribution types. Five realisations were generated from which the low, medium and high cases were realized. The result was a probabilistic distribution of the STOIIP: P_{10}, P_{50} and P_{90} which were taken as the low, medium and high case STOIIPs respectively. The results of the uncertainty analysis are shown in Appendix 3.3.7

Sensitivity analysis was also done to investigate the relative importance of each uncertain parameter on the STOIIP. It was achieved by varying all the uncertain parameters successively and separately while keeping the remaining ones constant. The results showed that the STOIIP is most sensitive to the oil-water contact.

The figure below shows the probabilistic spread of STOIIP.

Table 3.3.7: Summary of STOIIP estimation for Reservoir X

Sand	Oil Volume, STOIIP (MMSTB)			
	Stochastic			Deterministic
	P_{10}	P_{50}	P_{90}	
	23.15	34.76	40.45	35

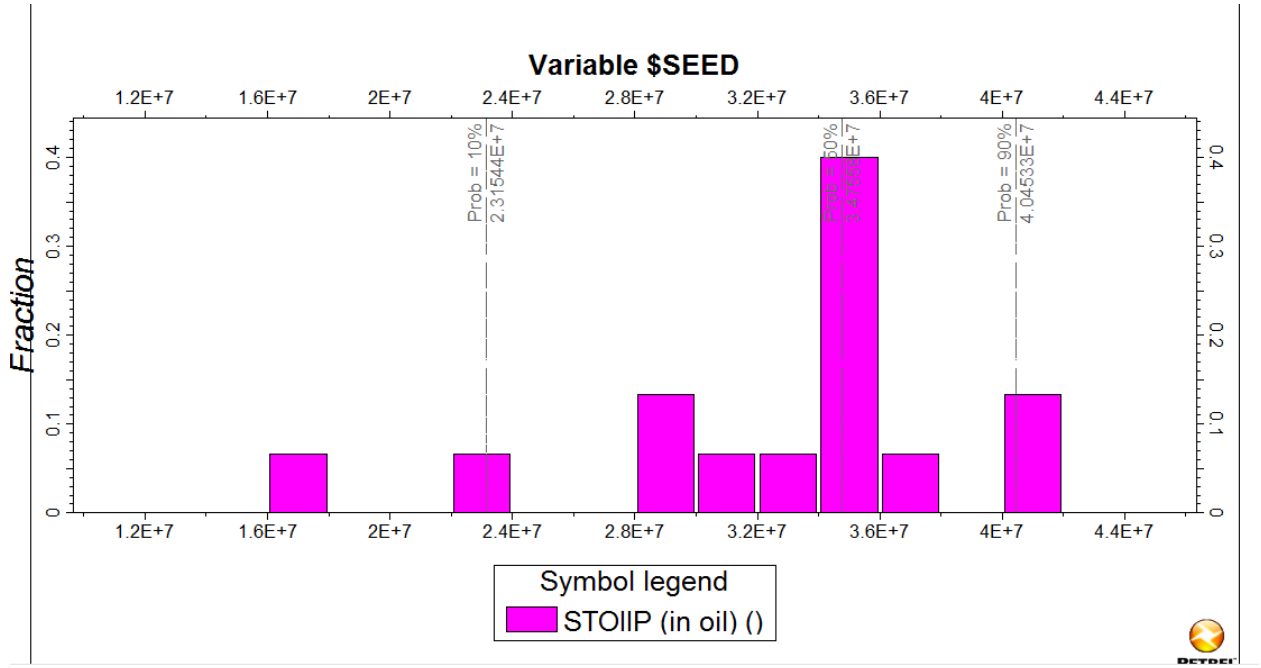

Figure 3.3.7: Probabilistic spread in STOIIP

CHAPTER 4

DISCUSSION AND ANALYSES OF RESULTS

4.1 Structural and Stratigraphic

The model reveals that the reservoir is a rollover anticline with dip closure to the south, east and west then bounded by growth faults to the north and north-west located on the footwall of the major (northern) growth fault. The major (regional) growth fault is an elongate east-west trending fault that assisted the reservoir dip closure in trapping the reservoir oil.

The paleoreconstruction indicates that the reservoir sedimentary setting is predominantly deltaic (paralic facies) and comprises Shoreface/ barrier bar sand deposits (since the GR log signature generally coarsens upward) which suggests that was the position of shoreline/ beach at that time. The sequence stratigraphic analyses revealed that the reservoir exists within Lowstand Systems Tract and that the reservoir was bounded on top by field-wide correlatable marine shales corresponding to regional flooding surface which serves as the top-seal for oil trapping in the reservoir. Well correlation shows lateral continuity of this sand (typical of barrier bar deposits) which pinches out to the southern and eastern part and implies that the reservoir producibility will be poor towards the south due to poor sand development. Hence, there are intra-reservoir heteroliths in some parts of the reservoir as observed in some wells.

4.2 Reservoir Properties

Reservoir properties (especially porosity, permeability and Net to Gross) are generally good except in the southern and eastern part of the reservoir where a pronounced heterogeneity/ variability exists. The average effective porosity ranges between 9 and 37% while the core permeability ranges between 5 and 4300md which is expected because reservoirs in Niger Delta basin are generally unconsolidated and have moderate to high porosity and permeability. NTG ranges between 5 and 99% which support the fact that the reservoir's environment of deposition is barrier bar/ shoreface. Water saturations in wells 1, 4, 6 and 9 are very good ranging between 5 and 15% while very poor in some other wells as high as 98%. The reservoir temperature is about 181^0F circa which shows that the reservoir exists within the "oil window". The pressure data indicates that the reservoir is an undersaturated reservoir with good API gravity and viscosity. The performance plot indicates that the reservoir drive mechanism is water drive (Fig 2.1.7) which justifies while the recovery factor of the reservoir can be as high as 70%. From the plot, the reservoir pressure is fairly constant and the wells completed on it had produced a lot of water leading to shutting-in of some of the wells. As at 1/1/2011, the reservoir had produced around 20MMSTB corresponding to almost 60% recovery factor (RF). This means 93,000bbls of oil was produced for each drop in psi because of almost 1:1 voidage replacement ratio (VRR).

4.3 Fluid Distribution

Pressure and log data indicate that the only hydrocarbon in the reservoir is oil (because it's undersaturated) while the contact analyses (using logs) suggests that the deepest initial Oil-Water contact (OWC) in oil wells is 6936ft TVDSS and the Shallowest Known Oil(SKO equivalent to GOC) is 6550ft TVDSS. This forms the reason why 6936ft and 6550ft were used as OWC and OUT respectively. This is even conservative as OUT indicates that there is still oil potential up-dip the reservoir. Nevertheless, absence of capillary pressure data to accurately validate the initial contacts represents a major uncertainty in estimating the reservoir STOIIP and reserves.

4.4 Geostatistical/ 3D Modelling

Having established reservoir properties at the well locations, geostatistical algorithms were employed to statistically distribute properties in the inter-well spaces in the reservoir. Variogram maps for the properties were generated. Variogram map is used to identify anisotropy in the properties and infer the direction of maximum continuity and anisotropy. Ellipsoidal shape in the map usually signifies anisotropy. From the variogram map in figure 3.3.5.3a, porosity is fairly isotropic in all directions due to absence of ellipsoid in its variogram map; the variogram model parameters also show less heterogeneity due to low nugget (0.2) and high ranges (4200). The up-scaled facies log showed a bit of anisotropy (Appendix 3.3.5.3_1a) with maximum continuity at azimuth of about $N210^0$; the nugget and

range in the major direction for facies log were 0.05 and 3770 respectively which also imply less heterogeneity. Water saturation also showed fairly good isotropy (Appendix 3.3.5.3_3a) while the nugget and range in the major direction were 0.2 and 4200 respectively (Appendix 3.3.5.3_3b) indicating less heterogeneity. Lastly, permeability showed a bit anisotropy with major direction of about N 230^0; nugget and range values of 0.2 and 4200 indicate less heterogeneity. All these variograms were applied in property modelling (especially using Sequential Gaussian simulation) to describe the spatial variation of the properties.

Both deterministic (Kriging) and stochastic (SGS) algorithms were used in generating the property models. The results of the property modelling show that stochastic models (SGS models) of the various properties are more realistic compared to deterministic (Kriging) models, thus SGS models were generally adopted in estimating STOIIPs. Appendices 3.3.5.3_1-5 compare the various reservoir property models.

Well Prognosis

Traditional well prognosis is done using 2D reservoir map which may be the cause of high incidence of dry holes during the pre-3D model era. Well prognosis or well placement could be easily done using 3D reservoir property models since they clearly show areas with low water saturation; moderate to high porosity; moderate to high NTG, high STOIIP etc. Figures 4.4 a and b compare well placement of infill well using a 2D map

and a 3D model of the reservoir. A chance of drilling a dry hole is lower in the 3D model than in the 2D reservoir map.

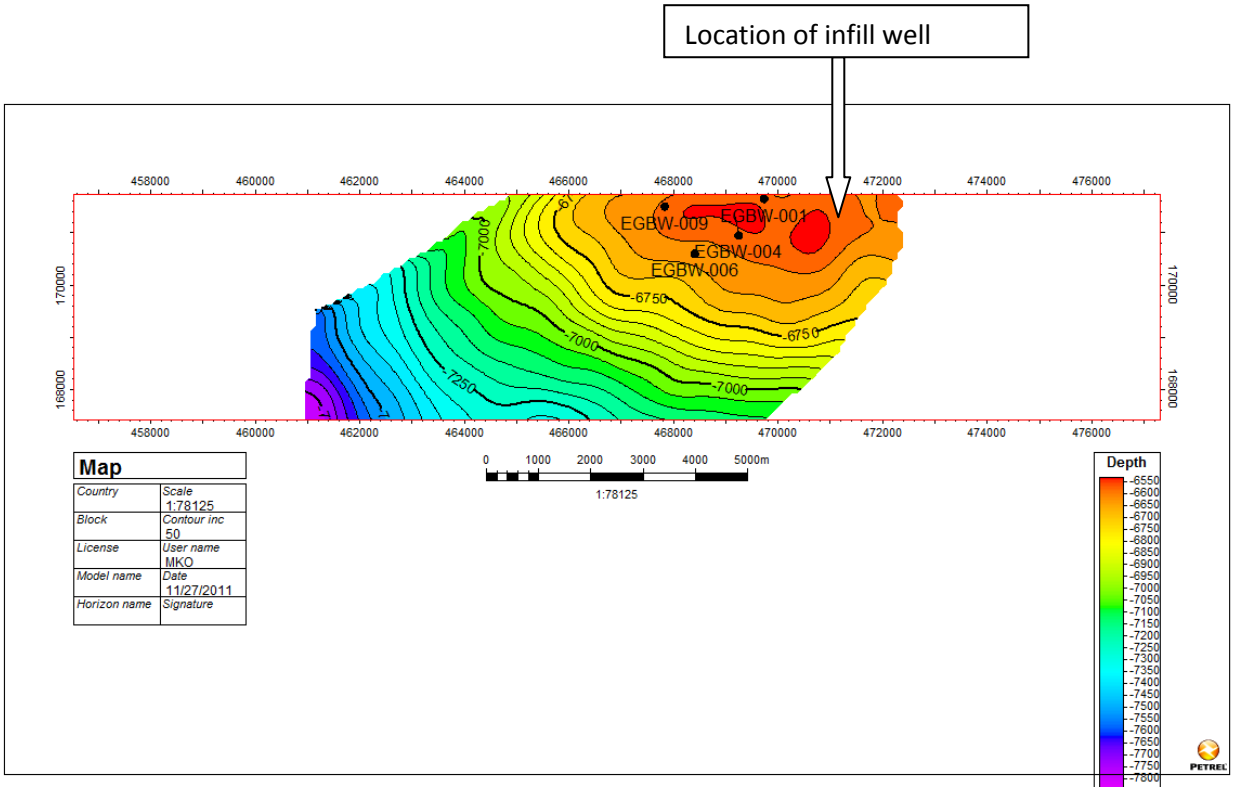

Figure 4.4 a: 2D Top structure map of Reservoir X

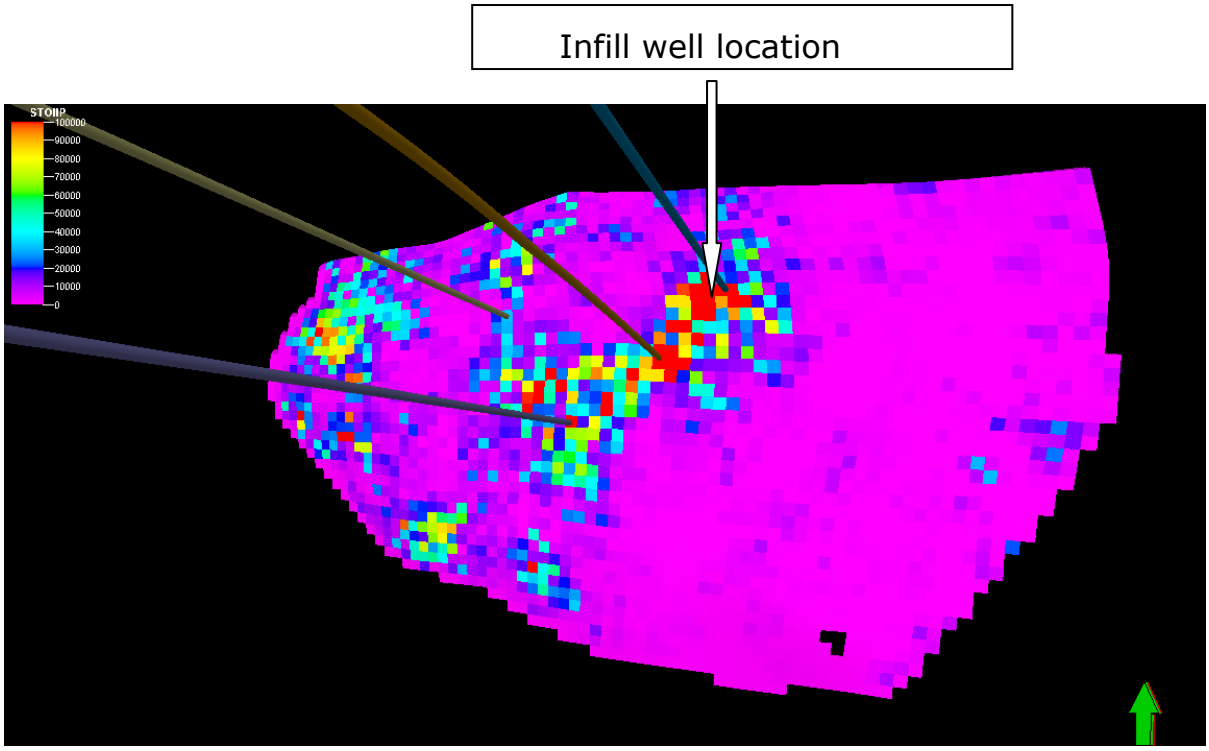

Figure 4.4 b: 3D STOIIP model of Reservoir X

It makes absolute sense for 3D well placement to be better down 2D because 2D map only considers structural and stratigraphic frameworks while 3D model considers gridded reservoir properties in addition to structural and stratigraphic framework. However, well placement is best done by integrating simulation with static reservoir models. With 3D dynamic STOIIP model, the current hydrocarbon saturation can be predicted and used in identifying new drillable prospects.

3.5 Volume Estimates

Bulk volume was generated using 3D reservoir model as 55,298 acre-ft and compared with Gross Rock Volume (GRV) generated using the reservoir 2D map (55412 acre-ft); they show a good match. These volumes were then compared with the existing GRV of the reservoir,

which is 46944 acre-ft[13]. There is a 15.28% difference in this study GRV and the existing GRV which is not bad at all, owing to the fact that the interpretation was done by two different interpreters. Deterministic STOIIPs were estimated first using petrophysical averages and then using property models generated @OWC of 6656 TVDSS. The results were then compared with the existing STOIIP @ the existing OWC and OUT (i.e. 6656ft and 6550ft TVDSS respectively). The results as illustrated in table 3.3.6.2 gives average property STOIIP as 52MMSTB; property model STOIIP as 15MMSTB; and existing STOIIP (from "D map) as 44.9MMSTB. These results clearly show that OWC of 6656ft is too shallow since 3D property models are more realistic than the averages. Hence OWC of 6936ft was adopted and used to estimate a STOIIP of 35MMSTB using the property models. In the same vein, Recovery factor (RF) of 70% was adopted since the estimated RF (using Guthrie and Greenberger correlation) is 62%$\pm$9% and the reservoir had already produced close to 20MMSTB which is around 60% Actual RF.

Stochastic STOIIP estimation shows P_{10} of 23.15MMSTB, P_{50} of 34.76MMSTB, and P_{90} of 40.45MMSTB. The mean of the 3 probabilities is 32.79MMSTB which is comparable to the most likely, P_{50} (34.76MMSTB).

The Ultimate Recovery (UR) based on 70% RF for the deterministic STOIIP is 24.5MMSTB. For the stochastic STOIIPs, the URs @ 70% RF are 16.17MMSTB, 24.33MMSTB, and 28.315MMSTB respectively. For the deterministic UR, the remaining reserve in Reservoir X is 4.5MMSTB.

For the stochastic most likely UR (P_{50}), the remaining reserve is 4.33MMSTB.

Sensitivity analysis shows that STOIIP is very sensitive to OWC/ oil column height (Figure 3.5).

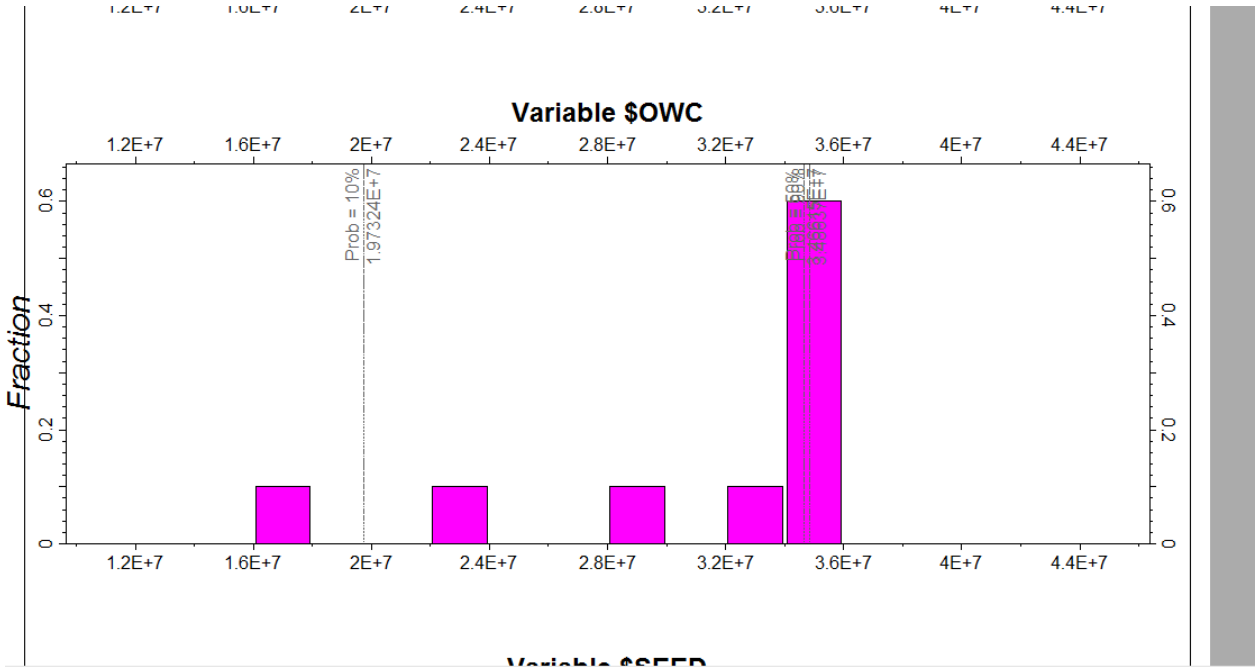

Figure 3.5 a: STOIIP is more sensitive to Contacts

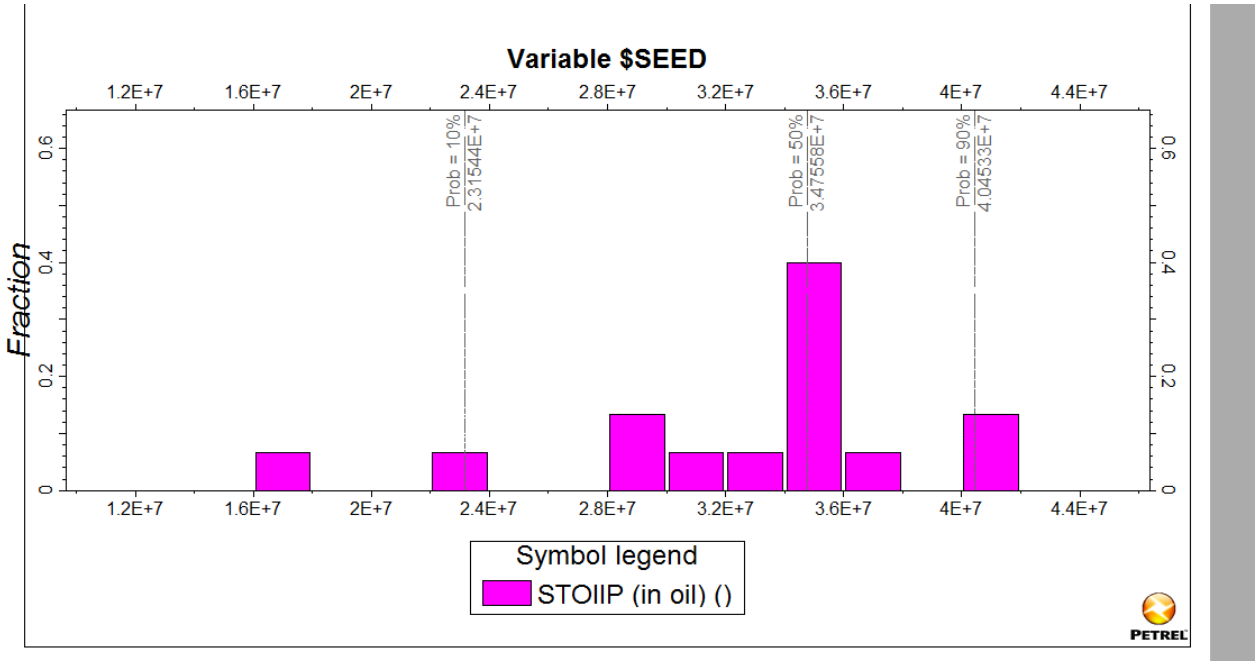

Figure 3.5 b: STOIIP sensitivity to Petrophysical properties (phi, k, S_w)

CHAPTER 5

CONCLUSIONS AND RECOMMENDATIONS

Conclusions

The integration of all available data (geophysical, geological, petrophysical, production, pressure, and PVT) has led to the building of a consistent high resolution 3-D static model of the reservoir which can serve as input into reservoir simulation model. The 3-D model can be better applied in well planning compared with the 2-D reservoir map conventionally used for the same purpose. Reservoir characterization of this reservoir has led to detailed description and understanding of the reservoir and has provided a very effective reservoir management strategy for the reservoir.

Recommendations

To maximally recover oil from Reservoir X, wells completed on the reservoir with high Water-Oil ratio (WOR) should be shut-in to conserve the reservoir energy (since it's an active water-drive reservoir). The wells completed down-dip (with early water breakthrough) should be re-perforated shallower. At least one well should be sunk (with the help of property models) into the reservoir to drain the remaining/ by-passed oil.

Conventional core should be taken within the reservoir interval to properly characterize the reservoir and reduce uncertainties. Complete LWD (logging while drilling) suites should be taken when drilling the next well.

RST (Reservoir Saturation Tool) data should be taken to ascertain the present contacts so as to more accurately book the reserve.

Dynamic modelling/ simulation should be done to be sure of the optimal location of infill well and further oil development. Future work should be focussed on improving on the current geostatistical property modelling algorithms.

* Simulation should have been done in this study but for time constraint.

REFERENCES

John W. Kramers: 'Integrated Reservoir Characterization: From the well to the numerical model'; Alberta Research Council, P.O. Box 8330, Edmonton, Alberta, Canada T6H 5x2

Fadase, B.: 'AUST Lecture Materials on Petroleum Geology (PE 500), Abuja, Nigeria, 7-25 June, 2010

Onuoha, K.M.: '3D Static Models and Reservoir Simulation', AUST Lecture note on Advanced Reservoir Characterization course (PE 613), Abuja, Nigeria, 14 Feb. - 4 March, 2011

XYZ E&P Company: 'Reservoir X Study Report'; 2001

XYZ E&P Company: 'Annual Review of Hydrocarbon Resources'; January 2011

Sessions, K. P. and Lehman, D. H.: 'Nurturing the Geology-Reservoir Engineering Team: Vital for Efficient Oil and Gas Recovery'; SPE Paper 19780, SPE Annual Technical Conference and Exhibition, 8-11 October 1989, San Antonio, Texas

Harris, G.D.: 'The Role of Geology in Reservoir Simulation Studies'; SPE Paper 5022, 49th Annual SPE of AIME Fall Mgt., Houston, TX,USA, 6 Oct. 1974

Haldorsen, H.H. and Lake, L.W.: SPE Journal, 1984, 24447-457

Begg, S.H., and King P.R.: Modelling the effects of shales on reservoir performance: calculation of effective vertical permeability. SPE Paper No. 13529, 1985

Lake, L. W. and Carroll, Jr., H. B. (eds): 'Reservoir Characterization'**,** Proceedings of the Reservoir Characterization Technical Conference, Dallas, April 29-May1, 1985, Orlando, Florida, Academic Press Inc., 1986,659

Lake, L. W., Carroll, Jr., H. B. and Wesson, T. C. (eds): 'Reservoir Characterization II', Proceedings of the Second International Reservoir Characterization Technical Conference, Dallas, June 1989, San Diego, California, Academic Press, Inc., 1991, 726.

Linville, B. (ed.): Reservoir Characterization III, Proceedings of the Third International Reservoir Characterization Technical Conference, Tulsa, November 1991, Tulsa, Oklahoma, PennWell Publishing Co.,1993,1008.

G.R. King et al: 'Reservoir Characterization, Geological Modelling, and Reservoir Simulation of N'Sano Field, Upper Pinda Reservoir'; SPE Paper 39760,1998 SPE Asia Pacific Conference on Integrated Modelling for Asset Management held in Kuala Lumpur, Malaysia, 23-24 March 1998.

Durlofsky, L. Et al: 'Application of a new scale-up methodology to the simulation of displacement processes in heterogeneous Reservoirs', SPE

Paper 28704, Presented at the SPE International Petroleum Conference and Exhibition of Mexico, Veracruz, Oct. 10-13, 1994)

P.K. Neog and N.M. Borah: 'Reservoir Characterization through Well Test analysis Assists in Reservoir Simulation: A Case Study'; SPE Paper 64447, prepared for presentation at the SPE Asia Pacific Oil and Gas Conference and Exhibition held in Brisbane, Australia, 16–18 October 2000.

M.A. Naguib et al: 'Improving Reservoir Management for a Mature field by Reservoir Characterization'; SPE Paper 64283, prepared for presentation at the SPE Asia Pacific Oil and Gas Conference and Exhibition held in Brisbane, Australia, 16–18 October 2000.

Fadase, B.: 'Depositional Environments', AUST Lecture note on Petroleum Geology course (PE 500), Abuja, Nigeria, 7-25 June, 2010.

Fadase, B.: 'AUST Lecture Materials on Petroleum Geology (PE 500), Abuja, Nigeria, 7-25 June, 2010

Schlumberger Oil Servicing Co.: Techlog Interactive Suite 2010 Help manual.

Tiab,D.: 'Drive Mechanisms, MBE and Reserves', AUST Lecture note on Properties of Reservoir Fluids and Reservoir Engineering, Abuja, Nigeria, 2-20 August, 2010.

NOMENCLATURE/ LIST OF ACRONYMS

API	-	American Petroleum Institute
ARHR	-	Annual Review of Hydrocarbon Resources
Av core K	-	Average core Permeability
Av eff Φ	-	Average effective porosity
Av eff S_w	-	Average effective water saturation
Av K	-	Average Permeability
Av Total Φ	-	Average Total Porosity
Av S_w	-	Average water saturation
Av V_{sh}	-	Average Volume of shale
bbl	-	Barrel
BHP	-	Bottom-hole pressure
b_{oi}	-	Formation Volume factor
BVWE	-	Effective Bulk Volume of water
cf	-	Cubic feet
cp	-	Centipoise
DPR	-	Department of Petroleum Resources
E&P	-	Exploration and Production
ftss	-	Feet sub-sea
HCPV	-	Hydrocarbon Pore volume
GOC	-	Gas-Oil contact
GOR	-	Gas-Oil ratio

GR	-	Gamma ray
GR_{index}	-	Gamma ray index
GR_{matrix}	-	Gamma ray log reading in 100% matrix
GR_{shale}	-	Gamma ray log reading in 100% shale
GRV	-	Gross rock volume
HST	-	Highstand Systems Tract
K	-	Permeability
K_c	-	Coates' constant
LST	-	Lowstand Systems Tract
m	-	Cementation exponent
md	-	Millidarcy
MBOPD	-	Thousand barrel of oil per day
MMSTB	-	Million Stock Tank barrel
n	-	Saturation exponent
NPV	-	Net Present Value
ODT	-	Oil down to
OIIP	-	Oil initially in place
OUT	-	Oil up to
OWC	-	Oil-water contact
P_{10}	-	Probability of 10%
P_{50}	-	Probability of 50%
P_{90}	-	Probability of 90%

Phi_e	-	Effective porosity
Phi_t	-	Total porosity
psig	-	Pounds per square inch gauge
PVT	-	Pressure, volume and Temperature
RB	-	Reservoir barrel
RF	-	Recovery factor
RFT	-	Repeat formation test
R_{sh}	-	Resistivity log reading in 100% shale
RST	-	Reservoir saturation tool
SGS	-	Sequential Gausian Simulation
S_h	-	Hydrocarbon saturation
SP	-	Spontaneous Potential
STB	-	Stock Tank Barrel
STOIIP	-	Stock Tank Oil Initially in Place
S_w	-	Water saturation
TSE	-	Transgressive Surface of Erosion
TST	-	Transgressive Systems Tract
TVDSS	-	True Vertical Depth Sub-sea
TWT	-	Two Way Time
UR	-	Ultimate Recovery
VRR	-	Voidage Replacement Ratio
V_{sh}	-	Volume of shale

WDT	-	Water Down to
3D	-	3 Dimensional
2D	-	2 Dimensional
Φ	-	Porosity

Appendix 3.3.3.2_1: North to South Well Correlation of Reservoir X showing thinning towards the basin

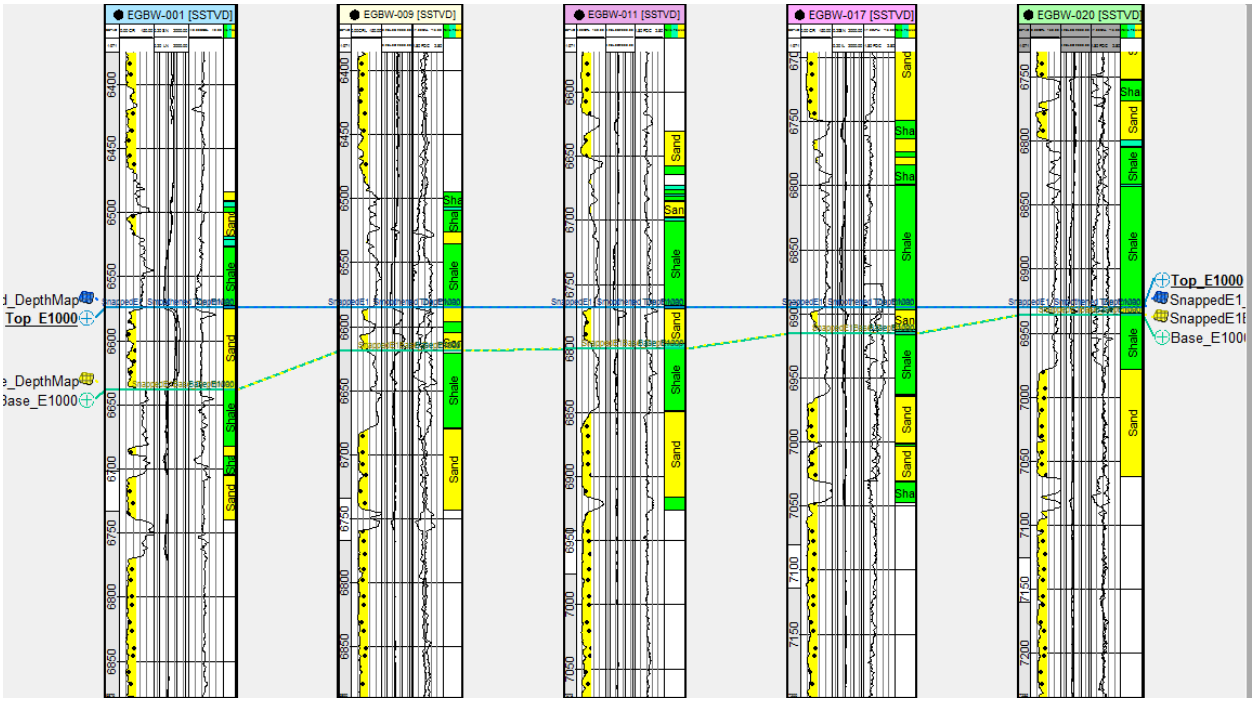

Appendix 3.3.3.2_2: West to East Well Correlation of Reservoir X showing poor sand development towards the eastern flank of the field.

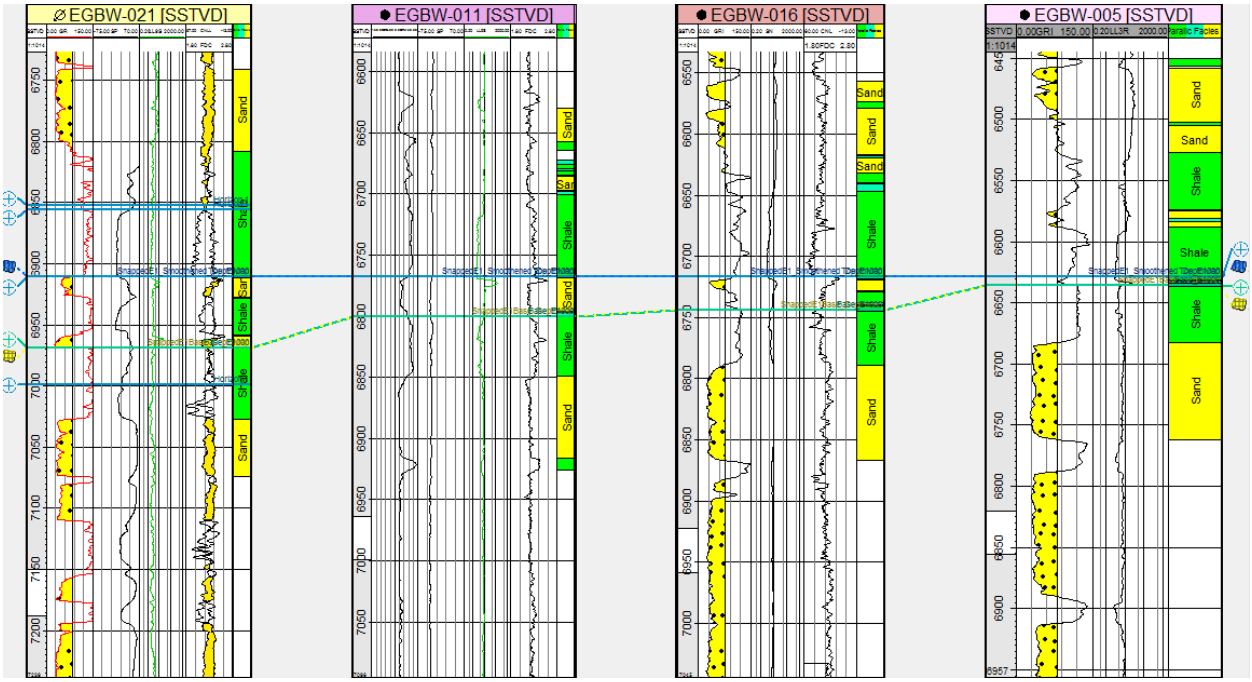

Appendix 3.3.3.2_1: West to East (Crossline) Cross sectional view of Reservoir X

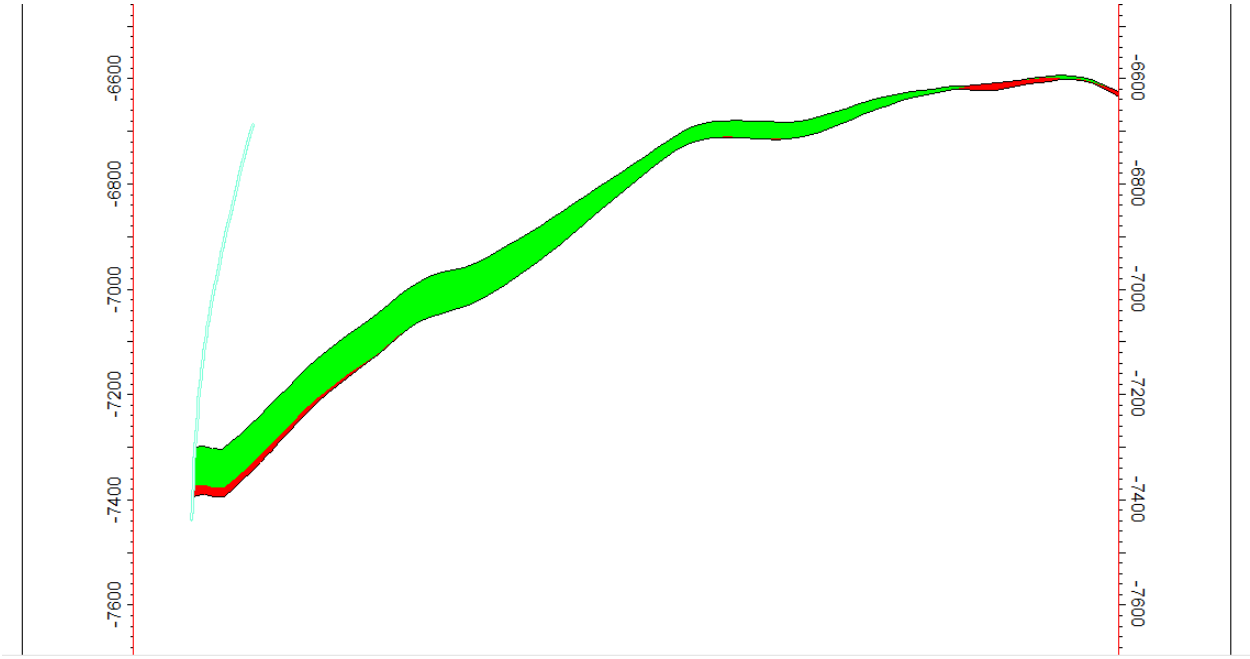

Appendix 3.3.3.2_2: South-North Cross-Sectional view of Reservoir X in the fields

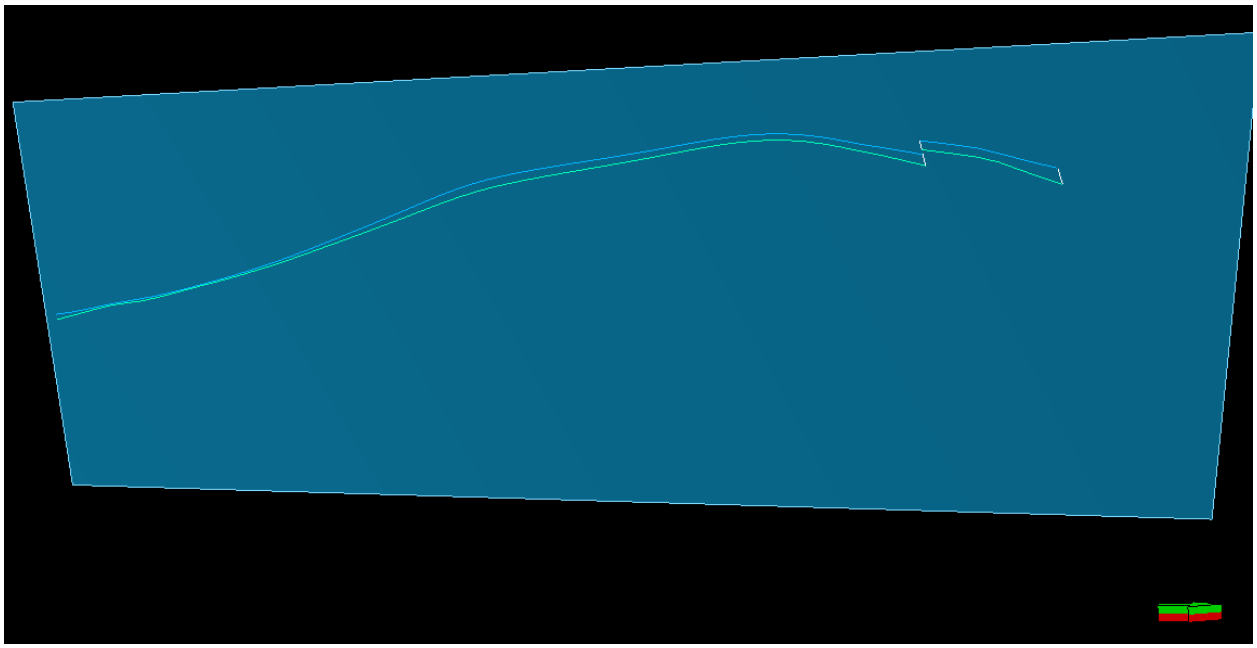

Appendix 3.3.4.3_2: Picket plot for well-6 indicating petrophysical properties

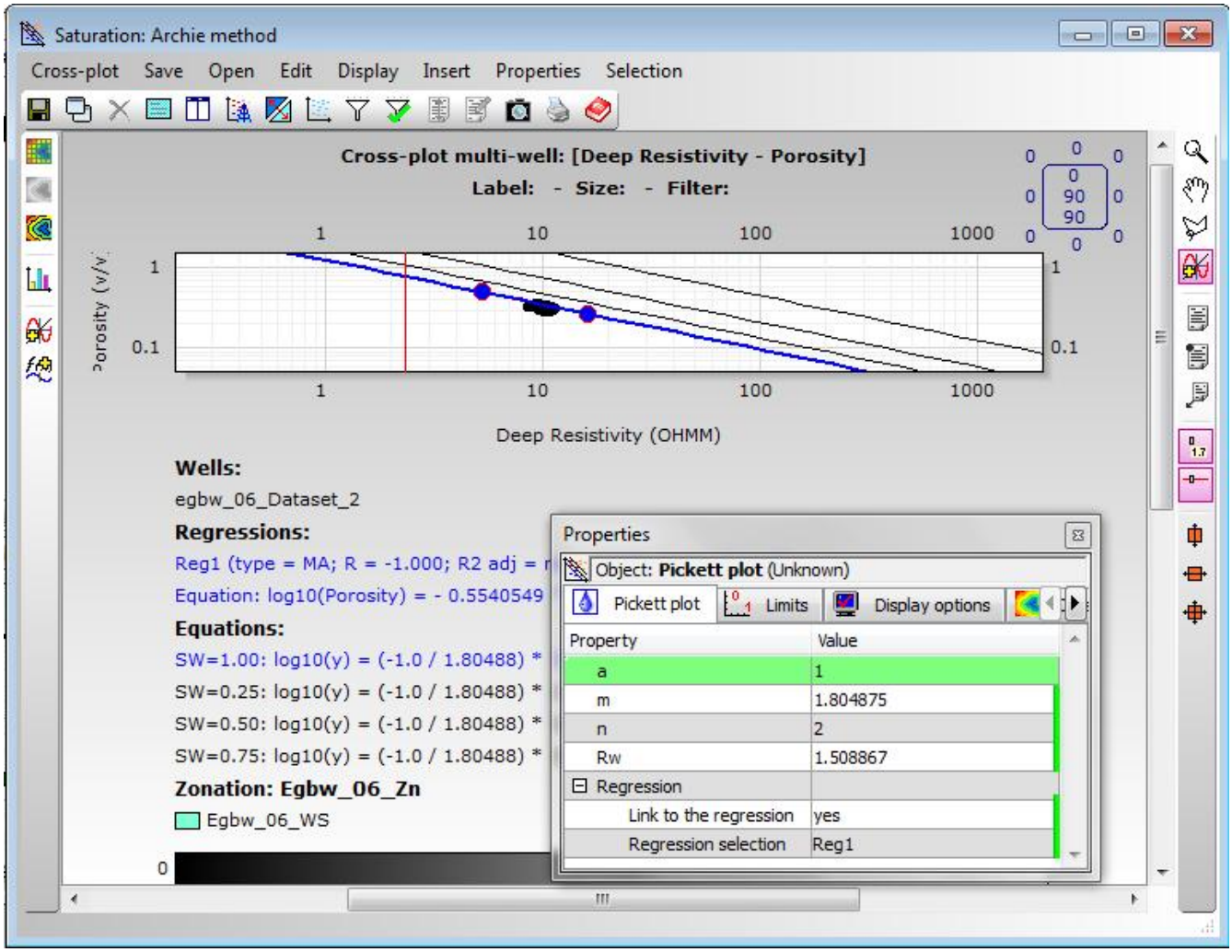

Appendix 3.3.4.3_3: Picket plot for well-7 indicating petrophysical properties

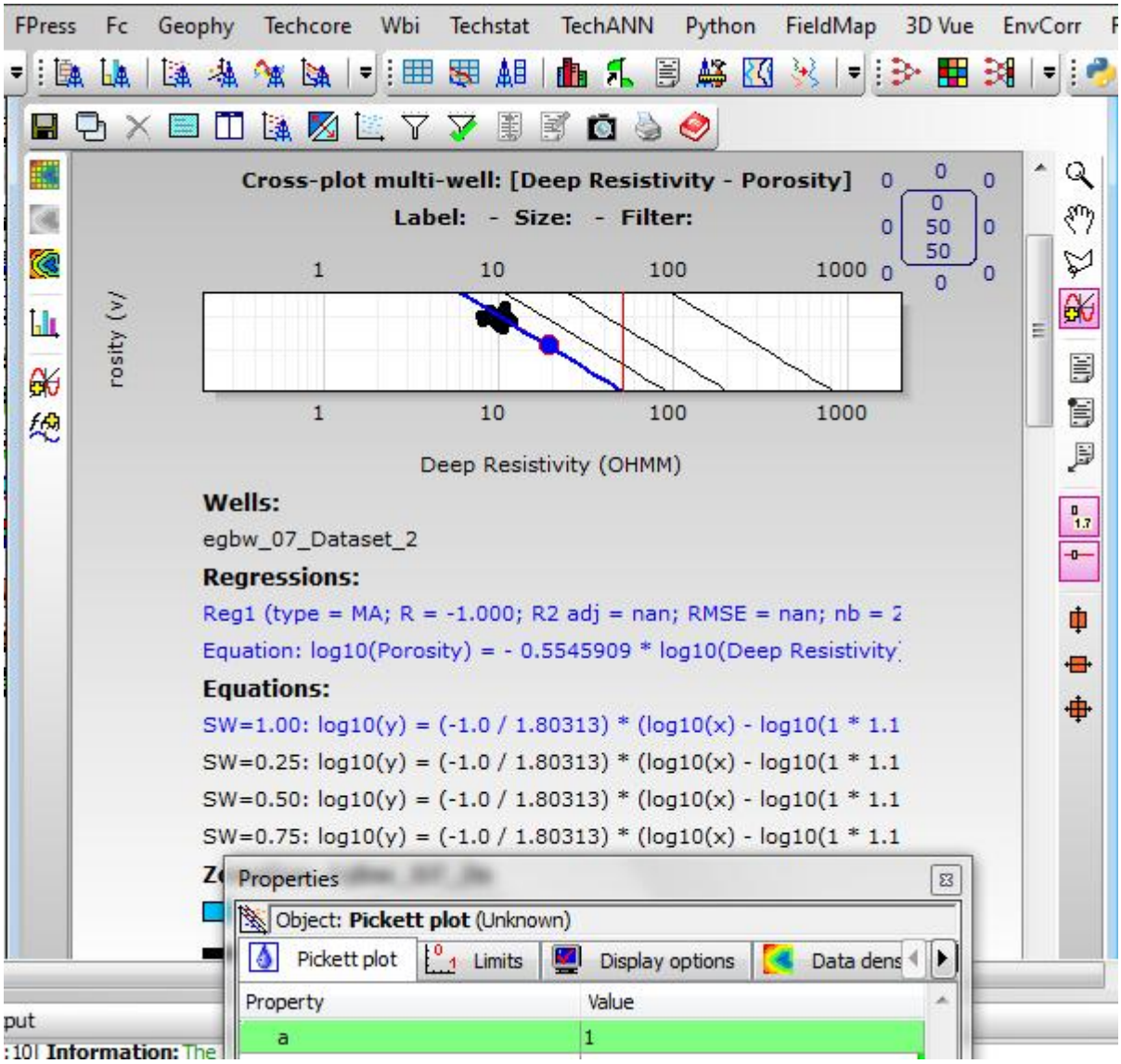

Appendix 3.3.4.3_4: Picket plot for well-8 indicating petrophysical properties

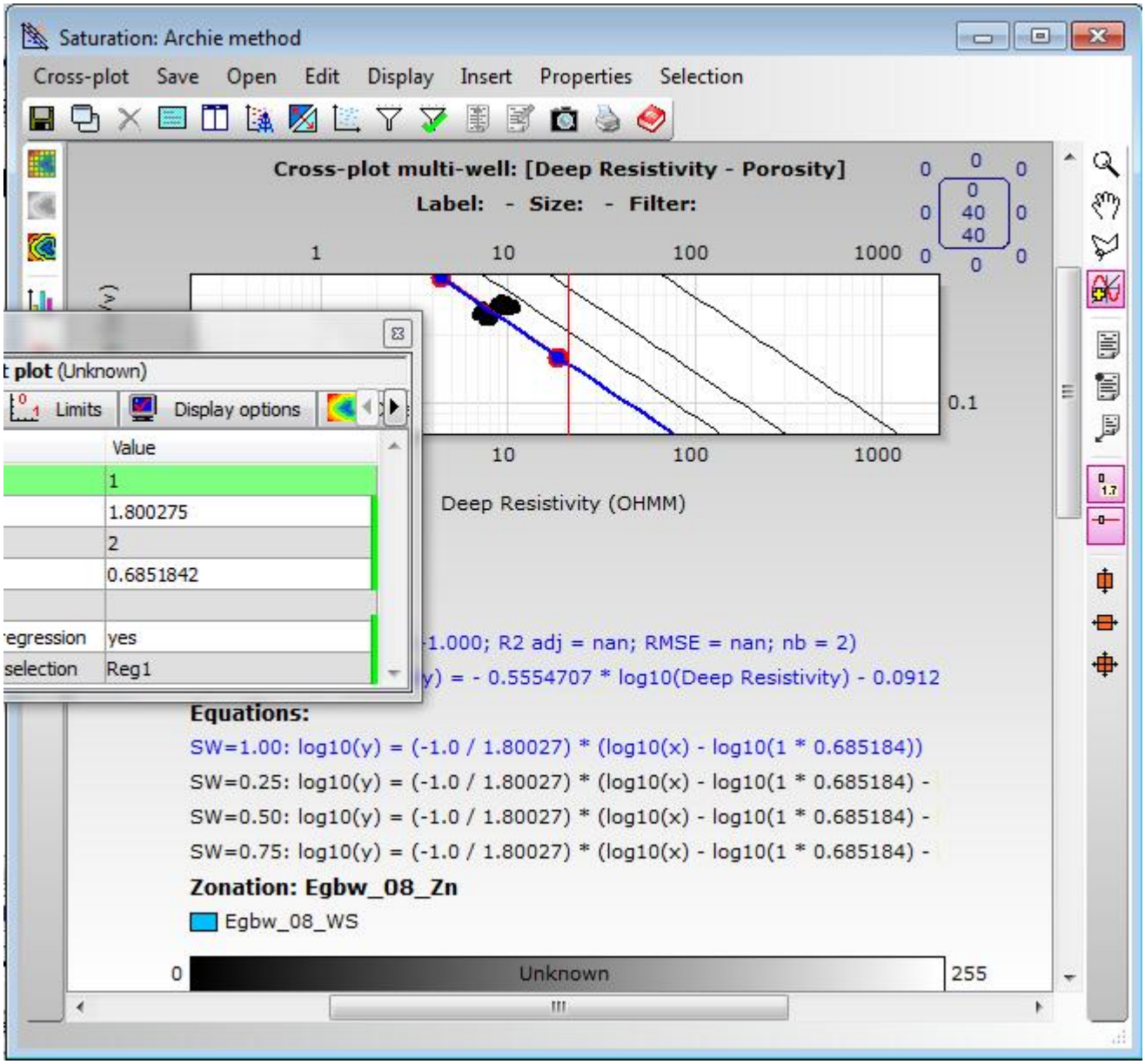

Appendix 3.3.4.3_5: Picket plot for well-9 indicating petrophysical properties

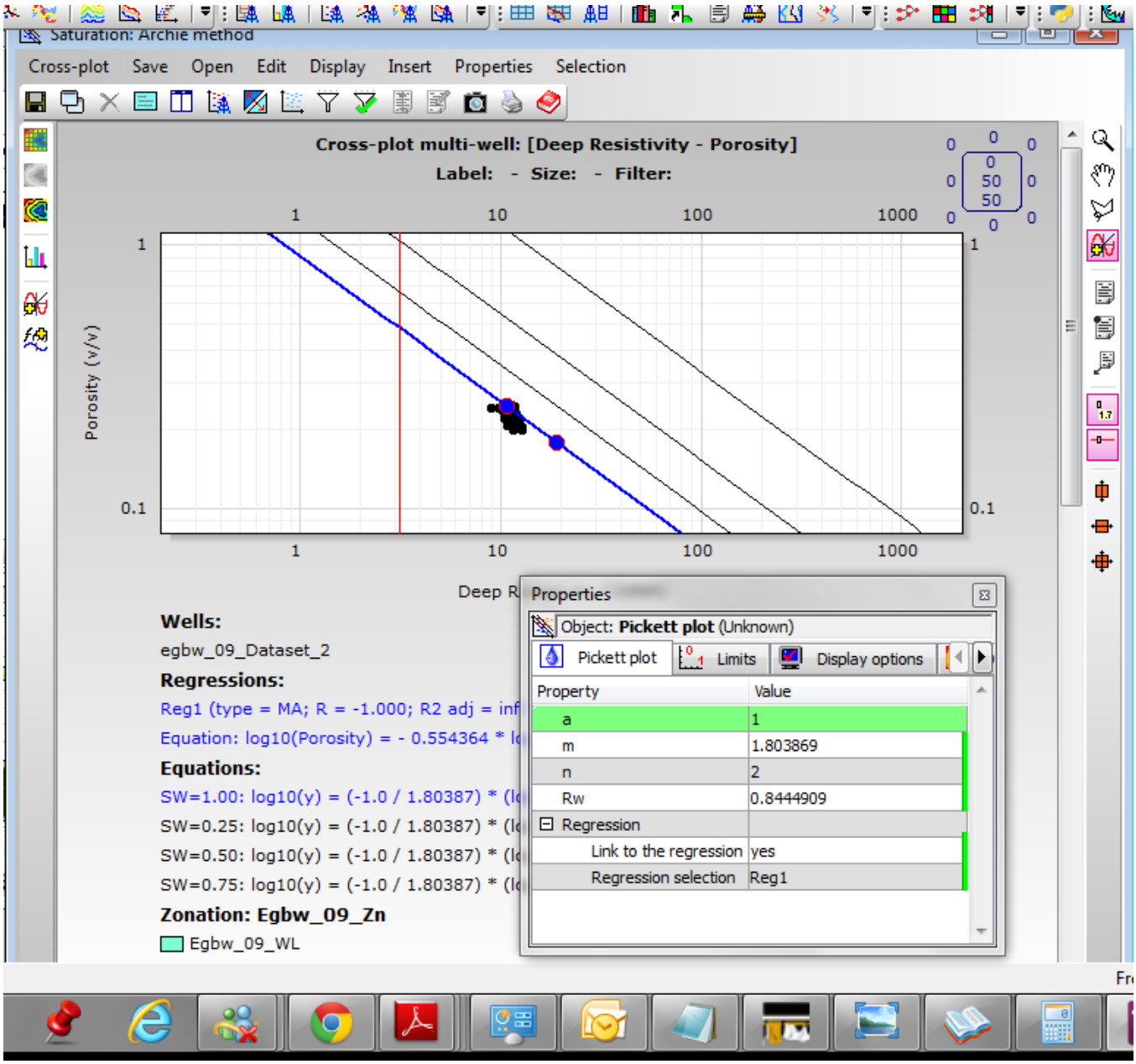

Appendix 3.3.4.3_6: Picket plot for well-11 indicating petrophysical properties

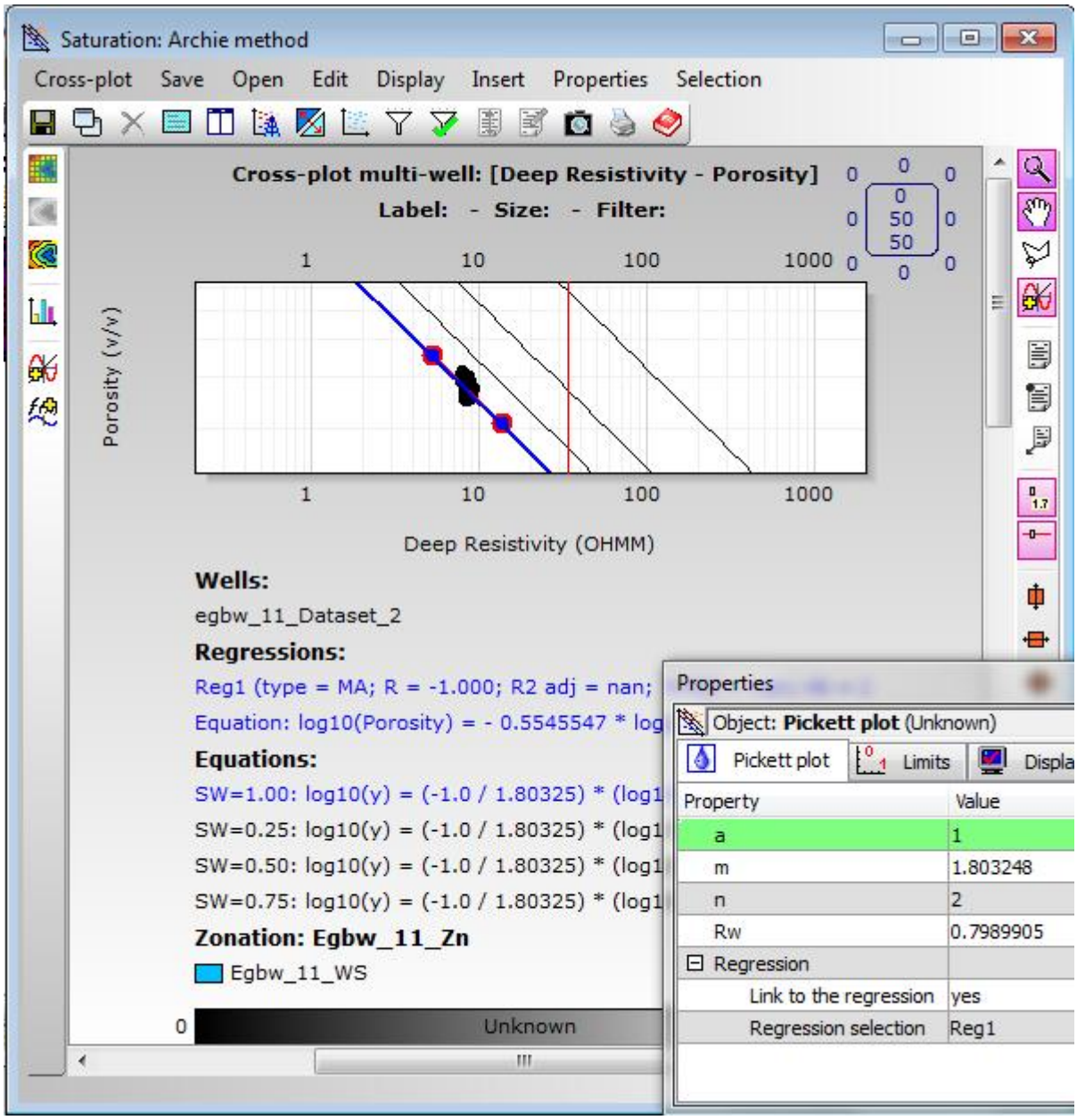

Appendix 3.3.4.3_7: Picket plot for well-12 indicating petrophysical properties

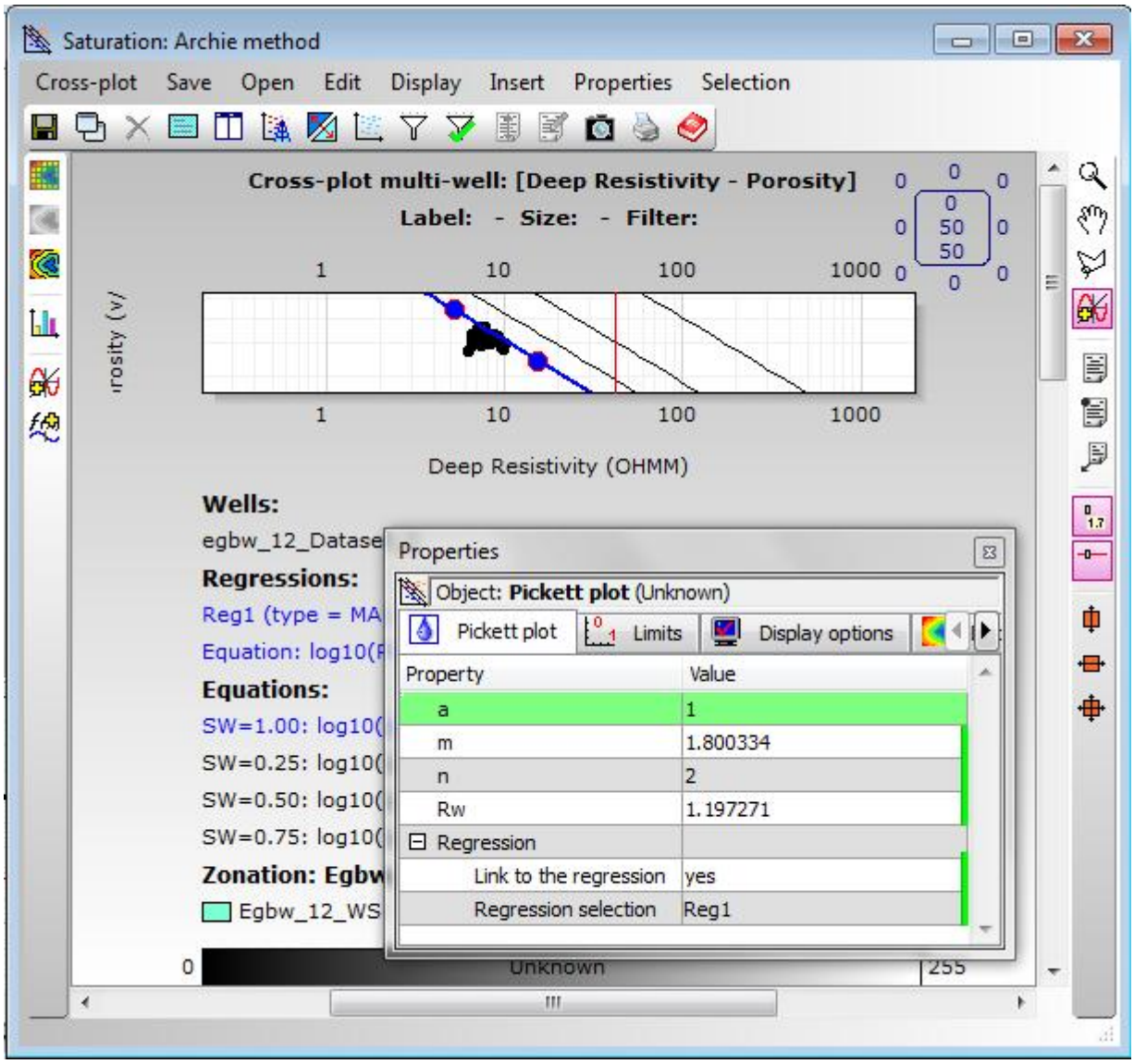

Appendix 3.3.4.3_8: Picket plot for well-14 indicating petrophysical properties

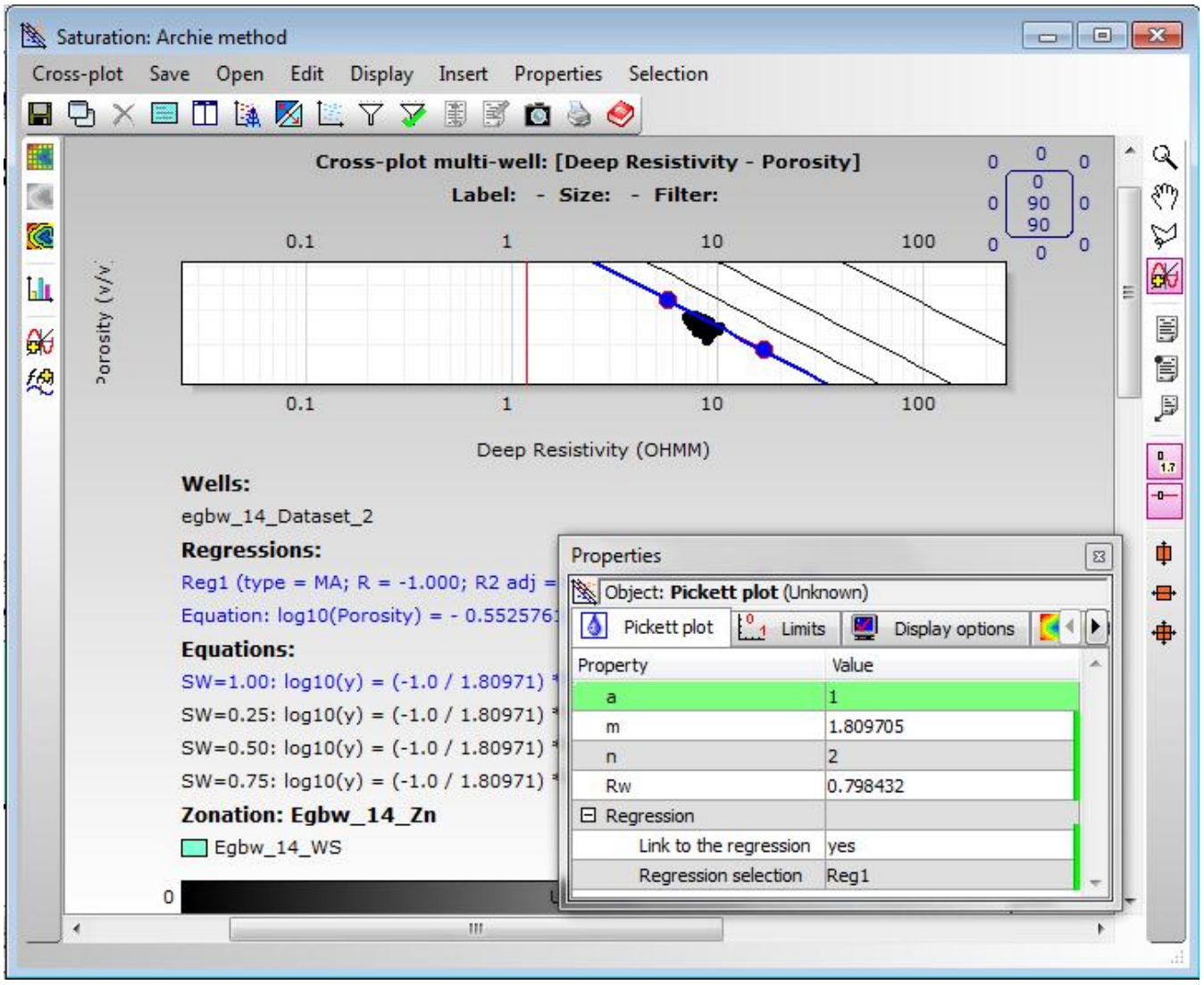

Appendix 3.3.4.3_9: Picket plot for well-17 indicating petrophysical properties

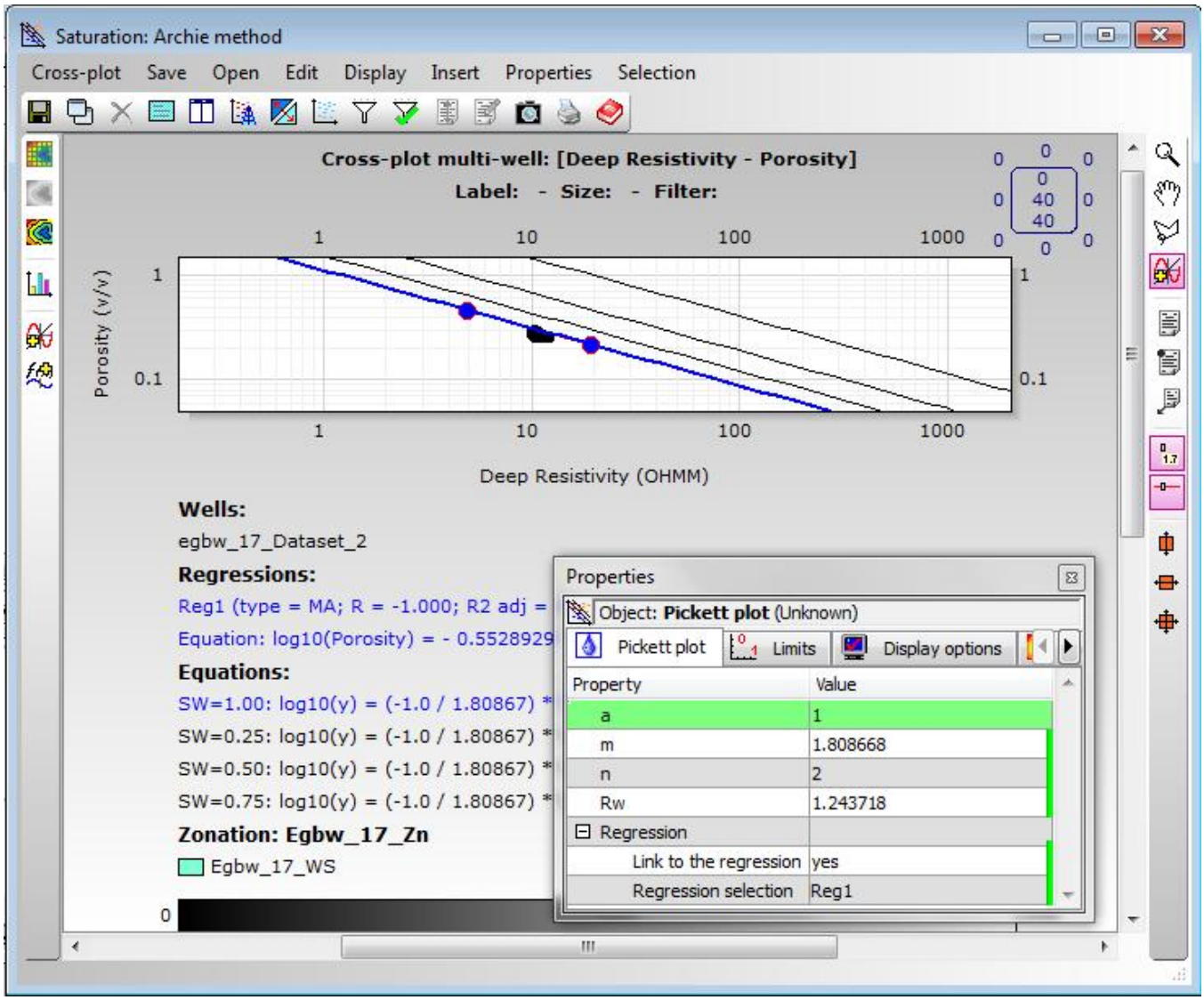

Appendix 3.3.4.3_10: Picket plot for well-18 indicating petrophysical properties

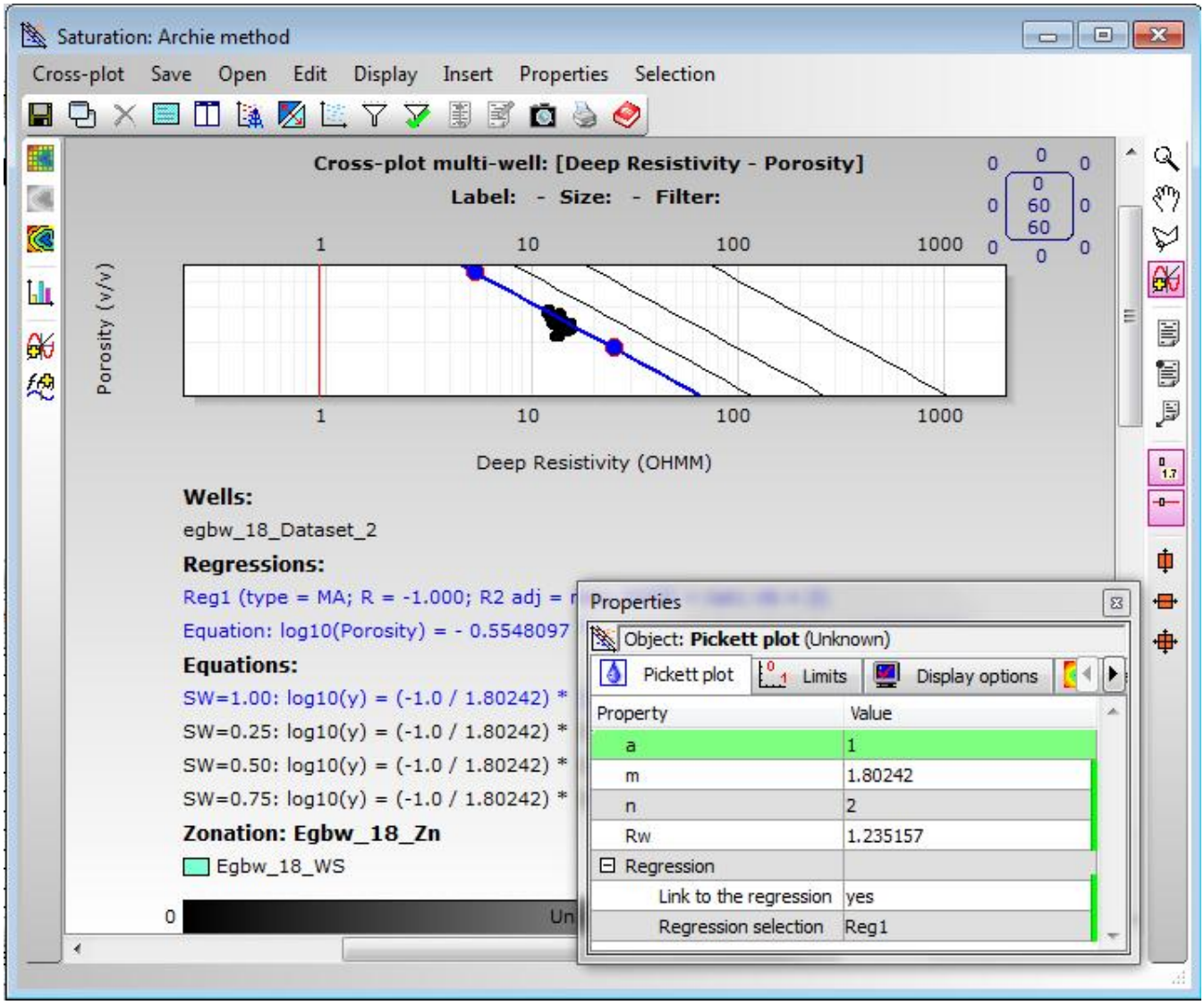

Appendix 3.3.4.3_11: Picket plot for well-19 indicating petrophysical properties

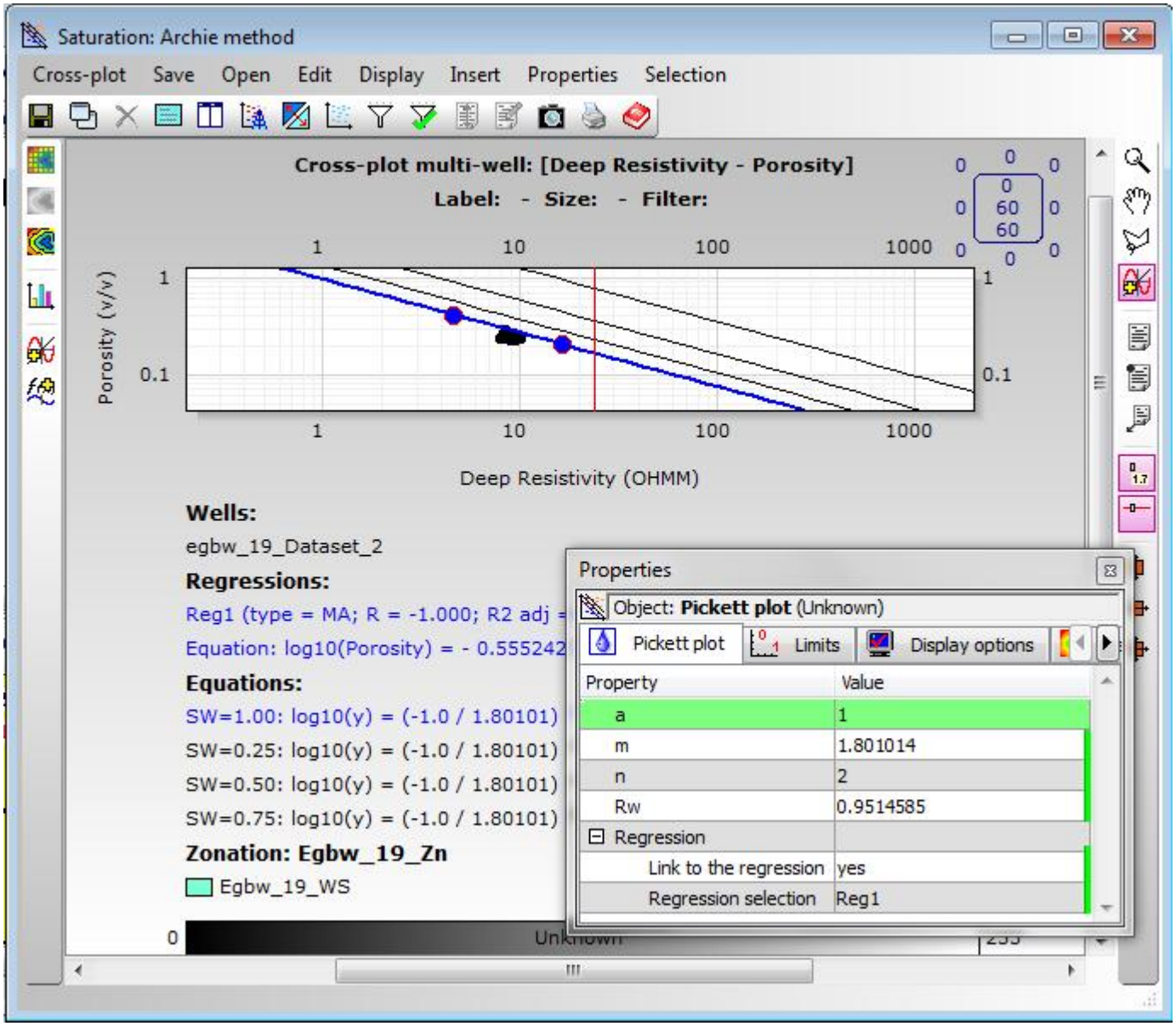

Appendix 3.3.4.3_12: Picket plot for well-20 indicating petrophysical properties

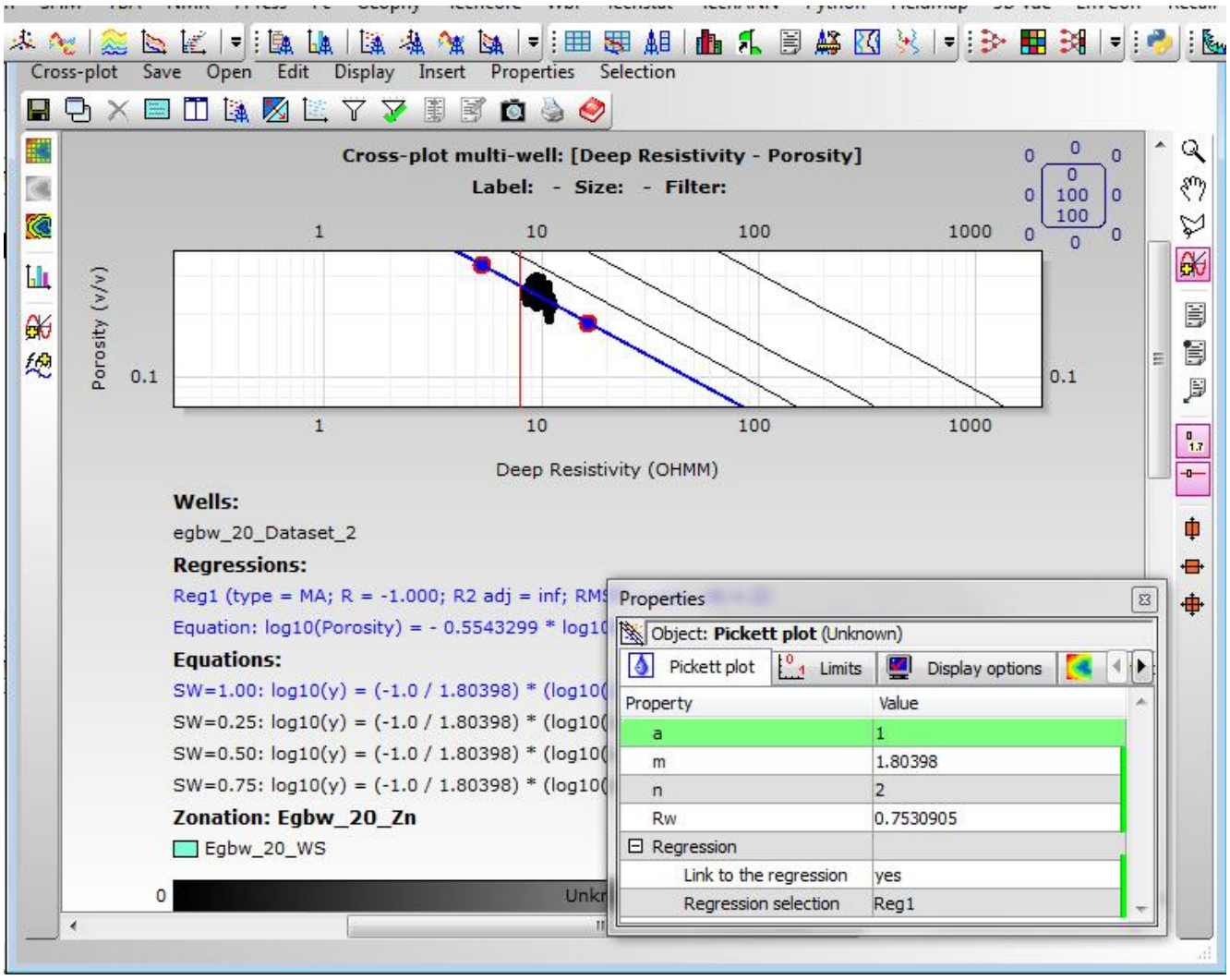

Appendix 3.3.4.3_13: Picket plot for well-21 indicating petrophysical properties

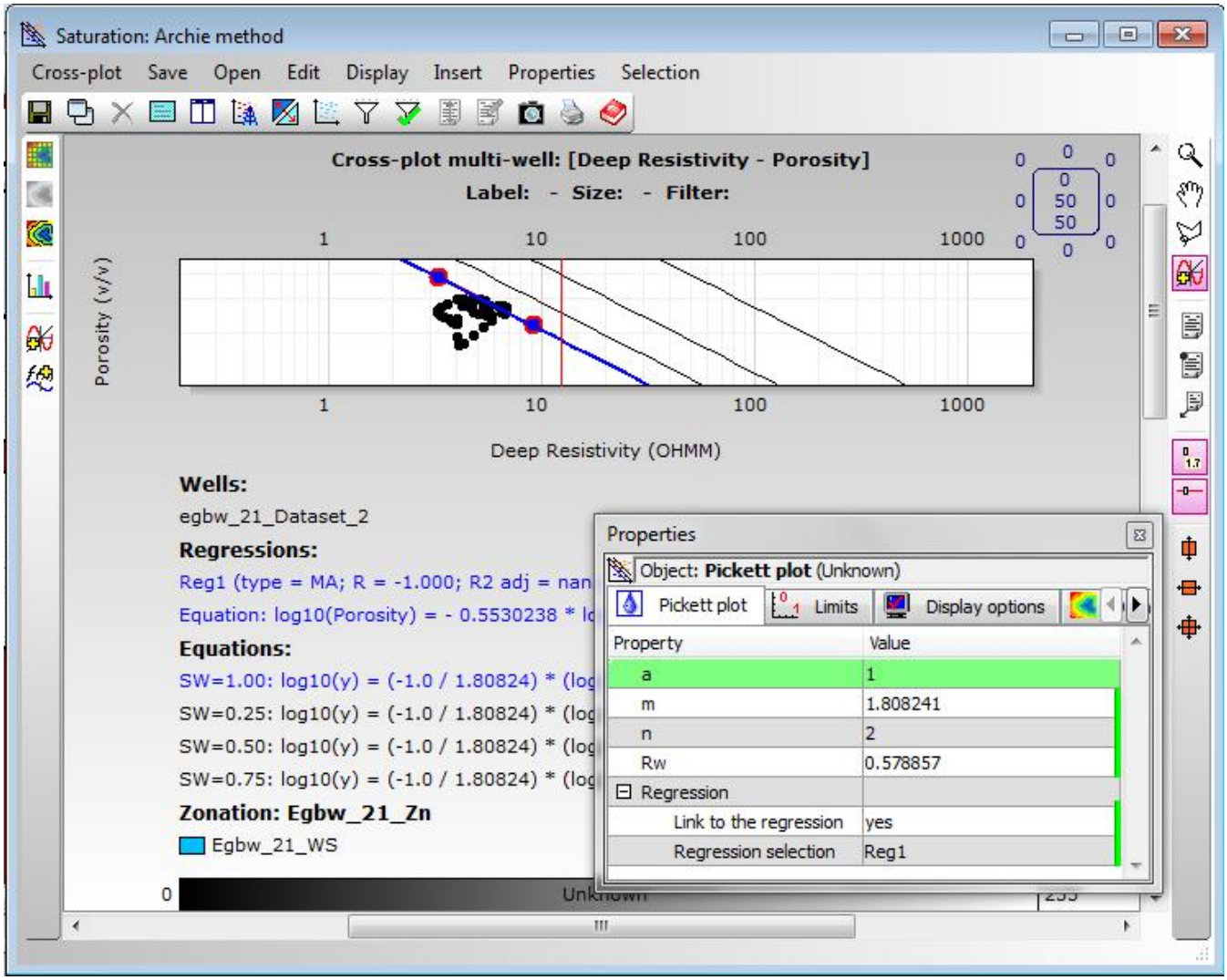

Appendix 3.3.5.3_1a: Variogram map from up-scaled facies log

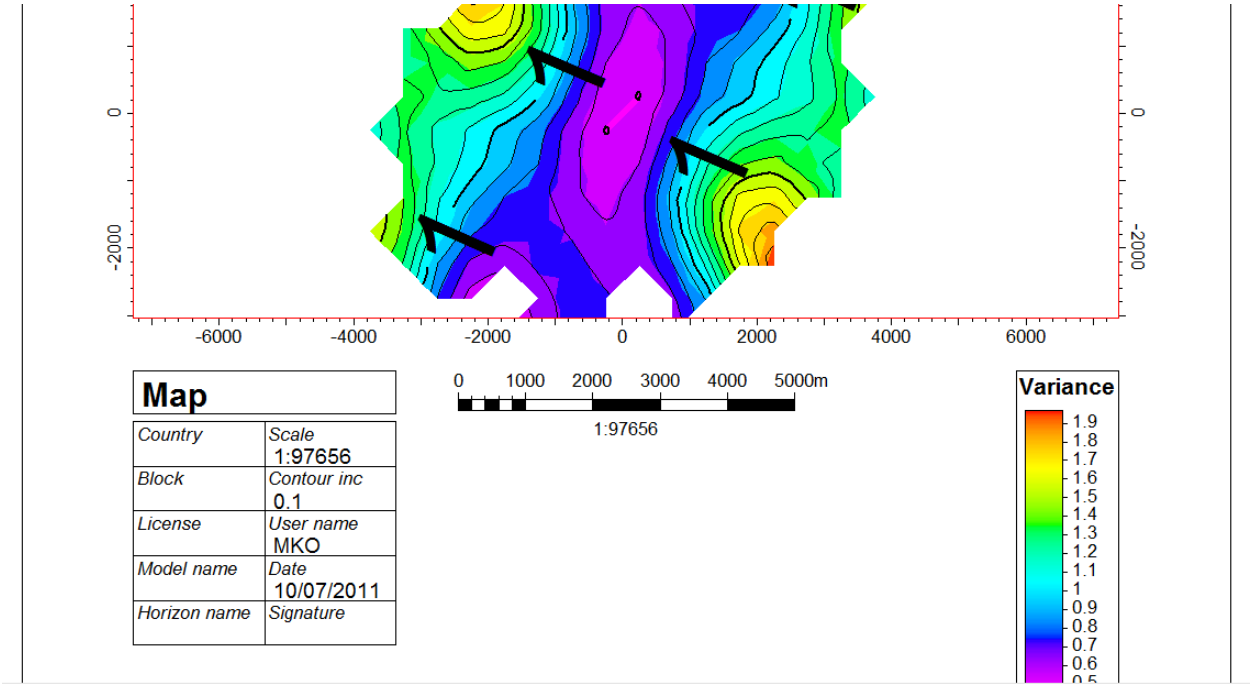

Appendix 3.3.5.3_1b: Sample Variogram and Variogram model from up-scaled Facies log

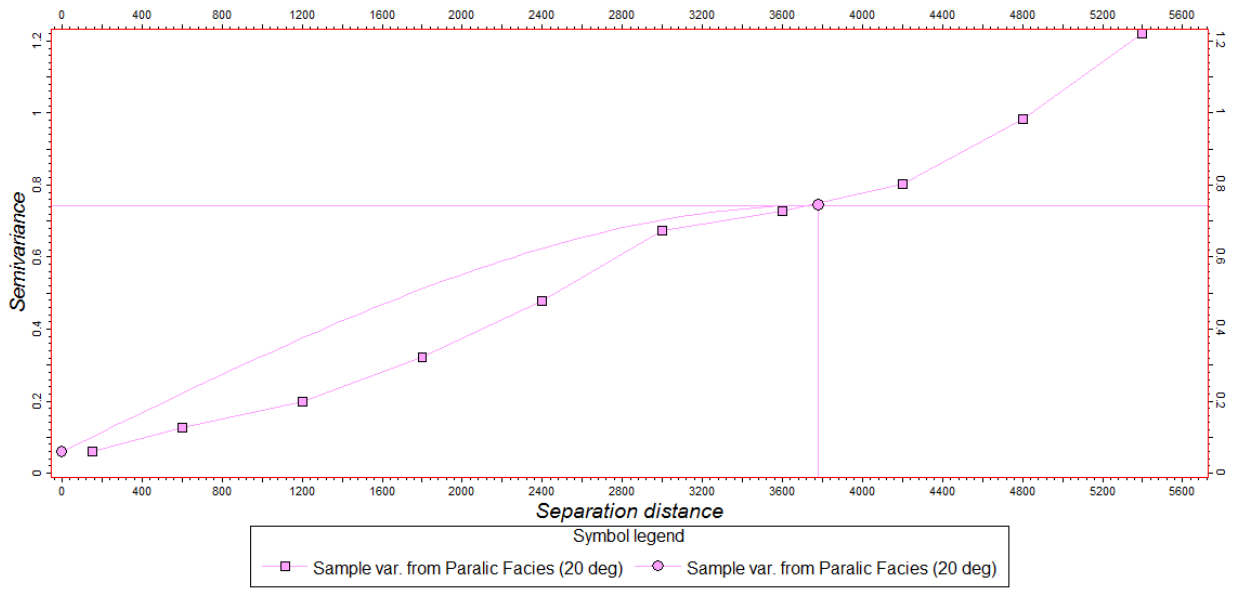

Appendix 3.3.5.3_1c: Facies model showing completed wells(using SGS algorithm)

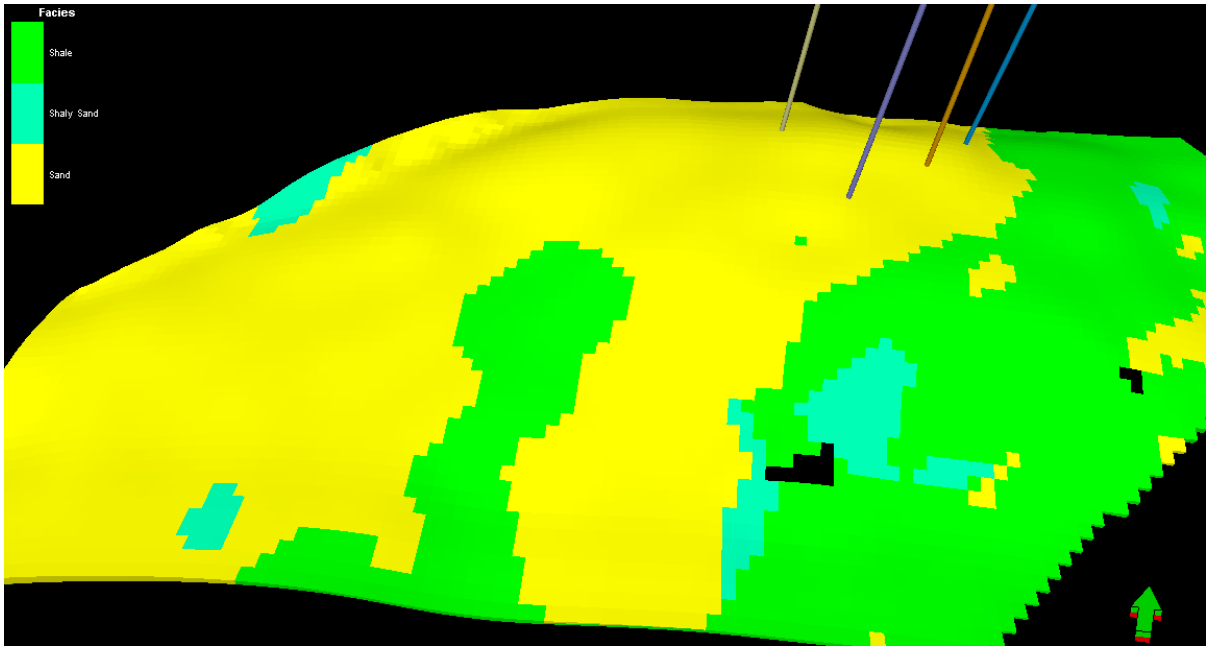

Appendix 3.3.5.3_1d: Facies model showing completed wells (using Kriging algorithm)

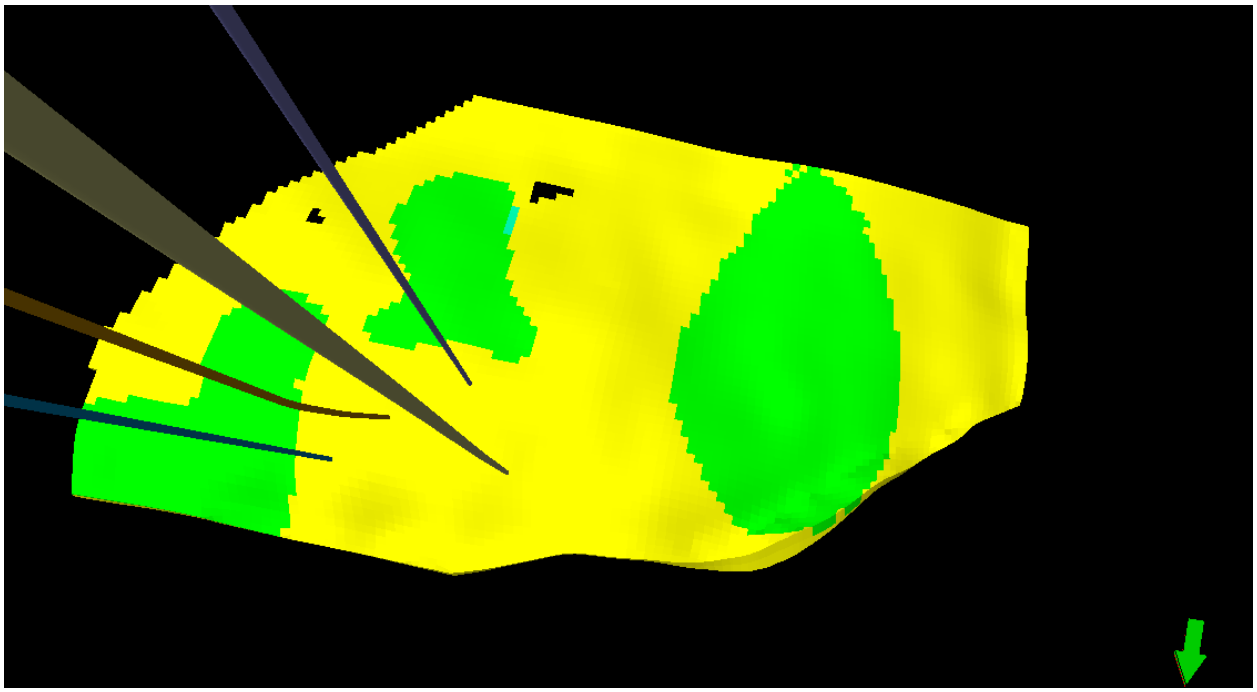

Appendix 3.3.5.3_2a: Variogram map from up-scaled porolog

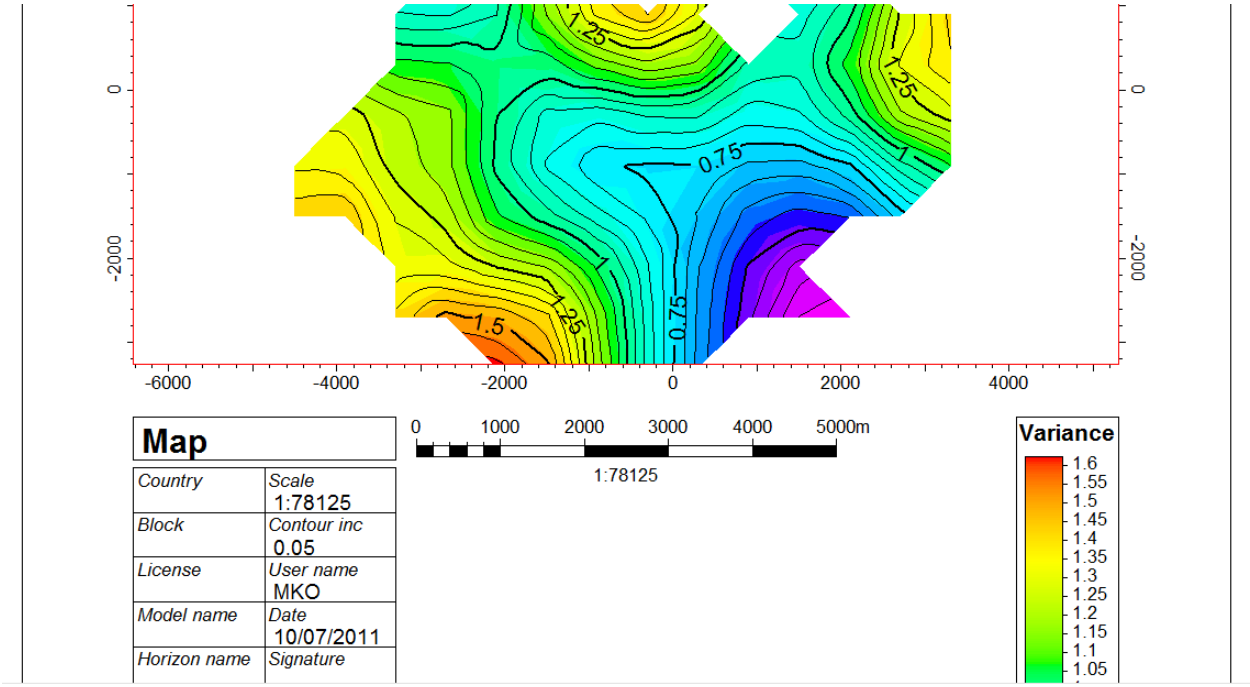

Appendix 3.3.5.3_2b: Sample Variogram and Variogram model from up-scaled porolog

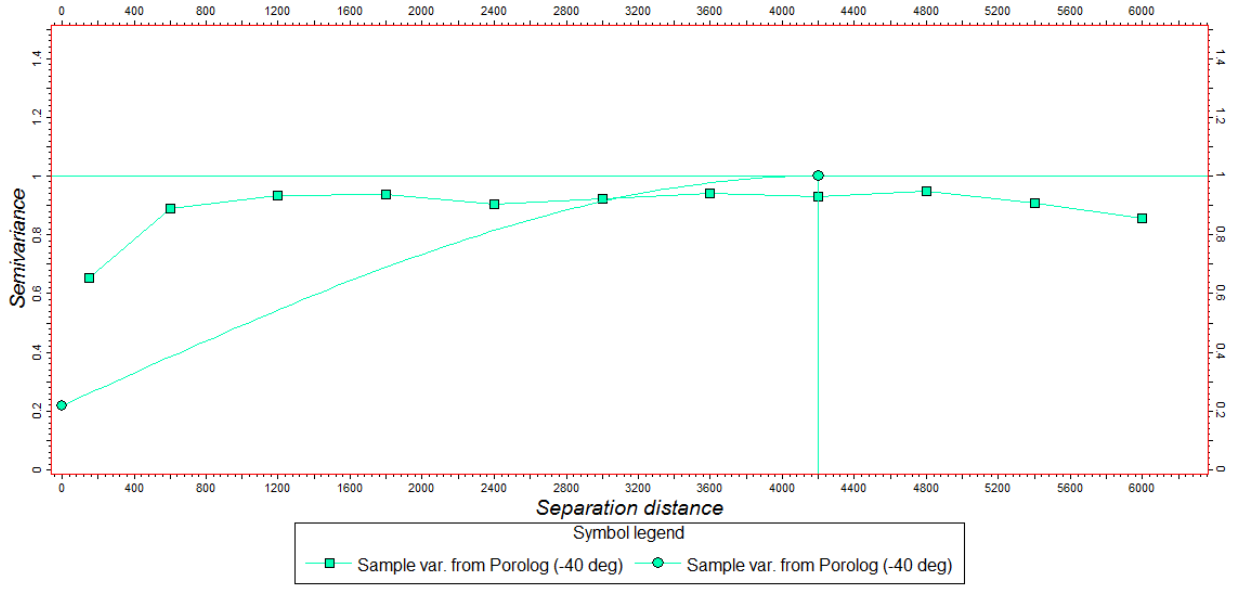

Appendix 3.3.5.3_2c: Porosity model showing completed wells (using SGS algorithm)

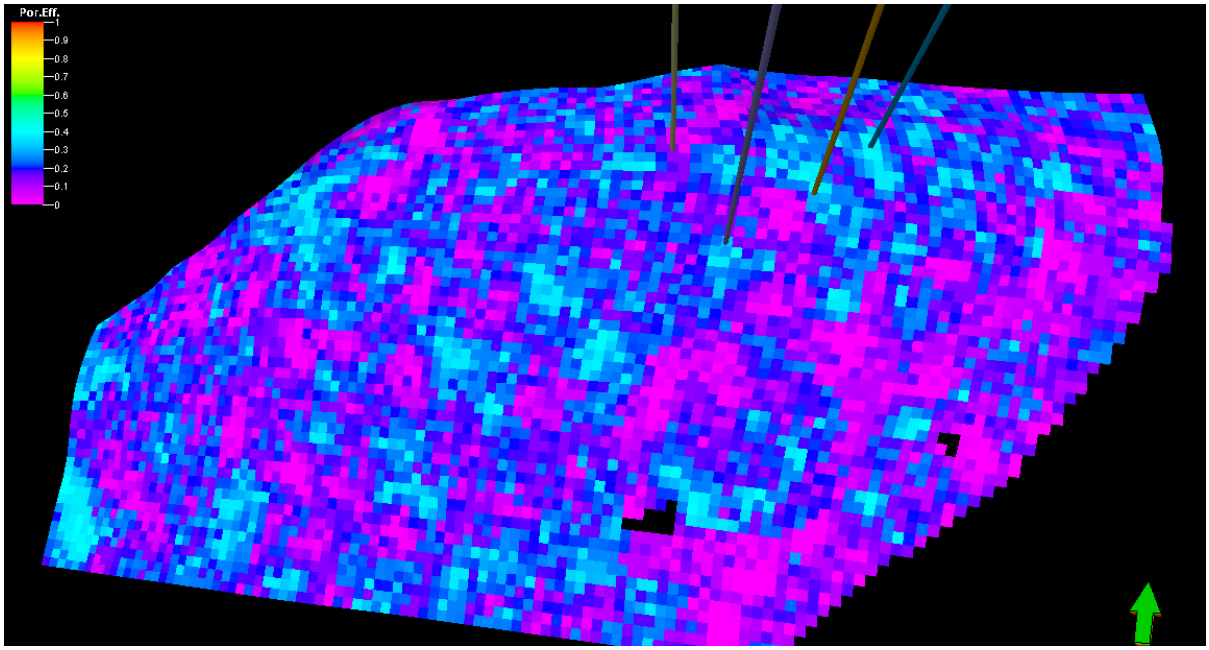

Appendix 3.3.5.3_2d: Porosity model showing completed wells (using Kriging algorithm)

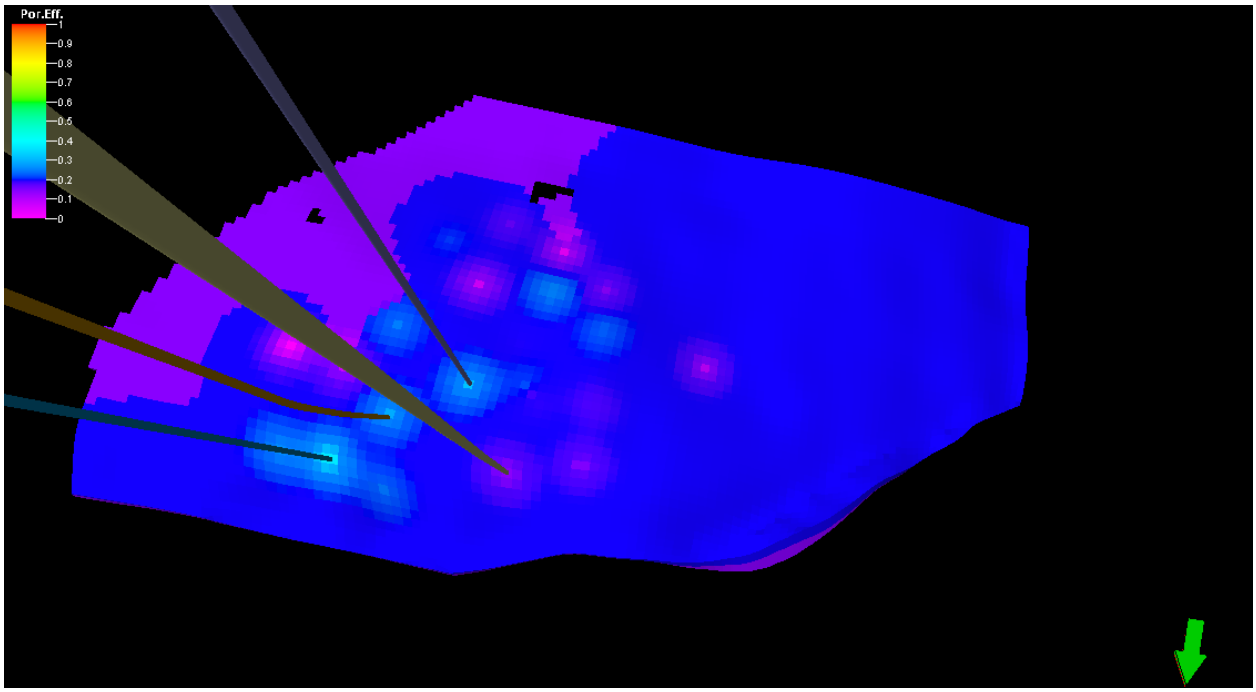

Appendix 3.3.5.3_2e: Porosity model with facies bias showing completed wells (using SGS algorithm)

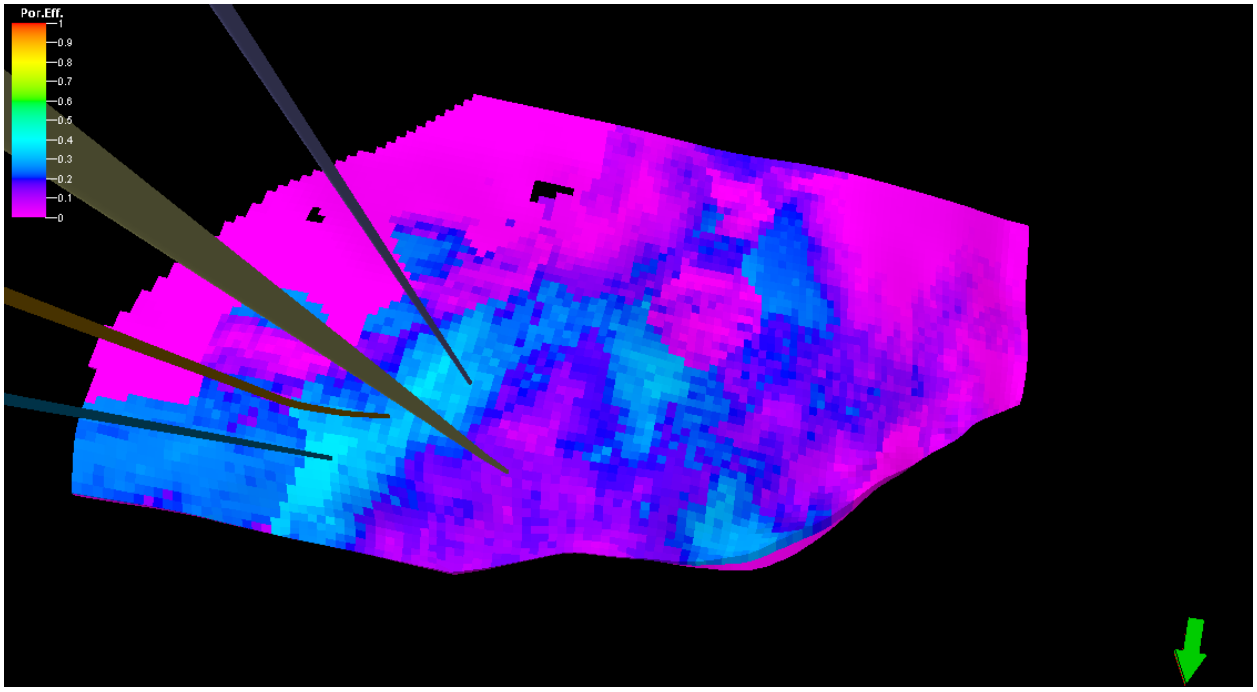

Appendix 3.3.5.3_3a: Variogram map from up-scaled $S_w$log

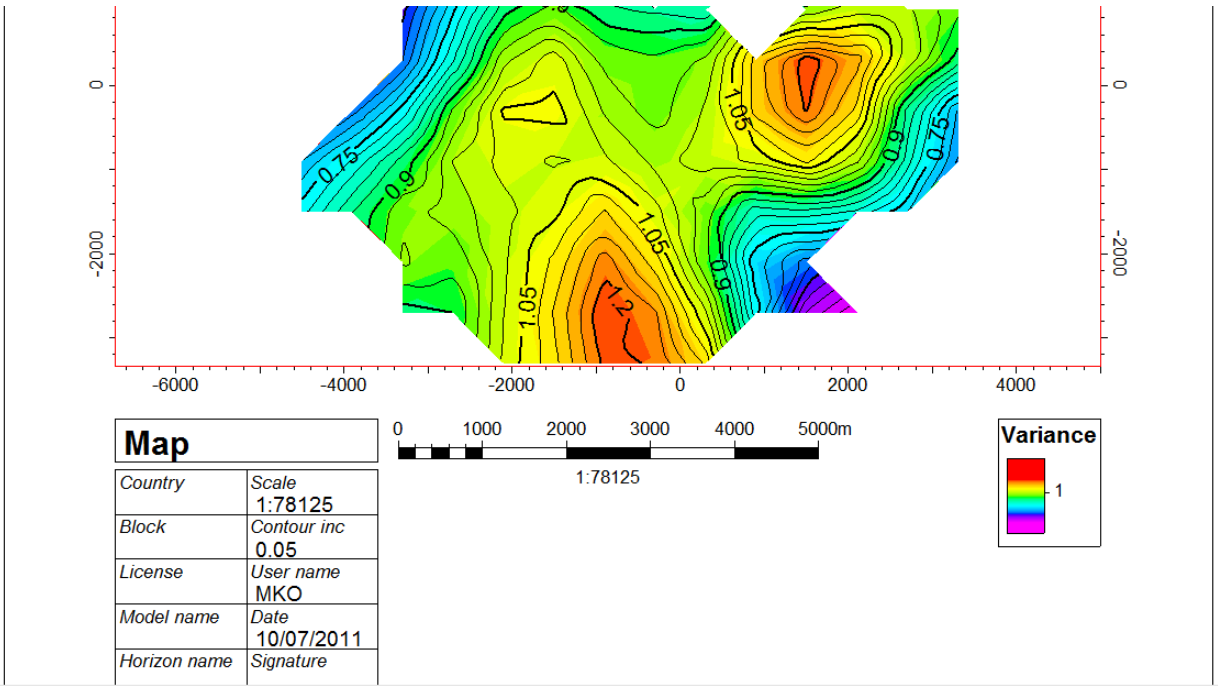

Appendix 3.3.5.3_3b: Sample Variogram and Variogram model from up-scaled $S_w$log

Appendix 3.3.5.3_3c: S_w model showing completed wells (using SGS algorithm)

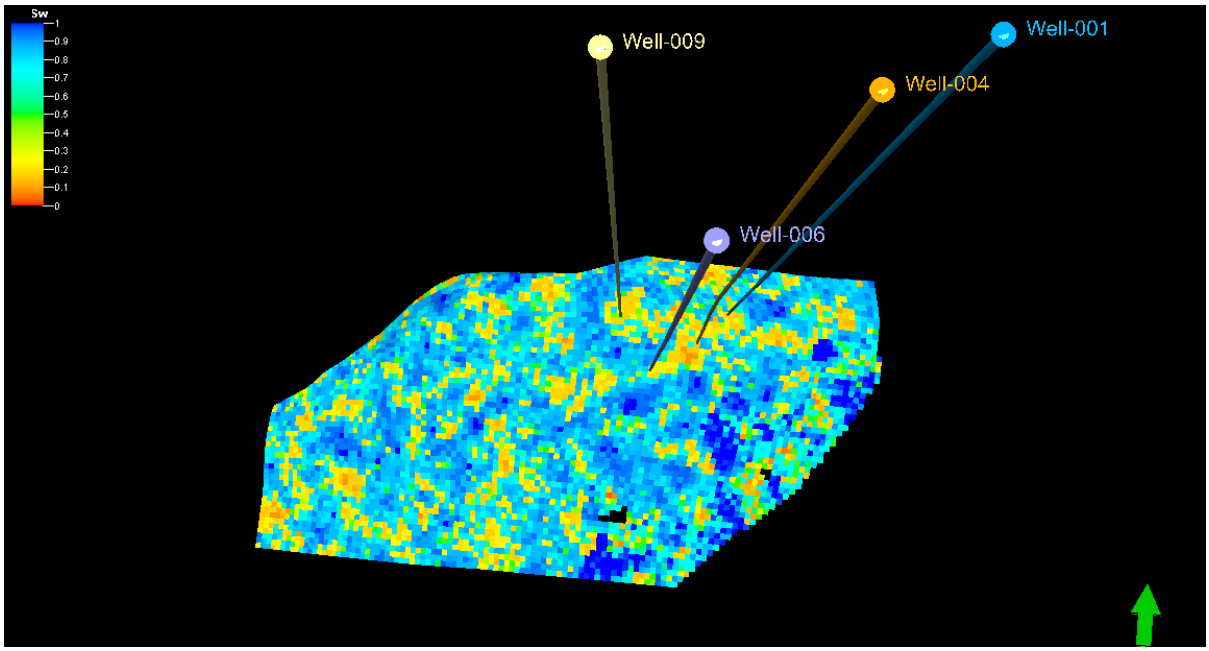

Appendix 3.3.5.3_3d: S_w model showing completed wells (using Kriging algorithm)

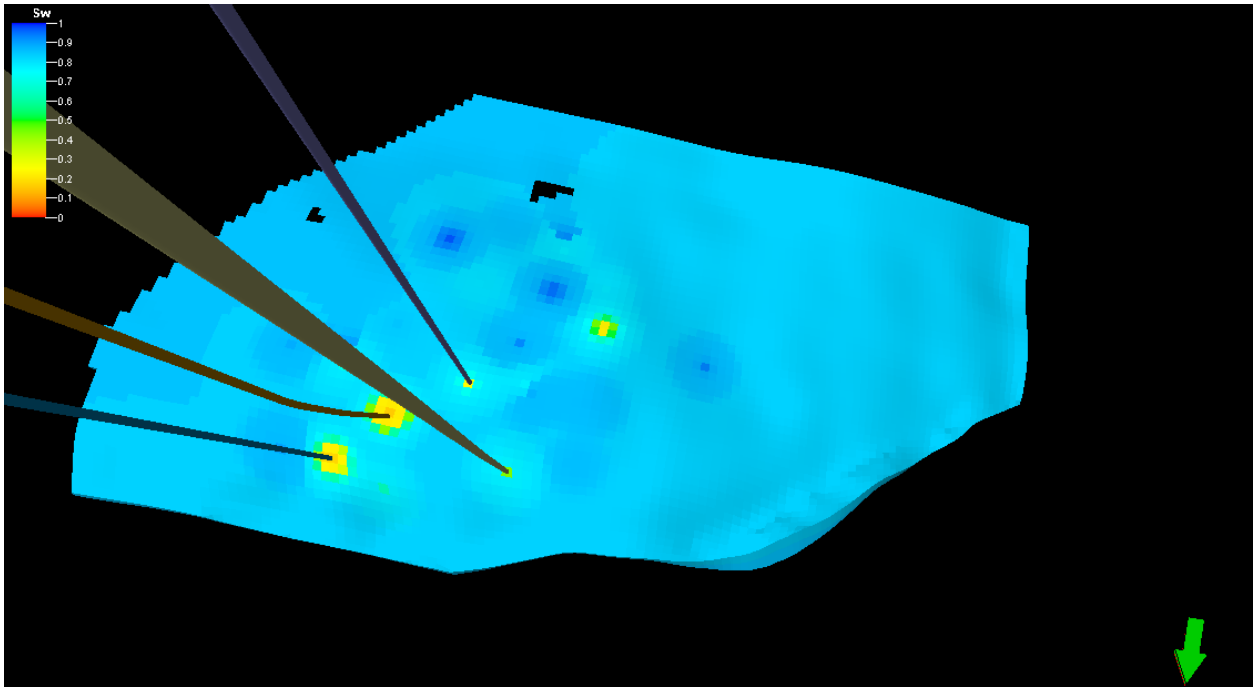

Appendix 3.3.5.3_3e: S_w model with facies bias showing completed wells (using SGS algorithm)

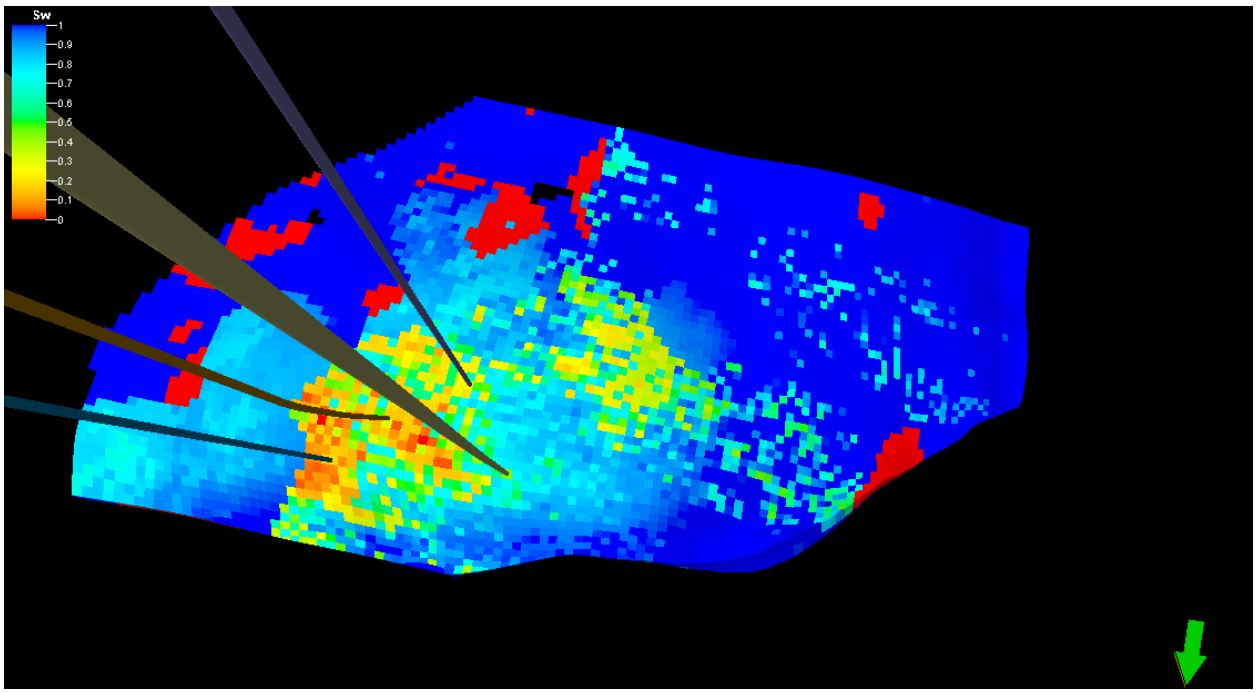

Appendix 3.3.5.3_4a: Variogram map from up-scaled NTG log

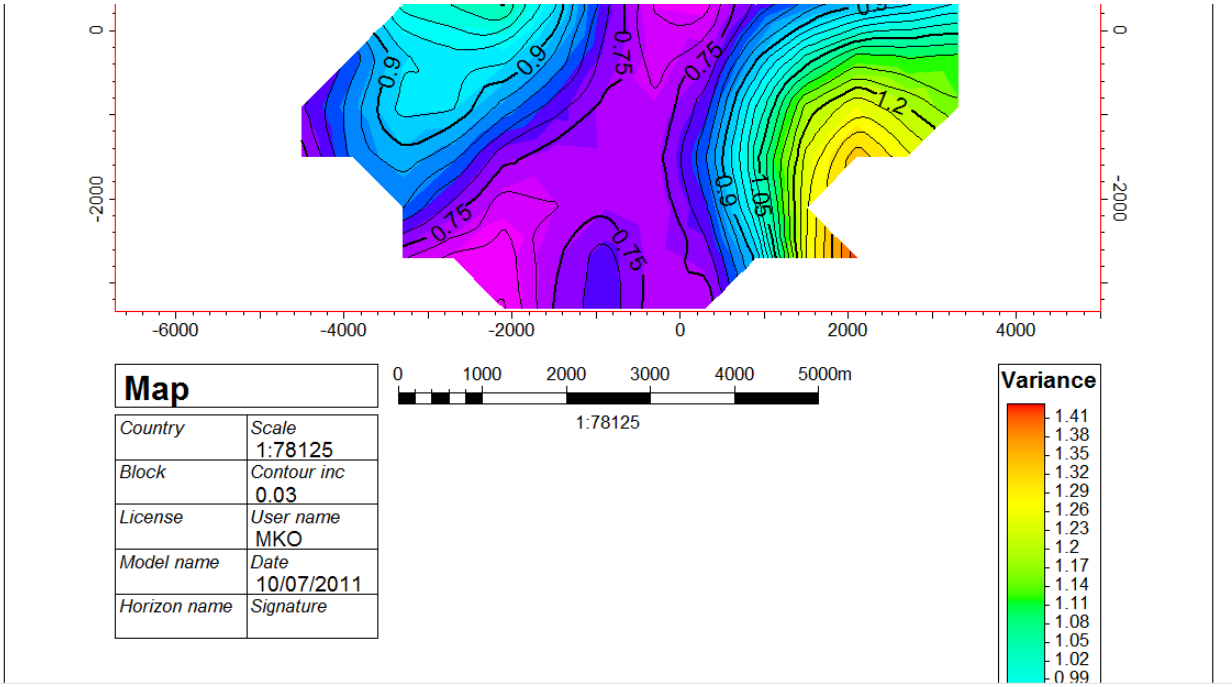

Appendix 3.3.5.3_4b: Sample Variogram and Variogram model from up-scaled NTG log

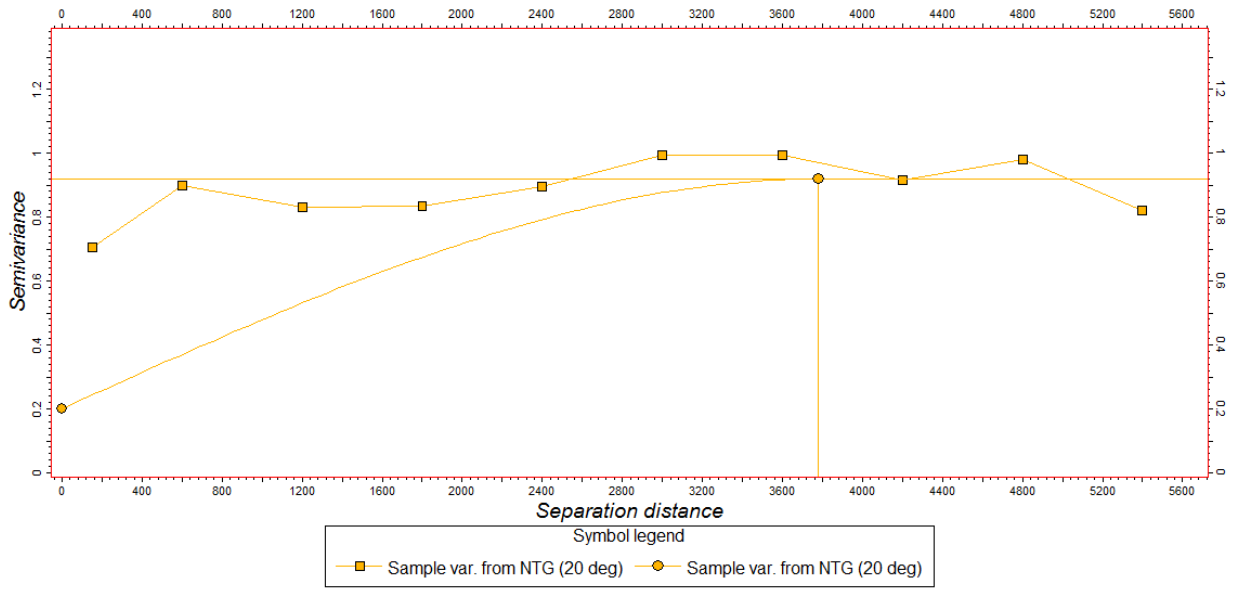

Appendix 3.3.5.3_4c: NTG model showing completed wells (using SGS algorithm)

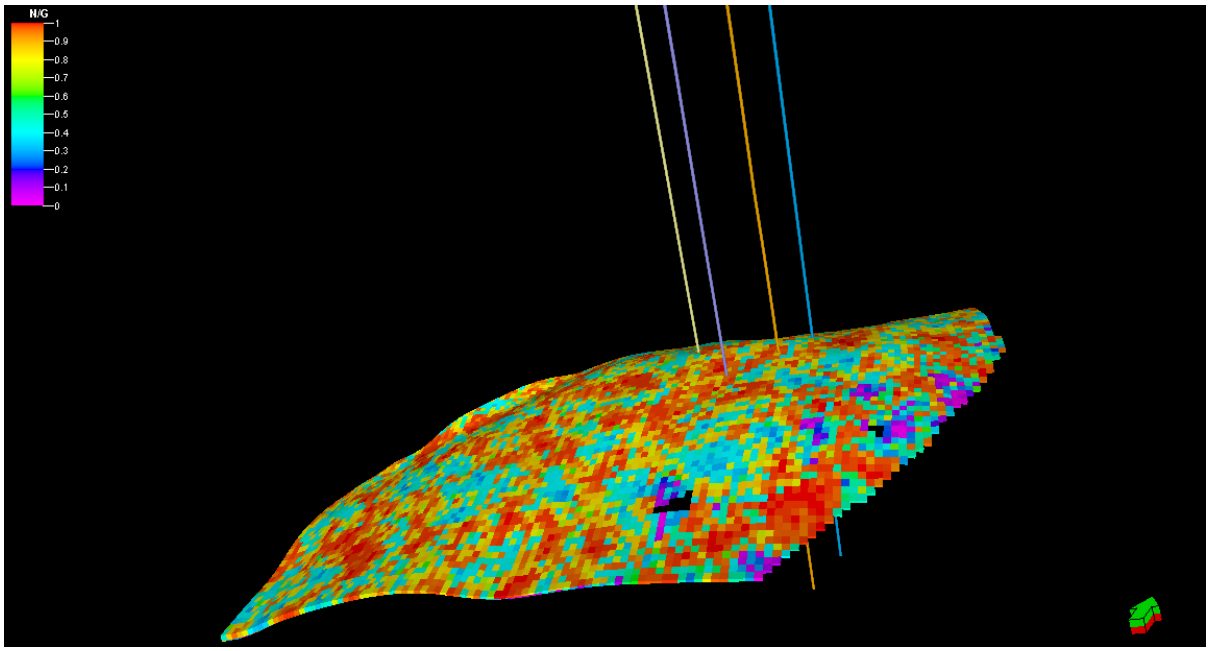

Appendix 3.3.5.3_4d: NTG model showing completed wells (using Kriging algorithm)

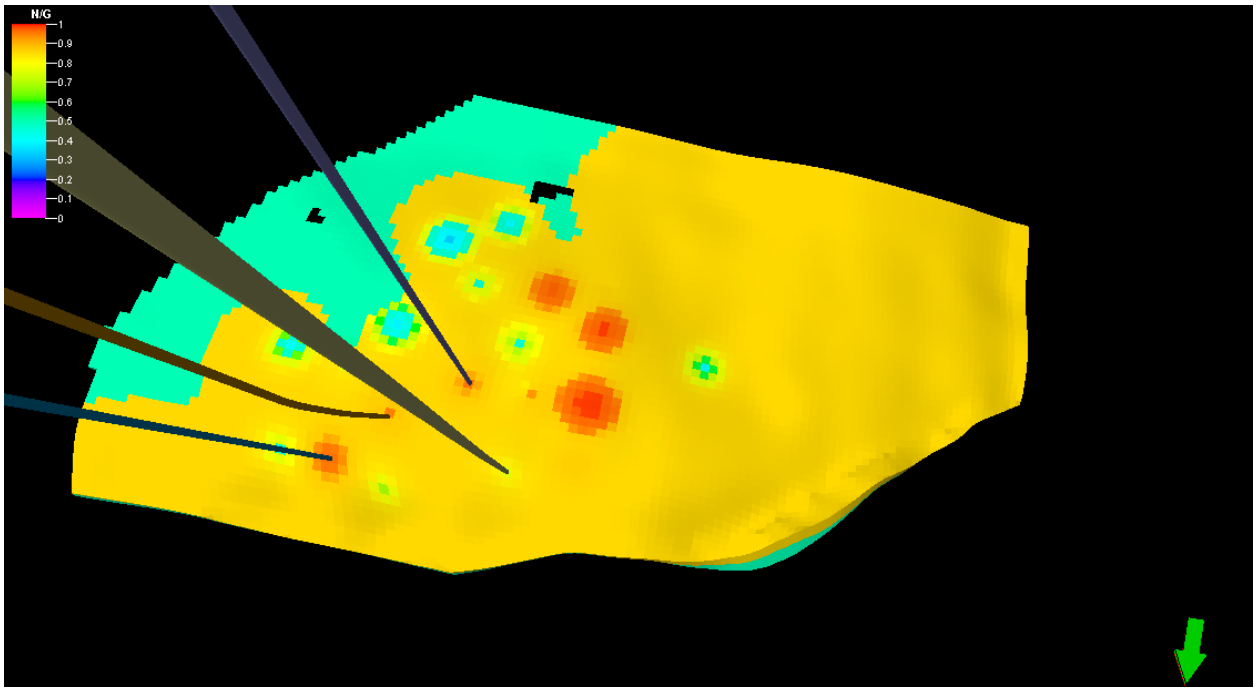

Appendix 3.3.5.3_4e: NTG model with Facies bias showing completed wells (using SGS algorithm)

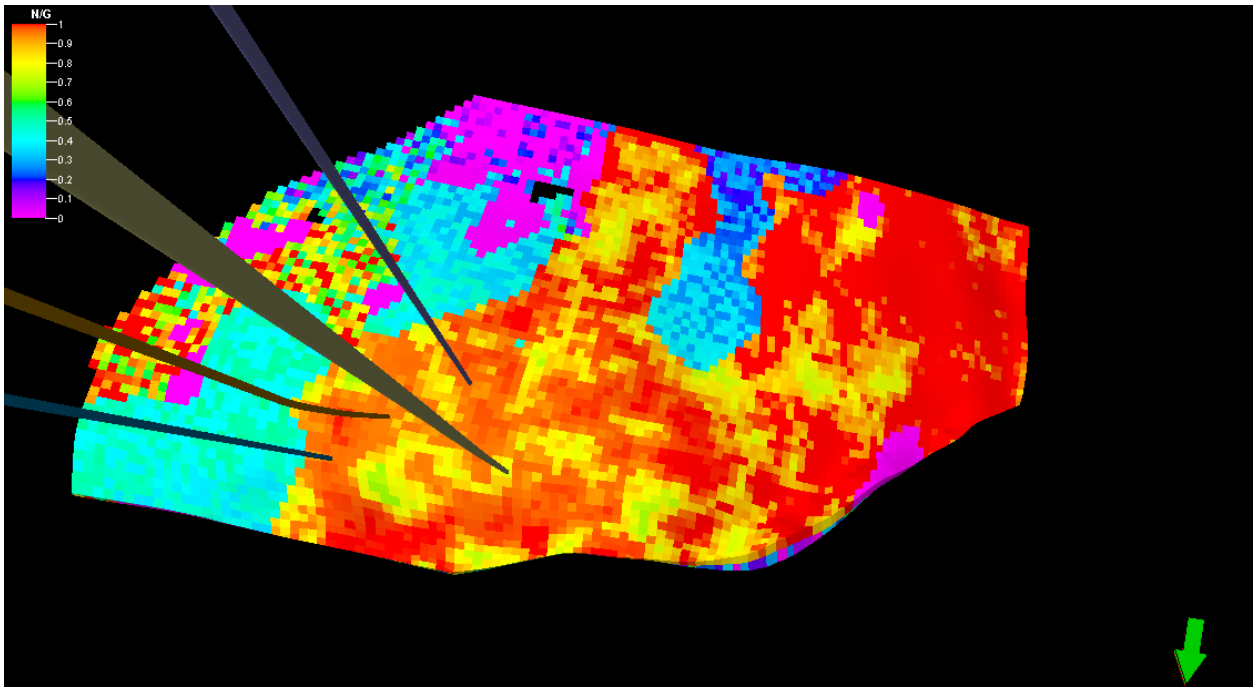

Appendix 3.3.5.3_5a: Variogram map from up-scaled Perm log

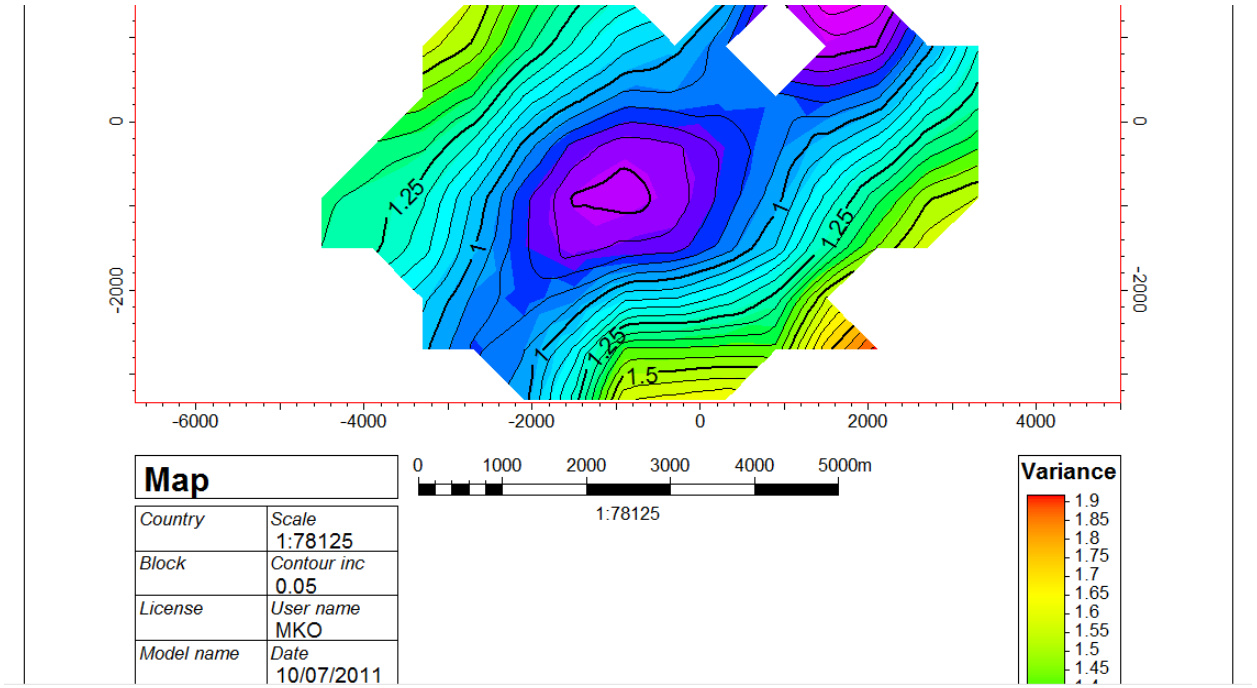

Appendix 3.3.5.3_5b: Sample Variogram and Variogram model from up-scaled Perm log

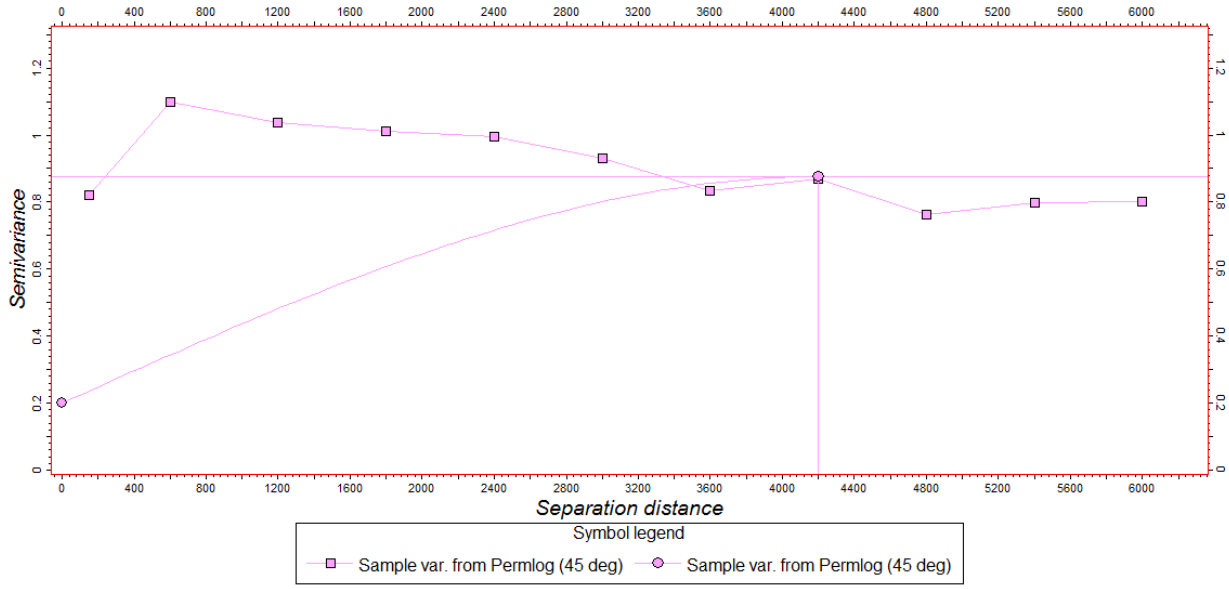

Appendix 3.3.5.3_5c: Perm model showing completed wells (using SGS algorithm)

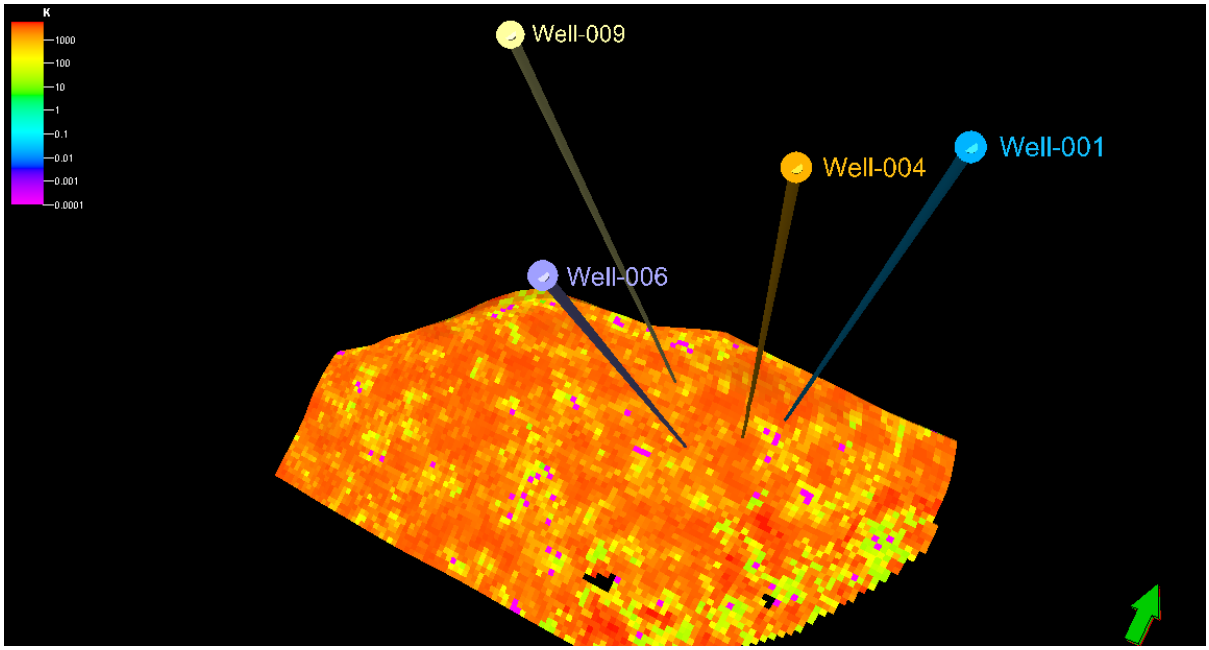

Appendix 3.3.5.3_5d: Perm model showing completed wells (using Kriging algorithm)

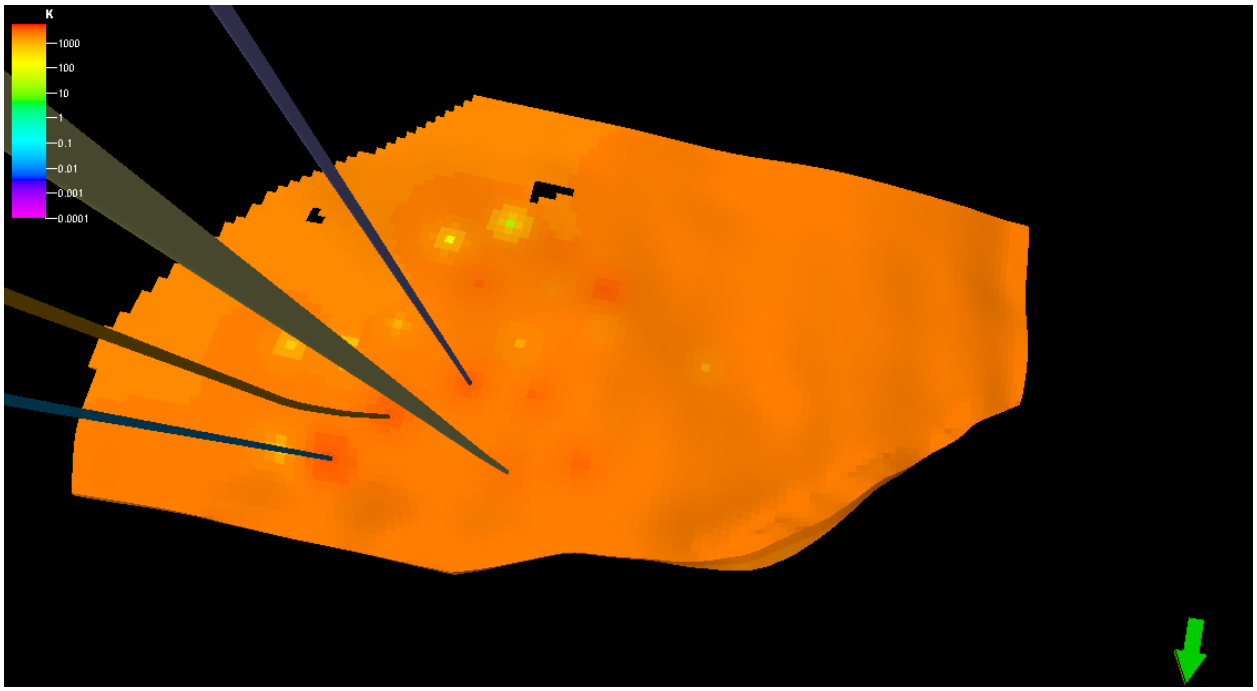

Appendix 3.3.5.3_5e: Perm model with facies bias showing completed wells (using SGS algorithm)

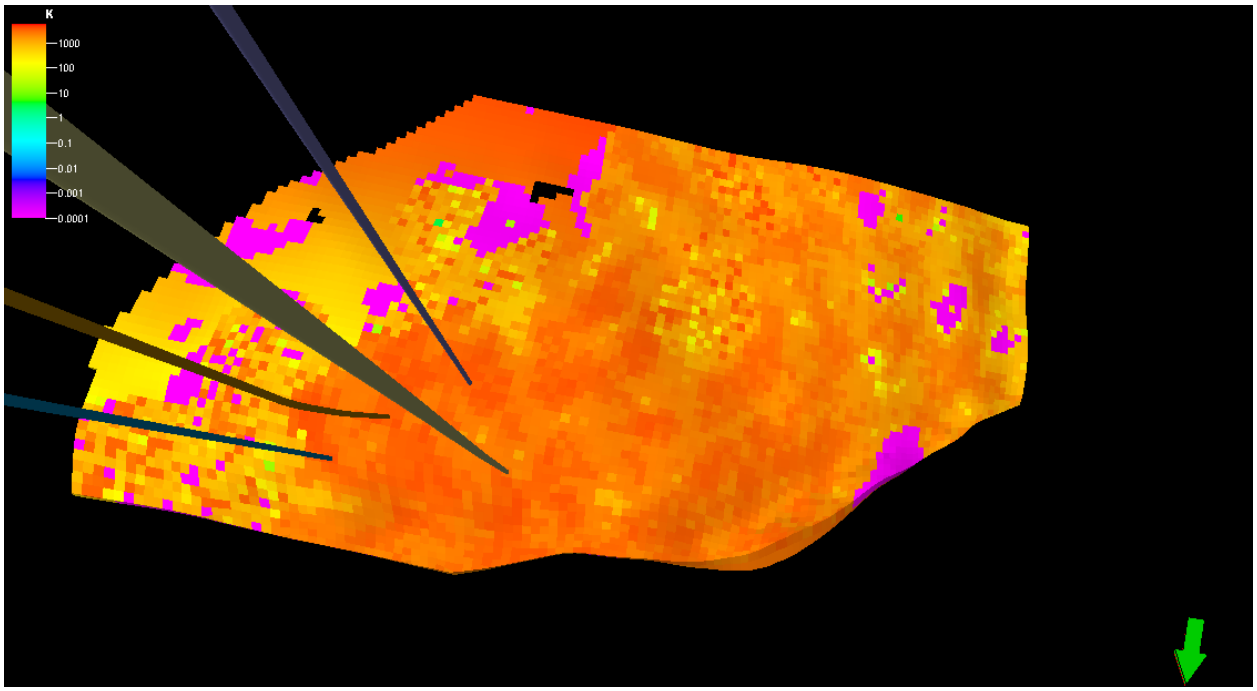

Appendix 3.3.5.2_1: Reservoir X surface showing the modelled faults

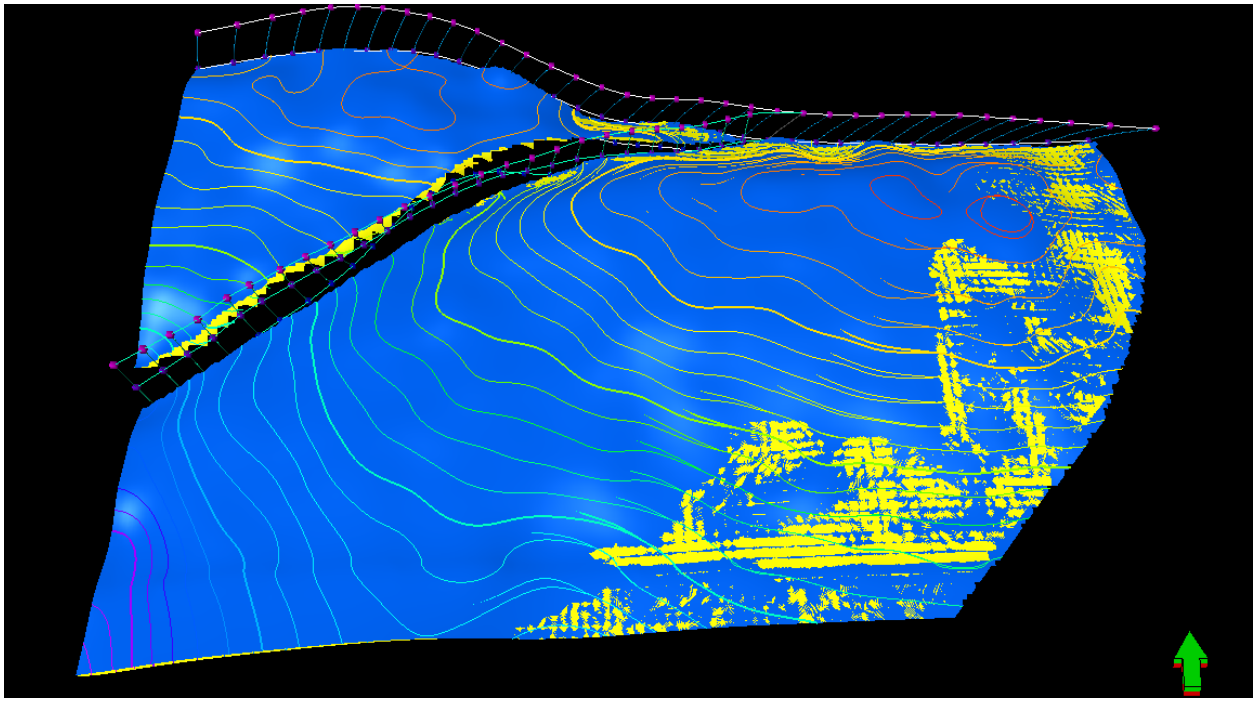

Appendix 3.3.5.2_2: Reservoir X horizon showing OWC and GOC

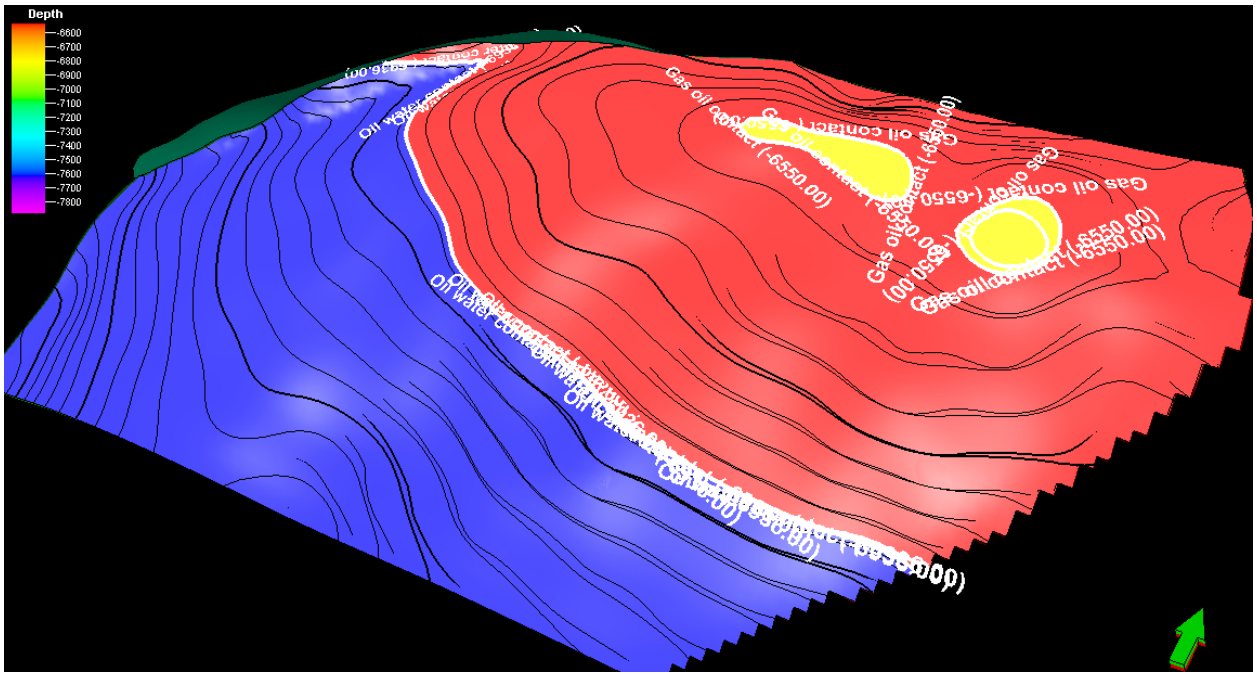

Appendix 3.3.2_4: Reservoir X map showing all the 21 wells

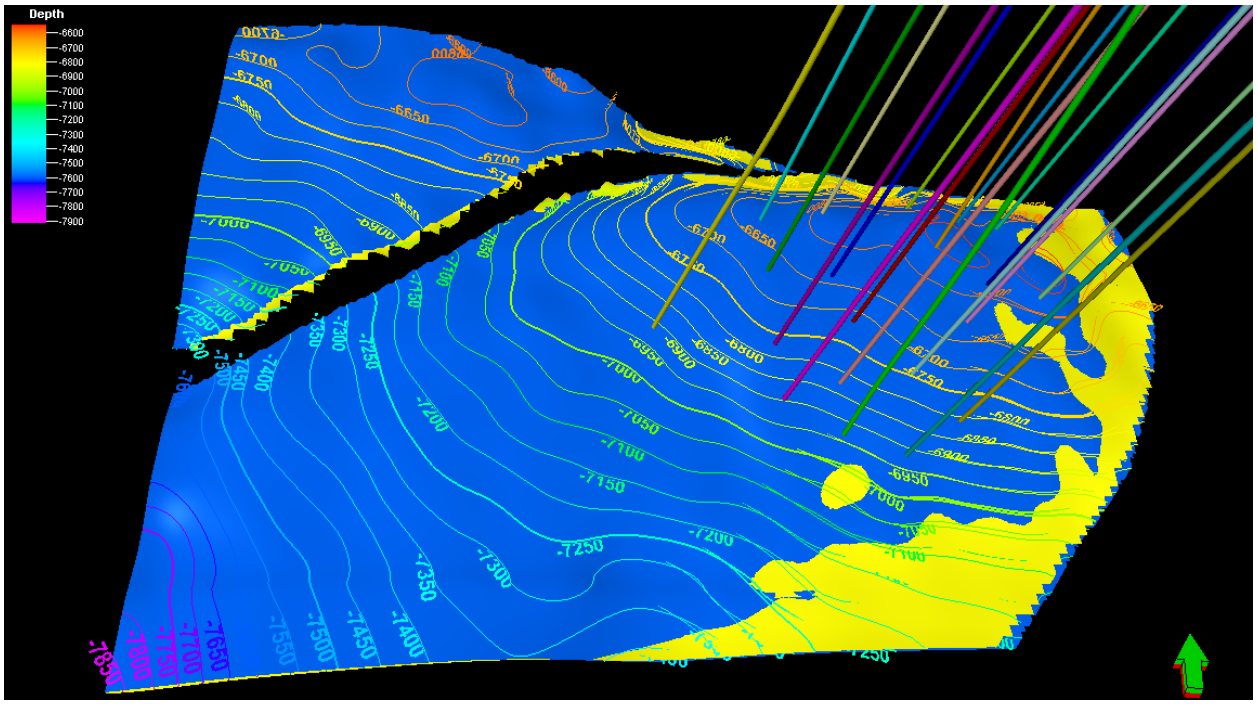

Appendix 3.3.6.2_1: Recoverable oil model of Reservoir X

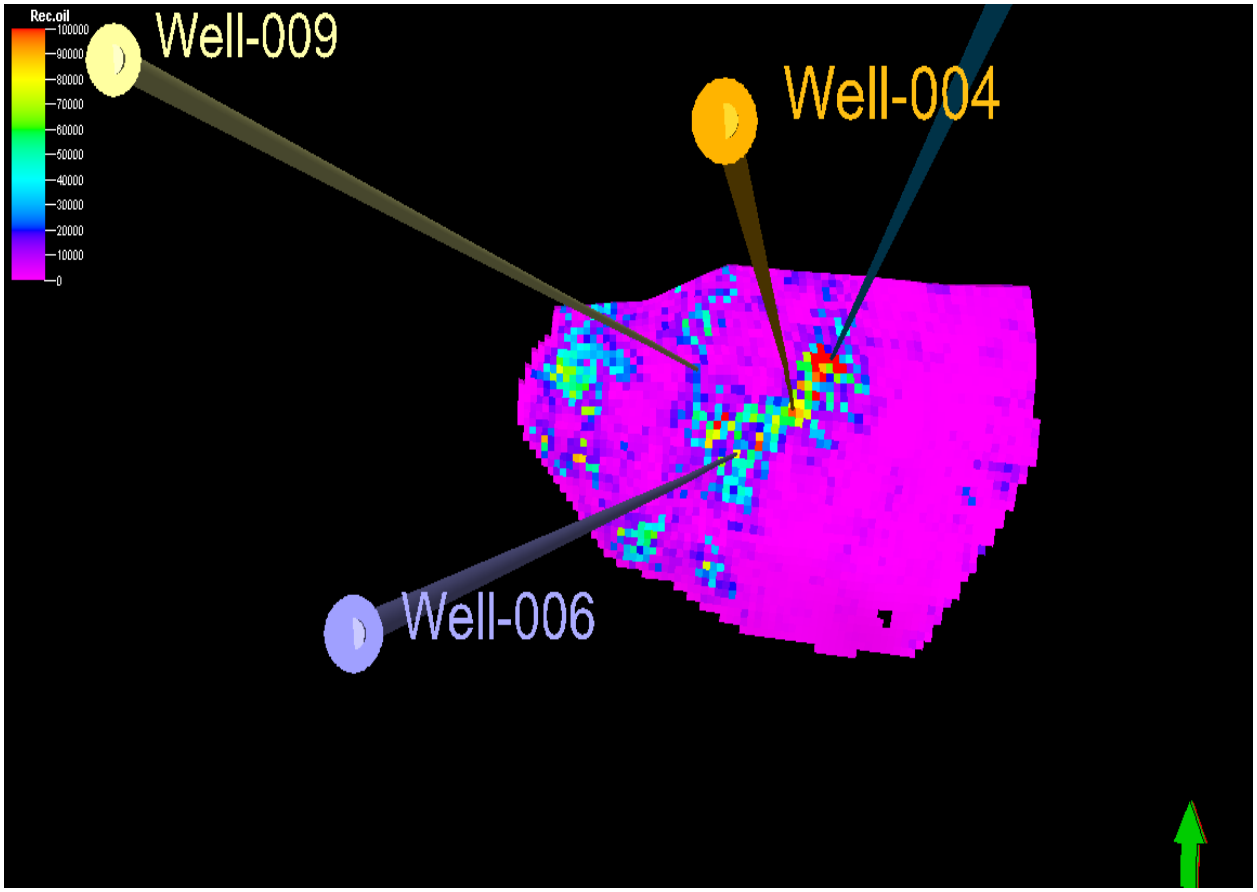

Appendix 3.3.6.2_2: STOIIP model of Reservoir X

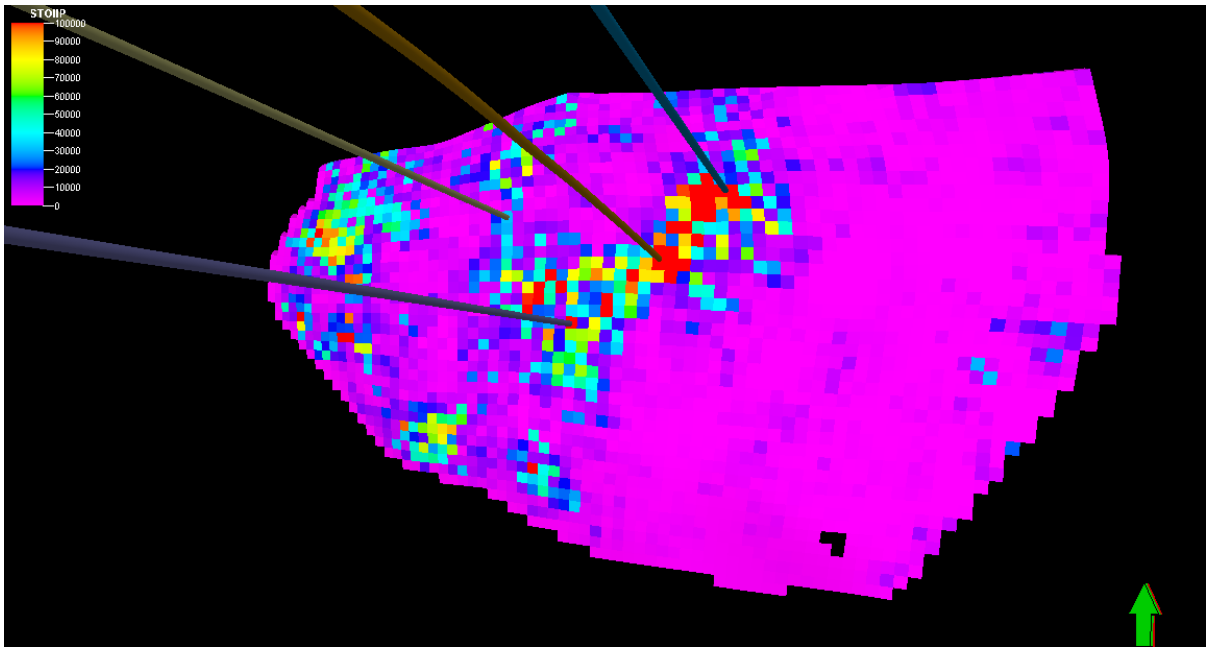

Appendix 3.3.6.2_3: Hydrocarbon Pore volume model of Reservoir X